Accepted Manuscript

Studies towards the development of a PET radiotracer for imaging of the $P2Y_1$ receptors in the brain: synthesis, ^{18}F-labeling and preliminary biological evaluation

Rareș-Petru Moldovan, Barbara Wenzel, Rodrigo Teodoro, Wilma Neumann, Sladjana Dukic-Stefanovic, Werner Kraus, Peijing Rong, Winnie Deuther-Conrad, Evamarie Hey-Hawkins, Ute Krügel, Peter Brust

PII: S0223-5234(19)30006-6

DOI: https://doi.org/10.1016/j.ejmech.2019.01.006

Reference: EJMECH 11013

To appear in: *European Journal of Medicinal Chemistry*

Received Date: 28 September 2018

Revised Date: 20 December 2018

Accepted Date: 4 January 2019

Please cite this article as: Rareș.-Petru. Moldovan, B. Wenzel, R. Teodoro, W. Neumann, S. Dukic-Stefanovic, W. Kraus, P. Rong, W. Deuther-Conrad, E. Hey-Hawkins, U. Krügel, P. Brust, Studies towards the development of a PET radiotracer for imaging of the $P2Y_1$ receptors in the brain: synthesis, ^{18}F-labeling and preliminary biological evaluation, *European Journal of Medicinal Chemistry* (2019), doi: https://doi.org/10.1016/j.ejmech.2019.01.006.

Graphical abstract

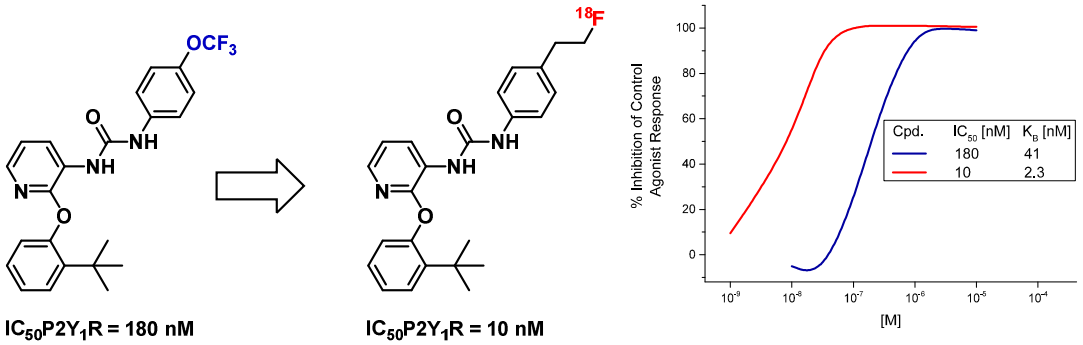

$IC_{50}P2Y_1R$ = 180 nM

$IC_{50}P2Y_1R$ = 10 nM

Studies towards the development of a PET radiotracer for imaging of the $P2Y_1$ receptors in the brain: synthesis, ^{18}F-labeling and preliminary biological evaluation

Rareş-Petru Moldovan[a,], Barbara Wenzel[a], Rodrigo Teodoro[a], Wilma Neumann[c], Sladjana Dukic-Stefanovic[a], Werner Kraus[b], Peijing Rong[e], Winnie Deuther-Conrad[a], Evamarie Hey-Hawkins[c], Ute Krügel[d§] and Peter Brust[a§]*

[a] Helmholtz-Zentrum Dresden-Rossendorf, Institute of Radiopharmaceutical Cancer Research, Permoserstraße 15, 04318 Leipzig, Germany

[b] BAM Federal Institute for Materials Research and Testing, Richard-Willstätter-Str. 11, 12489 Berlin, Germany

[c] Institute of Inorganic Chemistry, Faculty of Chemistry and Mineralogy, Universität Leipzig, 04103 Leipzig, Germany

[d] Rudolf Boehm Institute of Pharmacology and Toxicology, Medical Faculty, Universität Leipzig, 04107 Leipzig, Germany

[e] Institute of Acupuncture and Moxibustion, China Academy of Chinese Medical Sciences, 100700 Beijing, China

*Corresponding author: R.-P. Moldovan, E-mail address: r.moldovan@hzdr.de, Tel: +49 (0)341 234 179 4634

[§]Equal contribution

ABSTRACT Purine nucleotides such as ATP and ADP are important extracellular signaling molecules in almost all tissues activating various subtypes of purinoreceptors. In the brain, the $P2Y_1$ receptor ($P2Y_1R$) subtype mediates trophic functions like differentiation and proliferation, and modulates fast synaptic transmission, both suggested to be affected in diseases of the central nervous system. Research on $P2Y_1R$ is limited because suitable brain-penetrating $P2Y_1R$-selective tracers are not yet available. Here, we describe the first efforts to develop an ^{18}F-labeled PET tracer based on the structure of the highly affine and selective, non-nucleotidic $P2Y_1R$ allosteric modulator 1-(2-[2-(*tert*-butyl)phenoxy]pyridin-3-yl)-3-[4-(trifluoromethoxy)phenyl]urea (**7**). A small series of fluorinated compounds was developed by systematic modification of the *p*-(trifluoromethoxy)phenyl, the urea and the 2-pyridyl subunits of the lead compound **7**. Additionally, the *p*-(trifluoromethoxy)phenyl subunit was substituted by carborane, a boron-rich cluster with potential applicability in boron neutron capture therapy (BNCT). By functional assays, the new fluorinated derivative 1-{2-[2-(*tert*-butyl)phenoxy]pyridin-3-yl}-3-[4-(2-fluoroethyl)phenyl]urea (**18**) was identified with a high $P2Y_1R$ antagonistic potency (IC_{50} = 10 nM). Compound [^{18}F]**18** was radiosynthesized by using tetra-*n*-butyl ammonium [^{18}F]fluoride with high radiochemical purity, radiochemical yield and molar activities. Investigation of brain homogenates using hydrophilic interaction chromatography (HILIC) revealed [^{18}F]fluoride as major radiometabolite. Although [^{18}F]**18** showed fast *in vivo* metabolization, the high potency and unique allosteric binding mode makes this class of compounds interesting for further optimizations and investigation of the theranostic potential as PET tracer and BNCT agent.

Graphical abstract

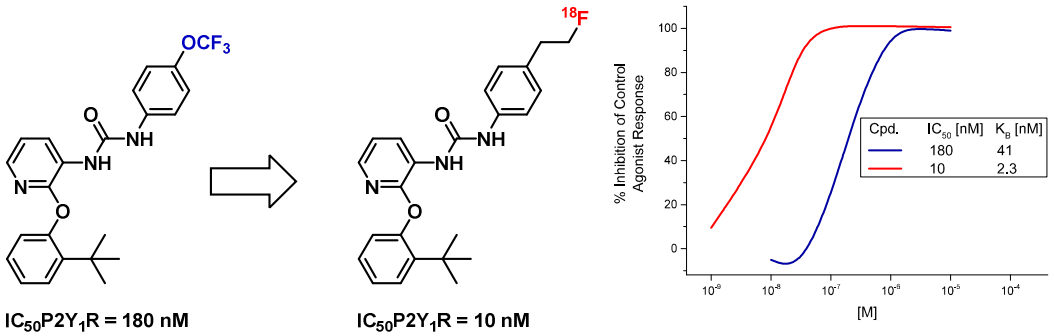

Keywords Purine $P2Y_1$ receptors, positron emission tomography, brain PET tracers, radiometabolites, micellar chromatography, hydrophilic interaction chromatography

Highlights

- A series of fluorinated, non-nucleotidic $P2Y_1R$ ligands was developed
- Derivative **18** was identified with an 18-fold higher antagonistic potency than the lead compound **7**
- [^{18}F]**18** was obtained in high radiochemical purity, yield and molar activities

INTRODUCTION

Purinoreceptors are a family of plasma membrane proteins found in almost all mammalian tissues including the brain.[1-3] The P1 receptors (R) are activated by extracellular adenosine. The P2R are further classified into the P2XR[4] and P2YR[5] families. P2XR are ligand-gated ion channels, preferentially activated by extracellular adenosine triphosphate (ATP).[6-8] P2YR are G protein-coupled receptors (GPCR)[9] activated by ATP, adenosine diphosphate (ADP), uridine triphosphate (UTP) and/or uridine diphosphate (UDP) as main endogenous ligands.[10] Dependent on the cellular activity of neurons or glial cells in the brain, ATP is released into the extracellular space where the nucleotide or its breakdown products interact with the corresponding cell surface purinoreceptors, thereby modulating fast cell-to-cell signaling such as neurotransmitter release, or long-term trophic processes like astrogliosis.[11-14]

So far, eight metabotropic P2YR subtypes have been identified, namely $P2Y_1$, $P2Y_2$, $P2Y_4$, $P2Y_6$, $P2Y_{11}$, $P2Y_{12}$, $P2Y_{13}$ and $P2Y_{14}$.[5, 10, 15-17] In particular, the $P2Y_1R$ subtype, which has

higher affinity to ADP than to ATP is involved in various physiological brain functions and processes related to mental and neurological disturbances.[12, 18]

Alterations in $P2Y_1R$ activity or expression are suggested to be part of the pathophysiology of neurodegeneration, like Alzheimer's disease,[19, 20] of neuroprotection and neuroregeneration in epilepsy,[21, 22] brain trauma[23] and stroke[24, 25] and of cellular proliferation of brain tumors.[16] Furthermore, behavioral and cognitive dysfunction in psychiatric diseases is attributed to the involvement of $P2Y_1R$ in synaptic transmission and plasticity.[26, 27]

The present knowledge on $P2Y_1R$ in the normal and diseased brain is limited and quantitative data on its protein density in brain are rare, mainly because of lack of highly receptor-selective compounds that readily pass the blood-brain barrier and allow *in vivo* imaging of this receptor subtype in the brain.[28, 29]

In chicken and rat brain membranes, a B_{max} for the nucleotidic ligand [^{35}S]dATPαS of 37 and 39 pmol/mg membrane protein, respectively, was reported. Levels of [^{35}S]dATPαS binding in individual structures (0.047–0.309 pmol/mg wet tissue) in chick brain are suggested to be comparable to those found for other G protein-linked receptors such as the muscarinic, dopamine and α2-adrenergic receptors and corresponded to their respective local transcripts.[17, 30] The distribution of [^{35}S]dATPαS specific binding sites was widespread throughout the rat brain, prominent in several regions including piriform cortex, ectostriatum, cerebellum and some nuclei in the telencephalon and mesencephalon.[31] Areas of high binding capacity in this autoradiographic brain study match to more recent data of mouse and human brain transcripts, which are available from the Allen Brain Atlas.[32] In addition, data from human brain[33] and studies on rat [34, 35]confirm a high distribution of $P2Y_1R$ at the protein level suggesting that this protein target is expressed at high enough local concentrations in health or disease for imaging.

The present study aims to explore strategies for the development of compounds of theranostic potential combining properties of an ^{18}F-labeled PET tracer and of a boron-based neutron capture therapeutic (BNTC) agent based on the structure of the highly affine and selective, non-nucleotidic $P2Y_1R$ allosteric modulator 1-(2-(2-(*tert*-butyl)phenoxy)pyridin-3-yl)-3-(4-(trifluoromethoxy)phenyl)urea (BPTU, **7** Figure 1).[36]

Given the nucleotidic nature of the endogenous $P2Y_1R$ ligand ADP (**1**, Figure 1), numerous synthetic ligands with a similar structural skeleton, and even sub-nanomolar affinity and high selectivity for the $P2Y_1R$ were developed to date.[15, 37, 38] Although **1** itself is a rather weak and

non-selective agonist at the $P2Y_1R$, chemical modifications of this molecule led to candidates applicable to prove $P2Y_1R$ as potential therapeutic target (e.g. compounds **2**, **3** and **4**, Figure 1A).[38, 39] Since nucleotidic ligands are thought to pass the blood brain-barrier only to a minor degree because of their negative charge at physiological pH and low capacity of the available transporters, they cannot be considered for development of PET tracers for brain imaging.[40-42]

Only a few non-nucleotidic $P2Y_1R$ ligands with sub-micromolar affinity have been reported so far.[43-45] The predominant scaffold, diarylurea, plays a crucial role for binding to the $P2Y_1R$ (Figure 1). As an example, compound **5** (K_i = 10 nM) was reported by Pfizer laboratories.[45] Similarly, GlaxoSmithKline laboratories identified compound **6**[43] with lower micromolar affinity (K_i = 0.6 µM),[14] and Bristol-Myers Squibb (BMS) laboratories identified compound **7** (K_i = 6 nM, Figure 1).[15, 36] Beside high affinity towards the $P2Y_1R$, compound **7** and related derivatives were highly selective, with no affinity towards $P2Y_2R$, $P2Y_6R$, $P2Y_{11}R$, $P2Y_{12}R$ and $P2Y_{14}R$ (K_i > 1000nM).

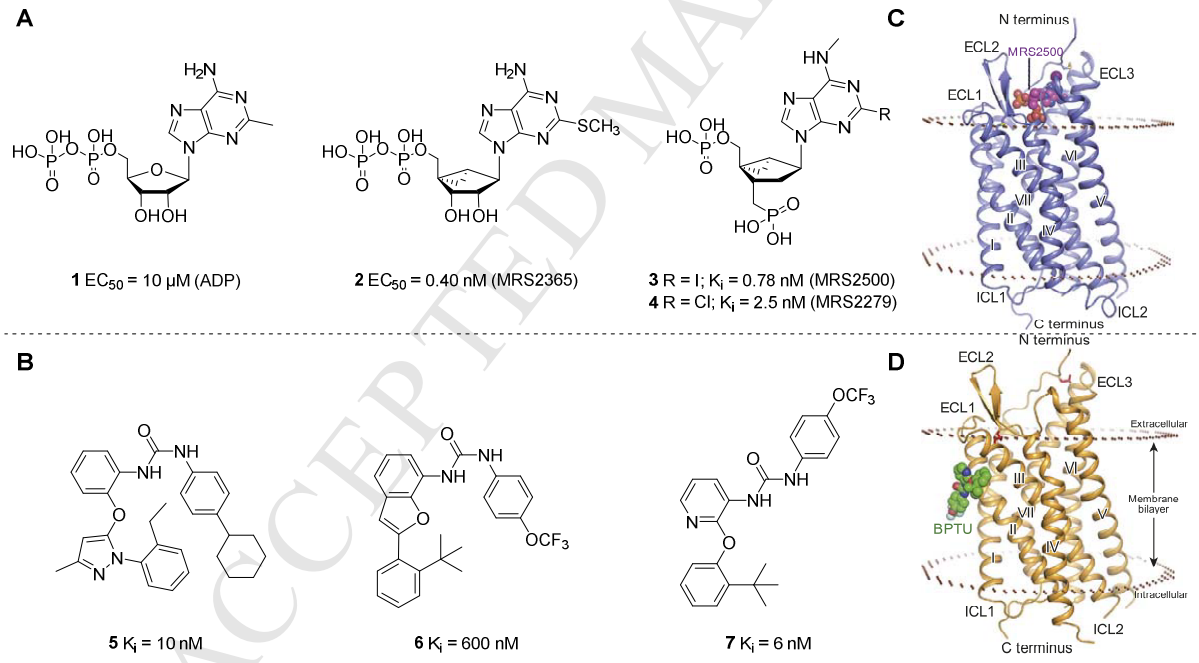

Figure 1. Selected $P2Y_1R$ ligands. (**A**) ADP (**1**) and the $P2Y_1R$ nucleotidic ligands **2**-**4**; (**B**) non-nucleotidic ligands **5**-**7**; (**C**) and (**D**) the structures of the $P2Y_1R$–**3** and $P2Y_1R$–**7** complexes with their orthosteric and allosteric ligand, respectively; the $P2Y_1R$ is shown in cartoon representation and ligands **3** and **7** are shown in sphere representation. For further details see ref. [46]. The picture is used by courtesy of Springer Nature License Number 4344250476031.

The functional antagonism and signaling patterns of the novel allosteric modulator **7** in combination with orthosteric antagonists was subject of various studies.[47 48 46, 49, 50] Recently, the binding mode of compound **7** to the $P2Y_1R$ was elucidated by X-ray crystal structure analysis revealing a unique, allosteric binding pocket, located entirely on the outer surface of the GPCR (Figure 1D). It illustrates that the affinity determination using binding assays with orthosteric radioligands is biased by the indirect rather than direct competition of allosteric modulators (e.g. **7**-**9**, Figure 2). Furthermore, the reported data highlight the potential of targeting the $P2Y_1R$ *via* the allosteric binding pocket, e.g., by the non-nucleotidic compound **7** or its analogues.

The low nanomolar $P2Y_1R$ affinity, the high selectivity and the non-nucleotidic nature of these diaryl-urea ligands[36] qualify this scaffold as a good starting point for the development of an ^{18}F-labeled tracer for brain PET imaging. Analogously to compounds **8** and **9** (Figure 2),[36] the introduction of a fluoroethyl or a fluoroethoxy group should be tolerated at the 4-position in phenyl ring D, enabling a facile S_N2 radiofluorination at an aliphatic position.

A major challenge in the developmental process of PET tracers for brain imaging, beside the brain permeability of the target radioactive compound, is the requirement of absence of brain penetrant radiometabolites. Wang et al.[51] identified the oxidative hydroxylation of the *tert*-butyl group as one of the major metabolic degradation pathways for this type of compounds. To overcome the risk for such metabolites, the *tert*-butyl subunit might be replaced by the metabolic more stable group like cyclopropy-CF_3. However, primarily, the fluorinated derivatives should be synthesized with *tert*-butyl and isopropyl as substituents. Although not described as a metabolic labile partial structure for this type of compounds we proposed the replacement of the urea (subunit C, Figure 2) by a metabolically more stable heterocycle like thiazole.[52] Moreover, the substitution of the fluorine at the 2-position of the pyridine ring B facilitates the introduction of the ^{18}F-label on an aromatic position which is described to be beneficial regarding metabolic stability.[53]

Beside the potential of such a PET tracer as diagnostic tool, it is worthwhile to explore the therapeutic potential of this scaffold in boron neutron capture therapy (BNCT). Therefore, we coupled a carborane, an icosahedral boron cluster that can serve as three-dimensional analog of aromatic hydrocarbons and that has been proposed as neutron capture moiety for BNCT, in compound **7**. Recently, we reported the possibility to replace phenyl rings with a carborane moiety in established cyclooxygenase (COX) inhibitors to generate highly potent and selective

inhibitors.[54-56] Likewise, our current approach is to replace the *p*-(trifluoromethoxy)phenyl subunit of compound **7** (ring D) by an *ortho*-carborane (partial structure IV, Figure 2). The successful implementation of a carborane at subunit D without affecting the binding affinity towards the $P2Y_1R$ will set the stage for introduction of fluorine at the 2-position of the pyridine (ring B, Figure 2). As a result, a bifunctional $P2Y_1R$-ligand is designed with the theranostic potential of being used as both ^{18}F-PET tracer and BNCT agent.

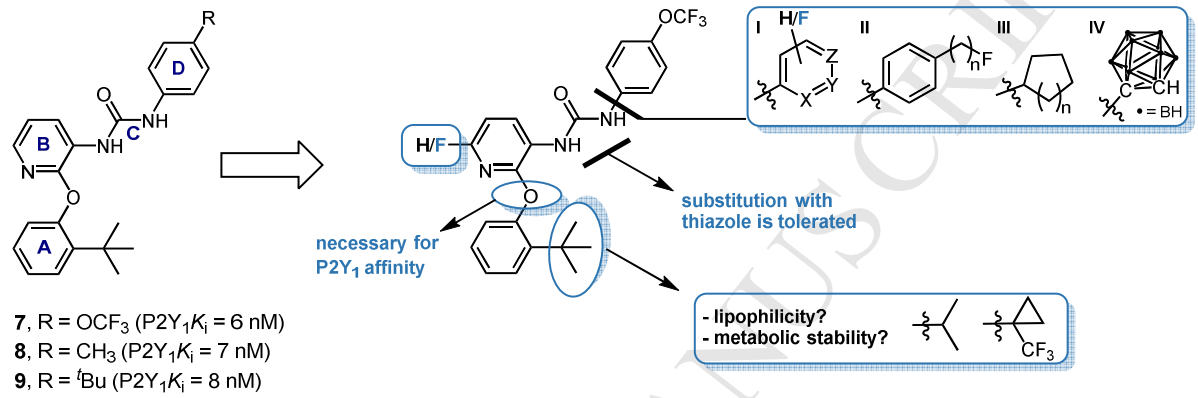

Figure 2. The structure of compounds **7**, **8** and **9** and proposed fluoro derivatization.[36, 52]

The investigation of the binding affinity of our newly designed ligands is currently hindered by the lack of a binding assay for allosteric $P2Y_1R$ modulators, making the in-vitro characterization of these ligands challenging. Here, we used a commercially available functional assay to assess the antagonistic potency of $P2Y_1R$ ligands as selection criteria for potential use in PET.

The successful development of a PET/BNCT tracer will enable the study of the role and distribution of the $P2Y_1R$ in the brain, as well as the involvement of the $P2Y_1R$ in various cancer types and brain diseases (e.g. neurodegeneration).

RESULTS AND DISCUSSION

Chemistry

The synthesis of the lead compound **7** (Figure 2 and Scheme 1) was performed as described by BMS with small modifications.[36] The coupling of the 2-*tert*-butylphenol (**10a**) with the pyridine derivative **11** in the presence of Cs_2CO_3 was followed by reduction of the nitro group (with Pd/C, H_2) to the corresponding amine **12a** and subsequent treatment with diphosgene in presence of Et_3N to give the isocyanate key intermediate **13a** in 55% yield over three steps. For several examples, isopropyl was used instead of a *tert*-butyl group (Scheme 1, R_1) in order to investigate

the influence of this position on the binding potency or metabolic stability. The herein obtained isocyanate was coupled without further purification with various amines to give the corresponding urea derivatives in high yields (>70%, see Experimental Section). The fluoroethyl compounds **18** and **19** were obtained from the alcohols **14** and **15**, respectively, by tosylation and subsequent fluorination with TBAF. The mono- and tri-fluoroethoxylated derivatives **22** and **23** were obtained starting from the methoxylated intermediate **20** upon deprotection to phenol derivative **21** and subsequent fluoroalkylation under basic reaction conditions (Scheme 1). Furthermore, compounds **24** and **25** bearing the fluorine in the 2-position of the phenyl ring were synthesized.

With large amounts of compound **12a** in our hands, we also prepared the 2-aminothiazole ring as previously described.[52] Accordingly, compound **12a** was treated with benzoyl isothiocyanate, hydrolyzed in the presence of LiOH and cyclized with 3-bromo-1,1,1-trifluoropropan-2-one in the presence of a base at elevated temperature to give compound **26**. Bromination at the thiazole 5-position of compound **27** gave the suitable precursor for the subsequent Suzuki coupling. We also introduced the fluorine atom at the 2-position of a pyridine ring due to the facile radiofluorination at this position. We chose the 2-fluoropyridin-5-boronic acid and 2-fluoropyridin-3-boronic acid as coupling partner for the Suzuki reaction[57, 58] and thus, compounds **28** and **29** were obtained in high yields (>70% yield, see Experimental Section) (Scheme 1). Additionally, the 4-fluorophenyl derivative **30** was synthesized.

Scheme 1. Synthesis of the fluorinated diaryl-urea derivatives 7, 14-25 and 2-aminothiazoles 28-30[a]

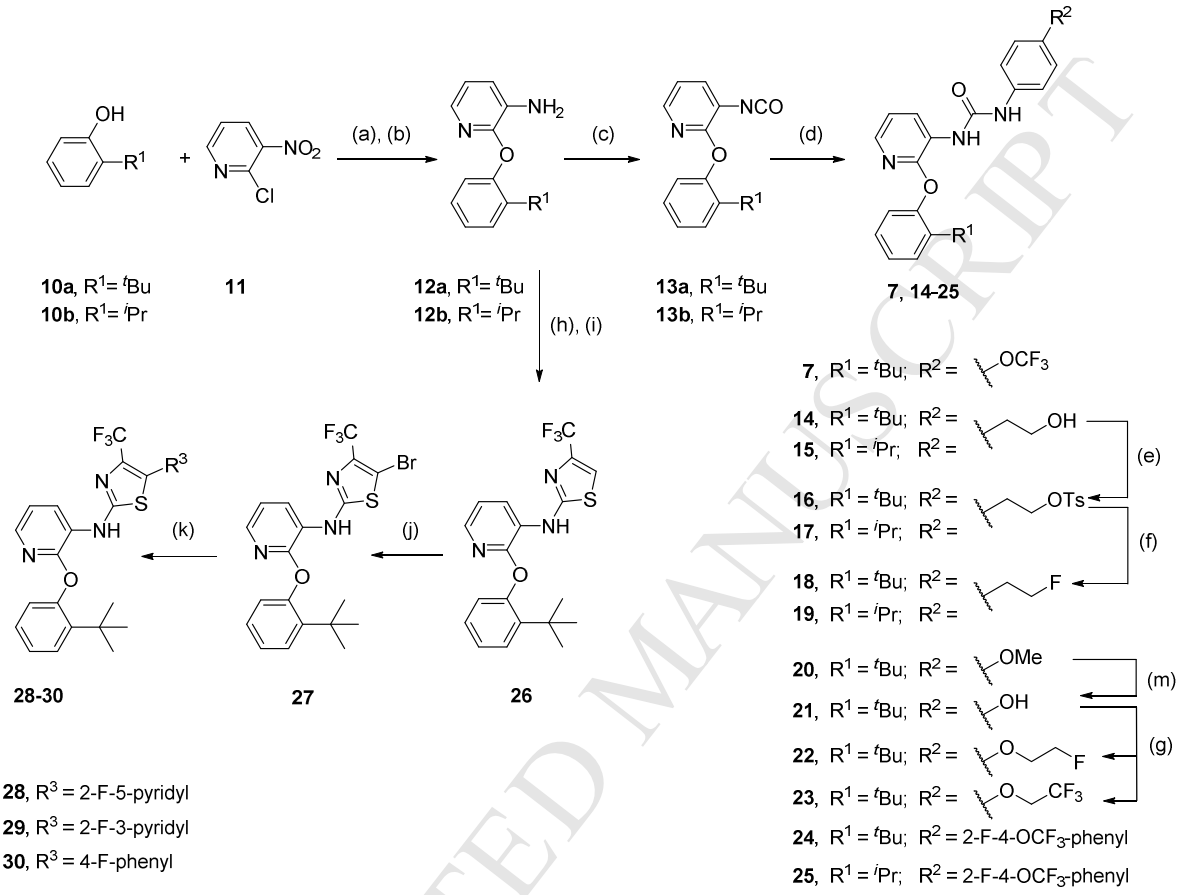

[a]Reagents and conditions: (a) Cs_2CO_3, DMF, 70 °C, 14 h; (b) Pd/C, H_2; (c) diphosgene, Et_3N, DCM, 0 °C to rt, 2 h; (d) corresponding substituted aniline, toluene, 80 °C, 1 h; (e) TsCl, pyridine, DCM, rt, 16 h; (f) TBAF, THF, rt, 16 h; (g) RX, K_2CO_3, CH_3CN, 80 °C, 16 h; (h) i. benzoyl isothiocyanate, DCM, 40 °C, 2 h; ii. 2M LiOH/MeOH, 50 °C, 2 h; (i) 3-bromo-1,1,1-trifluoropropan-2-one, 2,6-lutidine, EtOH, 80 °C, 24 h; (j) NBS, AcOH/THF, 0 °C, 2 h; (k) Suzuki coupling using $[Pd(PPh_3)_4]$, Na_2CO_3, toluene/EtOH, 95 °C, 16 h; (m) BBr_3, DCM; TsCl = *p*-toluenesulfonyl chloride; $[Pd(PPh_3)_4]$ = tetrakis(triphenylphosphine)palladium(0); TBAF = tetra-*n*-butylammonium fluoride; NBS = *N*-bromosuccinimide.

Apart from this series of fluorinated derivatives shown in Scheme 1, the *p*-(trifluoromethoxy)phenyl subunit of compound **7** was replaced with a carborane cluster using amino-carborane **31** as coupling partner for the isocyanate **13a**. Carborane **31** was obtained based

on a literature protocol from the commercially available *ortho*-carborane.[59] The formation of the urea function in compound **32** was much slower (24 h) compared to the other urea derivatives shown here, probably due to the low nucleophilicity of the amino group of the carborane derivative **31**.

Scheme 2. Synthesis of the carborane derivative 32[a]

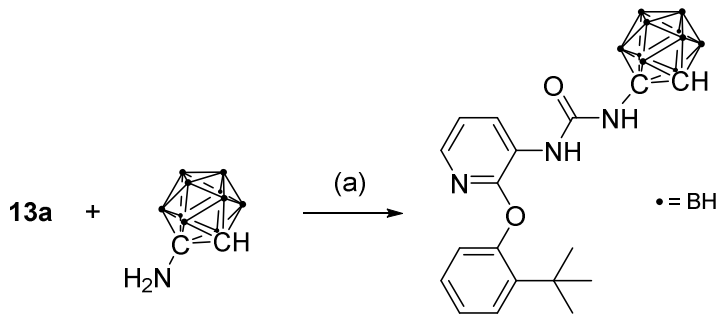

31 **32**

[a]Reagents and conditions: a) toluene, 80 °C, 24 h.

In addition, the incorporation of a fluorine atom at the 2-position of the pyridine (ring B, Figure 2) of **7** was performed. Compound **33** was reacted with 2-*tert*-butylphenol (**10a**) in the presence of a base to give the two regioisomers **34** and **35**. After separation of these regioisomers by flash chromatography and characterization by 2D-NMR spectroscopy, the formation of the urea group was performed as described above (Scheme 1 and Scheme 2) to afford the 2-fluoropyridine derivative **36** over three steps. Several further residues (R) were used to form analogues of **36** including 4-^{t}Bu-phenyl (**37**) and the more hydrophilic 4-hydroxyethanol phenyl **38**. Moreover, the non-aromatic adamantyl, cyclohexyl and cyclopentyl rings were implemented in order to assess the scope and limitation of this subunit regarding the biological activity (Scheme 2, compounds **39**-**41**). The same synthesis sequence (Scheme 2 (b)-(d)) was carried out starting from **35** to give **42**, a regioisomer of **36**. Additionally, the hydrophobic derivative **43** was synthesized. The molecular structure of **36** was unambiguously confirmed by single-crystal diffraction analysis to prove the molecular configuration shown in Figure 3 (for crystallographic data and structure refinement parameters see Supplementary Information).

Scheme 3. Synthesis of the 2-fluoropyridine compounds 36-43[a]

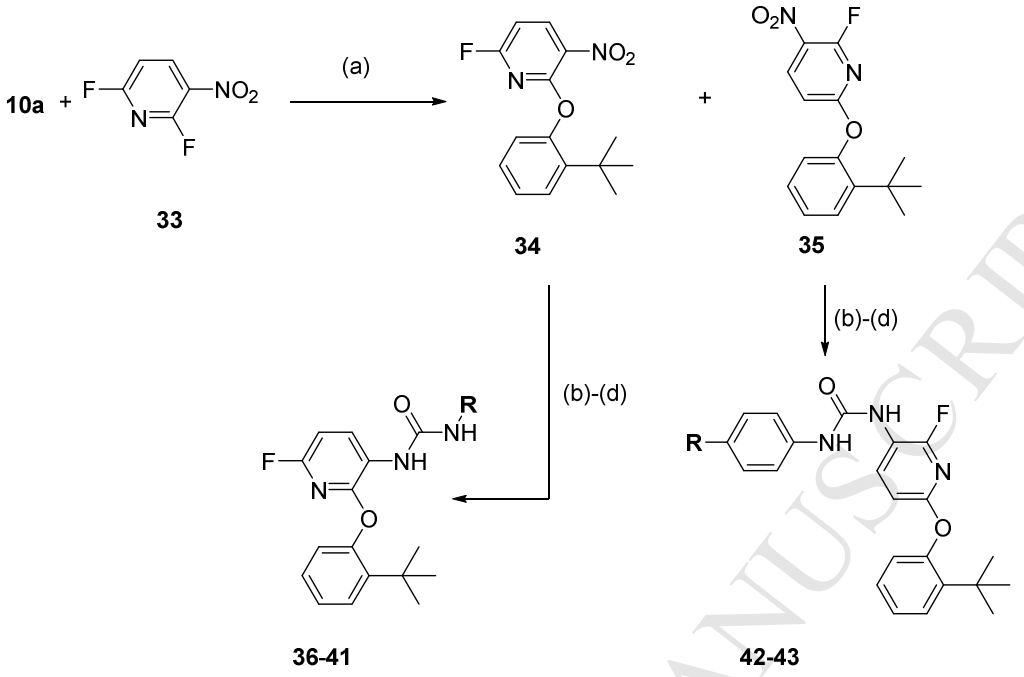

[a]Reagents and conditions: (a) Cs_2CO_3, DMF, 70 °C, 14 h (**34**, 43% and **35**, 35%); (b) Pd/C, H_2; (c) diphosgene, Et_3N, DCM, 0 °C to rt, 2 h; (d) corresponding substituted aniline, toluene, 80 °C, 1 h.

A new series of derivatives was developed by converting the two regioisomeric amines **44** and **50** into the corresponding 2-aminothiazoles **45** (Scheme 4) and **51** (Scheme 5), respectively. NBS-promoted bromination at the 5-position of the thiazole ring gave the precursors for the subsequent Suzuki coupling reactions to obtain compounds **46** and **52**, which were further coupled with selected boronic acids to give compounds **47**-**49** and **53**-**54** in moderate to high yields (see Experimental Section).

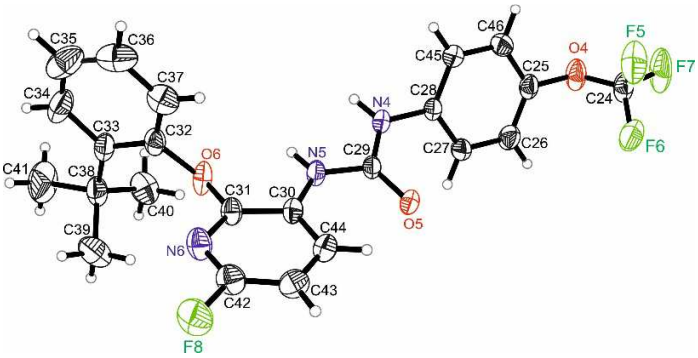

Figure 3. ORTEP representation of compound **36**. Atomic labeling is shown with 30% probability displacement ellipsoids (CCDC number 1849365).

Scheme 4. Synthesis of the 2-fluoropyridyl-5-(2-aminothiazoles) 47-49[a]

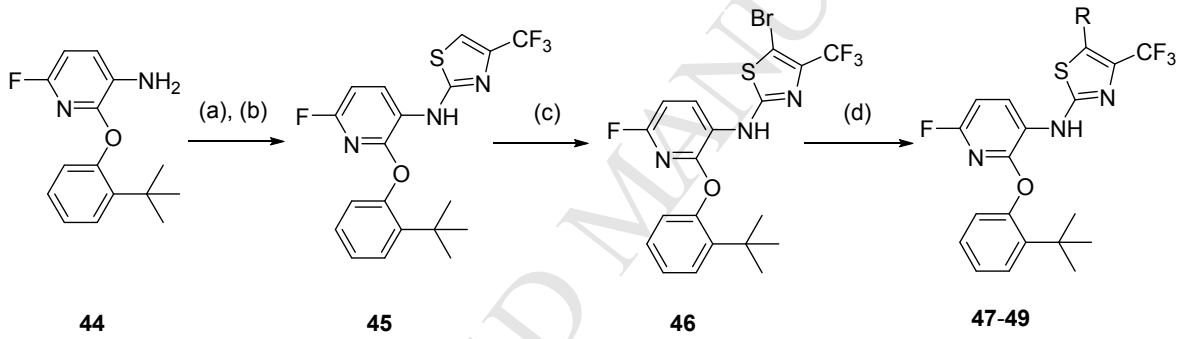

47, R = phenyl

48, R = 4-pyridyl

49, R = 3-pyridyl

[a]Reagents and conditions: (a) *i.* benzoyl isothiocyanate, DCM, 40 °C, 2 h; *ii.* 2M LiOH/MeOH, 50 °C, 2 h; (b) 3-bromo-1,1,1-trifluoropropan-2-one, 2,6-lutidine, EtOH, 80 °C, 24 h; (c) NBS, AcOH/THF, 0 °C, 2 h; (d) Suzuki coupling using $[Pd(PPh_3)_4]$, Na_2CO_3, toluene/EtOH, 95 °C, 16 h.

Scheme 5. Synthesis of the 2-fluoropyridyl-3-(2-aminothiazoles) 53 and 54[a]

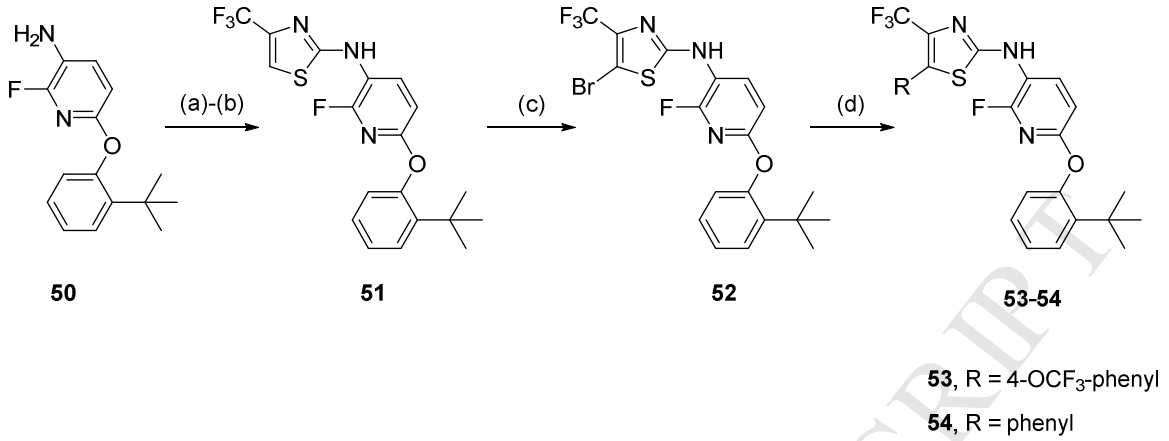

[a]Reagents and conditions: (a) *i.* benzoyl isothiocyanate, DCM, 40 °C, 2 h; *ii.* 2M LiOH/MeOH, 50 °C, 2 h; (b) 3-bromo-1,1,1-trifluoropropan-2-one, 2,6-lutidine, EtOH, 80 °C, 24 h; (c) NBS, AcOH/THF, 0 °C, 2 h; (d) Suzuki coupling using $[Pd(PPh_3)_4]$, Na_2CO_3, toluene/EtOH, 95 °C, 16 h.

In vitro biological evaluation

Using a commercially available cellular functional assay, the literature-known compound **7** together with the herein described new derivatives were studied for both agonistic and antagonistic effects. The agonistic effect was investigated using the known $P2Y_1R$ agonist **55** (MRS2365, {[(1*R*,2*R*,3*S*,4*R*,5*S*)-4-[6-amino-2-(methylthio)-9*H*-purin-9-yl]-2,3-dihydroxybicyclo[3.1.0]hex-1-yl]methyl} diphosphoric acid monoester trisodium salt) as reference compound at a single concentration (20 nM). The antagonistic effect was investigated using compound **3** as reference compound at two concentrations, 20 and 100 nM, respectively.[38] As expected,[36] these compounds are devoid of any agonistic effect. As shown in Table 1, at the given concentrations, the lead compound **7** has a low antagonistic effect. At a concentration of 20 nM, only compounds **18** and **38** had a slight antagonistic effect. However, at a concentration of 100 nM compound **18** strongly inhibited the agonist response, whereas compounds **7**, **24**, and **40** were only weak antagonists. Within the 2-fluoropyridine series, only compound **40** showed a slight antagonism at 100 nM. None of the 2-aminothiazole derivatives showed any potency. The regioisomeric derivatives **42**, **43**, **51**, **53** and **54** were also ineffective. To reinforce the results from Table 1, lead compound **7**, the fluoroethyl derivative **18**, the fluoropyridine **38** and the carborane **32** were subject of a detailed study on antagonist effectivity (Figure 4). Among them,

compound **18** (IC_{50} = 10 nM) possesses ~18-fold higher antagonistic potency than the starting compound **7** (IC_{50} = 180 nM). The 2-fluoropyridine derivative **38** is characterized by an IC_{50} value of 490 nM but the carborane **32** failed to have any antagonistic potency at the $P2Y_1R$.

Table 1. Results from cellular functional assays investigating antagonistic and agonistic effects of selected compounds

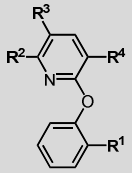	**R^1**	**R^2**	**R^3**	**R^4**	**Agonism**[a] (20 nM)	**Antagonism**[b] (20 nM)	(100 nM)
7	^{t}Bu	H	H	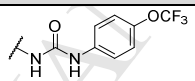	-12	-10	22
18	^{t}Bu	H	H	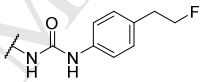	-14	26	73
19	^{i}Pr	H	H	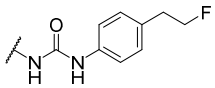	NA	-14	15
22	^{t}Bu	H	H	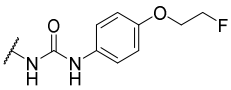	-15	-5	NA
23	^{t}Bu	H	H	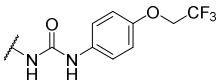	-14	-12	4
24	^{t}Bu	H	H	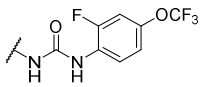	NA	6	16
25	^{i}Pr	H	H	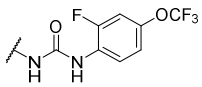	NA	-18	4

28	^{t}Bu	H	H	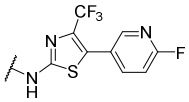	-11	-20	-5
29	^{t}Bu	H	H	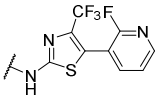	NA	7	-14
30	^{t}Bu	H	H	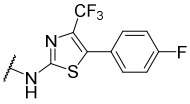	NA	-1	-15
32	^{t}Bu	H	H	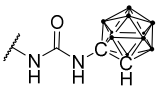	NA	1.5	NA
36	^{t}Bu	F	H	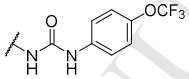	-9	-17	-19
37	^{t}Bu	F	H	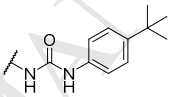	NA	3	-11
38	^{t}Bu	F	H	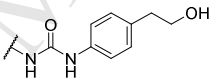	-7	18	NA
39	^{t}Bu	F	H	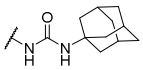	-8	-7	-7
40	^{t}Bu	F	H	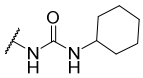	NA	7	26
41	^{t}Bu	F	H	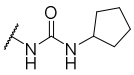	NA	6	2
42	^{t}Bu	F	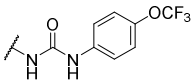	H	-1	-16	-24
43	^{t}Bu	F	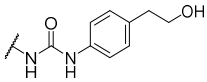	H		-13	-21
46	^{t}Bu	F	H	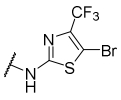	NA	-21	-4

47	^{t}Bu	F	H	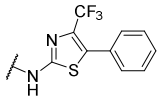	NA	-1	-14
48	^{t}Bu	F	H	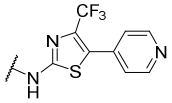	NA	10	10
49	^{t}Bu	F	H	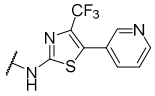	NA	0	6
51	^{t}Bu	F	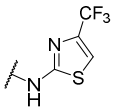	H	NA	-27	-16
53	^{t}Bu	F	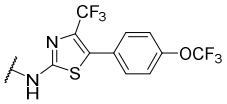	H	NA	-3	-17
54	^{t}Bu	F	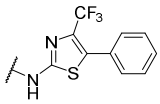	H	NA	11	-16

[a]% of control agonist response using **55** as reference compound (n = 2); [b]% inhibition of control agonist response using **3** as reference compound (n = 2); NA = not available.

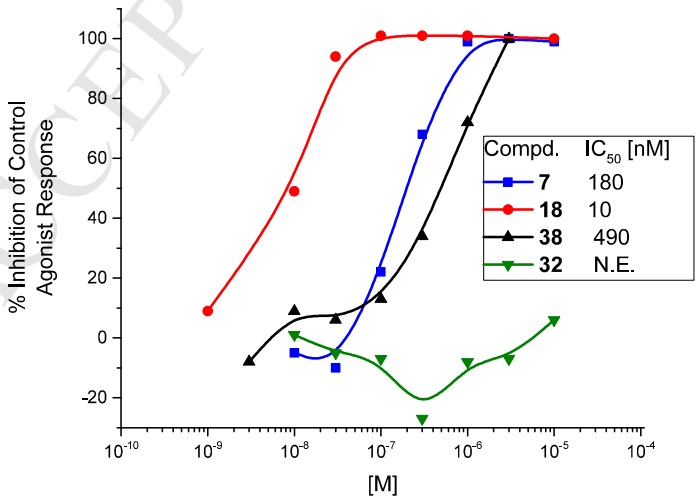

Figure 4. $P2Y_1R$ antagonistic properties of compounds **7**, **18**, **32** and **38**. (N.E. = no effect)

Radiochemistry

As derivative **18** demonstrated the strongest antagonistic response, it was selected for ^{18}F-labeling. The new radioligand [^{18}F]**18** was prepared by nucleophilic substitution of the tosylate group of precursor **16** (Scheme 1) using anhydrous [^{18}F]TBAF in *tert*-BuOH (Scheme 6). Under conventional heating at 90 °C and 10 min reaction time, radiochemical yields (RCY) of 58.0 ± 6.4% (n = 5) were achieved for the labeling process. According to radio-TLC analysis, two radioactive by-products were observed in the reaction mixture accounting for about 15% of total radioactivity. Interestingly, when the classical K[^{18}F]F-$K_{2.2.2}$-carbonate complex system and acetonitrile (CH_3CN) at 90 °C were used, a considerably lower RCY was achieved (< 9%). The precursor **16** remained stable under all conditions tested as proven by HPLC.

Scheme 6. ^{18}F-Radiolabeling of compound 16

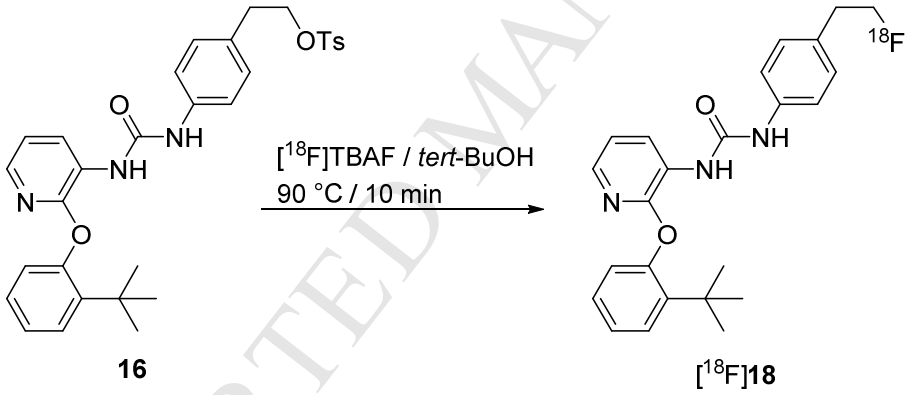

16 **[^{18}F]18**

The isolation of [^{18}F]**18** was performed by semi-preparative RP-HPLC (Figure 5A). The collected product was purified using solid-phase extraction on an RP cartridge and formulated in sterile isotonic saline containing 10% of EtOH for better solubility. Analytical radio- and UV-HPLC of the final product, spiked with the nonlabeled reference compound, confirmed the identity of [^{18}F]**18** (Figure 5B). Finally, the formulated radiotracer was obtained with a radiochemical purity of ≥ 99%, in a radiochemical yield (EOB) of 28.2 ± 0.8% (n = 4, decay corrected), and molar activities (EOS) in the range of 153–283 GBq/µmol using starting activities of 2-3 GBq. The logD value of [^{18}F]**18** was experimentally determined by the shake-flask method to be 3.64 ± 0.33 (see Experimental Section).

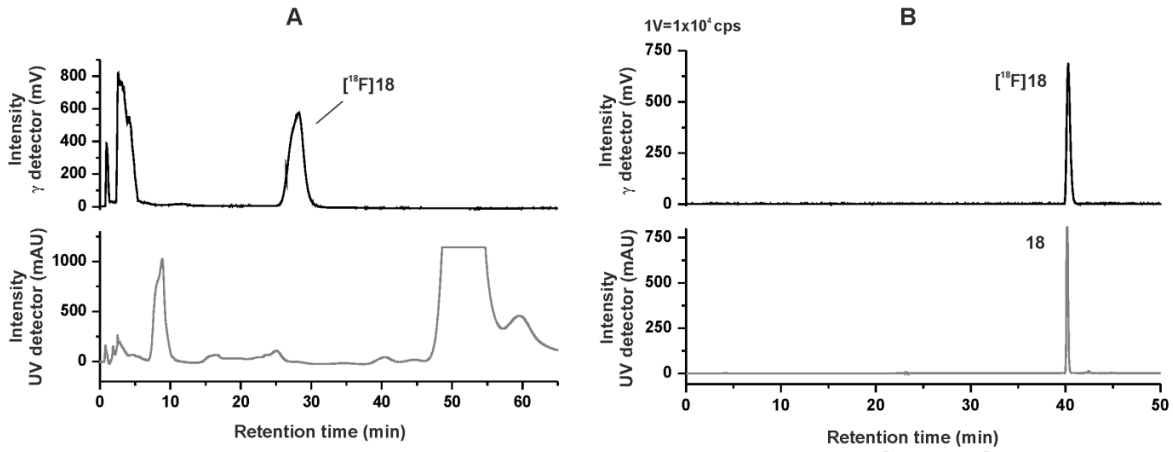

Figure 5. A: Semi-preparative radio- and UV-HPLC chromatograms of [^{18}F]**18** (conditions: Reprosil-Pur C18-AQ, 250 x 10 mm, 62% CH_3CN/20 mM aq NH_4OAc., 4.0 mL/min). **B**: Analytical radio- and UV-HPLC chromatograms of the final product of [^{18}F]**18** spiked with the nonradioactive reference **18** (conditions: Reprosil-Pur C18-AQ, 250 x 4.6 mm, gradient with eluent mixture of CH_3CN/20 mM aq NH_4OAc, 1.0 mL/min).

*Metabolism studies of [^{18}F]**18** in vivo*

Metabolism of [^{18}F]**18** *in vivo* was investigated in plasma and brain samples obtained from CD-1 mice (mice lacking the cluster of differentiation 1 molecules) in two independent experiments at 30 min after injection of the radioligand. At this time point, the activity in plasma and brain accounted for 1.7 and 1.7% ID/g respectively. Sample analysis was performed by micellar chromatography (MLC) and RP-HPLC. MLC allows a direct injection of samples into the HPLC system without eliminating the tissue matrix, whereas samples for RP-HPLC analysis need to be treated with a mixture of methanol/water to precipitate the proteins, resulting in recoveries of about 70% and 60% of activity for plasma and brain samples, respectively.

Data obtained with both methods indicated a fast metabolic degradation of the radiotracer. Radio-MLC and radio-RP-HPLC chromatograms of plasma and brain samples showed only negligible amounts of [^{18}F]**18** and the formation of a main radiometabolite representing more than 85% of total activity (Figure 6). Due to the high amount of activity found in the brain at this time point (1.7% ID/g), it can be excluded that the activity found there is related to contaminations with residual blood. The very fast elution in both chromatography systems indicates a high polarity of the radiometabolite. Moreover, the observed low recovery during the extraction procedure indicates free [^{18}F]fluoride as the main radiometabolite that partially binds

to the precipitated proteins. To verify this assumption, brain homogenate samples were investigated for the first time with hydrophilic interaction chromatography (HILIC). Due to the use of a polar stationary phase and a mobile phase with a high content of organic solvent, the retention of analytes is prolonged with their increasing polarity.[60] Therefore, the elution order in HILIC is more or less the opposite of the elution order in RP-HPLC as illustrated by chromatogram (c) in Figure 6C. Accordingly, [^{18}F]**18** elutes at a very short retention time of about 3 min followed by the much more polar [^{18}F]fluoride at about 14 min. The assumption of defluorination is supported by comparing chromatogram (b) in Figure 6C obtained from a brain sample spiked with [^{18}F]fluoride and chromatogram (a) representing a corresponding non-spiked brain sample. A potential mechanism for radiodefluorination of a fluoroethyl chain bound to an aromatic ring was already proposed by Lee et al.[61-64] involving an α-carbon hydroxylation followed by oxidation and slow α-elimination with the formation of the halide. As fluoride does not pass the blood-brain barrier in a considerable extent, the [^{18}F]fluoride detected in the brain may be due to local metabolism or to degradation during sample preparation. The latter can be excluded, because the stability of the radiotracer has been proven under the conditions used for MLC. Drug metabolism in the brain is a phenomenon that is currently under investigation.[65] In particular, the central expression and function of several cytochrome P450 containing enzymes (CYP) enzymes support this hypothesis. Despite low CYP levels in the brain with approximately 0.5-2% of those in the liver,[65] it is conceivable that a CYP-mediated metabolism influences radiotracer stability because of its negligible injected mass. This is in agreement with Coenen et al.[66] who determined a certain level of [^{18}F]fluoride in mouse brain samples. Thereupon Welch et al.[67] postulated a metabolic process within the brain as a possible explanation.

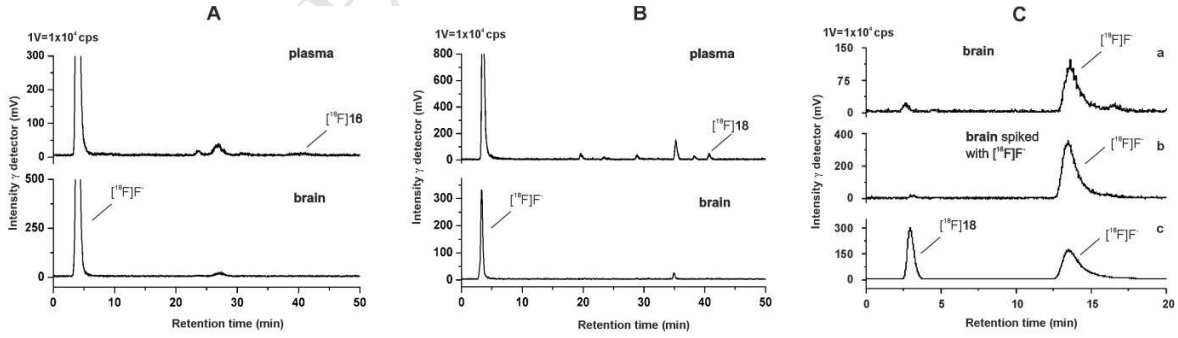

Figure 6. Representative radio chromatograms of a mouse plasma and brain sample of [^{18}F]**18** at 30 min p.i.. **A**: Micellar chromatography (conditions: Reprosil-Pur C18-AQ, 250 x 4.6 mm, gradient: 3-30-3% PrOH/100 mM SDS_{aq}, 10 mM Na_2HPO_{4aq}; flow: 0.75 mL/min). **B**: Reversed

phase chromatography (conditions: Reprosil-Pur C18-AQ, 250 x 4.6 mm, gradient: 10-90-10% MeCN/20 mM NH_4OAc_{aq}; flow 1.0 mL/min). **C**: Hydrophilic interaction chromatography; **a**: radio chromatogram of a mouse brain sample, **b**: radio chromatogram of a mouse brain sample spiked with [^{18}F]fluoride, **c**: chromatogram of a mixture of [^{18}F]**18** and [^{18}F]fluoride (conditions: Nucleodur HILIC, 250 x 4.6 mm, 74% MeCN/20 mM NH_4OAc_{aq}, flow 1.0 mL/min).

Finally, the observed strong radiodefluorination of [^{18}F]**18** was rather unexpected, considering that a 2-fluoroethyl aryl group is thought to be slightly more stable than the corresponding 2-fluoroethoxy aryl analogue (compound **22**, Scheme 1) which is known to be metabolized quite fast *via* CYP-mediated *O*-dealkylation. Recently, we reported on the development of an ^{18}F-labeled radiotracer for imaging the oxytocin receptor,[68] which also contains a fluoroethyl function and did not demonstrate such a fast metabolic degradation. Nevertheless, the metabolic stability of a particular ^{18}F-bearing functional group considerably depends on the entire molecular structure of the compound. As reviewed by Kirchmair and co-workers, the prediction of potential target sites within a compound for metabolic degradation is challenging and needs further research.[69]

These results might support but do not prove the brain-penetrant nature of this class of compounds, however the fast metabolization of [^{18}F]**18** hinders any further investigation of the $P2Y_1R$ *in vivo* with PET. Several methods to increase the metabolic stability of ^{18}F-labeled tracers are described in the literature.[53] One option might be a deuterated fluoroethyl chain to decelerate the defluorination process. Alternatively, the ^{18}F-label could be introduced at an aromatic ring, e.g. at the 2-pyridine position.

CONCLUSIONS

In summary, a novel, small series of fluorinated compounds was synthesized to develop an ^{18}F-PET radiotracer for $P2Y_1R$ imaging in the brain by modifying the structure of the highly affine and selective $P2Y_1R$ ligand **7**. Additionally, the boron-rich derivative **32** was designed by replacing the *p*-(trifluoromethoxy)phenyl subunit with an *ortho*-carborane as potential tool for BNCT for cancer treatment. Preliminary *in vitro* investigations revealed a strong antagonistic effect for the fluorinated compound **18**. Therefore, **18** was selected for ^{18}F-labeling. A manual radiosynthesis procedure was developed to generate [^{18}F]**18** with suitable radiochemical parameters. First *in vivo* experiments performed with CD-1 mice revealed a fast metabolism with

nearly no intact [^{18}F]**18** at 30 minutes post injection in plasma and brain samples. The main radiometabolite was identified by HILIC to be [^{18}F]fluoride. Future efforts will focus on the development of an analogue of [^{18}F]**18** with a deuterated fluoroethyl chain or investigation of alternative labeling positions (e.g. the 2-pyridine position) to obtain metabolically more stable compounds suitable for the *in vivo* mapping of the $P2Y_1R$.

EXPERIMENTAL SECTION

Chemistry

General methods

Unless otherwise noted, moisture-sensitive reactions were conducted under dry nitrogen or argon. All chemicals and reagents were purchased from commercially available sources and used without further purification. Thin layer chromatography (TLC): Silica gel 60 F254 plates (Merck KGaA, Darmstadt, Germany). Flash chromatography (fc): Silica gel 60, 40-64 μm (Merck). Room temperature (rt) was 21 °C. MS: MAT GCQ (Thermo Finnigan MAT GmbH, Bremen, Germany). ^{1}H, ^{13}C and ^{19}F NMR spectra were recorded on VARIAN "MERCURY plus" (300 MHz for ^{1}H NMR, 75 MHz for ^{13}C NMR, 282 MHz for ^{19}F NMR) and VARIAN "MERCURY plus" and BRUKER DRX-400 (400 MHz for ^{1}H NMR, 100 MHz for ^{13}C NMR, 377 MHz for ^{19}F NMR); δ in ppm related to tetramethylsilane; coupling constants (*J*) are given with 0.1 Hz resolution. Multiplicities of NMR signals are indicated as follows: s (singlet), d (doublet), t (triplet), m (multiplet), dd (doublet of doublets), dt (doublet of triplets). ESI/Ion trap mass spectra (LRMS) were recorded with a Bruker Esquire 3000 plus instrument (Billerica, MA, USA). High resolution mass spectra were recorded on a FT-ICR APEX II spectrometer (Bruker Daltonics; Bruker Corporation, Billerica, MA, USA) using electrospray ionization (ESI) in positive ion mode. The purity of all the tested compounds was ≥95% as determined by HPLC [unless otherwise noted: Jasco, MD-2010Plus, LG-2080-04S, DG-2080-54, AS-2055Plus, LC-NetII/ADC, λ = 254 nm, column ReproSil-Pur Basic C18-HD (250 x 4.6 mm, 5 μm, Dr. Maisch GmbH), gradient MeCN/20mM NH_4OAc_{aq} from 10/90 to 90/10, (v/v) over 35 min, flowrate 1 mL/Min].

Procedures and compound characterization

General procedure A: 2-Halo-3-nitropyridine (1 eq, 7.3 mmol) in DMF (6 mL) was treated with 2-isopropylphenol (1 eq, 7.3 mmol) and Cs_2CO_3 (1.5 eq, 10.9 mmol) and heated at 70 °C

for 14 h. Afterwards, the reaction mixture was cooled to room temperature, and DMF was evaporated. The residue was dissolved in ethyl acetate (EA, 20 mL) and washed with 5% LiCl aq sol. (3 × 7 mL) and brine (3 × 7 mL). Drying ($MgSO_4$) and removal of solvent afforded a brown solid which was recrystallized from ethanol to afford the corresponding ether as yellow needles.

General procedure B: A solution of nitro compound (1 eq, 7.4 mmol) in MeOH/THF (1:4, 16 mL) was reduced under H_2 atmosphere (1 atm) in the presence of Pd/C (10 mol%) overnight at room temperature. The reaction mixture was filtered over Celite and concentrated to afford a white solid which was recrystallized from EA to afford the corresponding amine as a white powder.

General procedure C: A solution of dichloromethane (DCM, 10 mL) containing Et_3N (3 eq, 13 mmol) was added dropwise to a solution of the amine (1 eq, 4.4 mmol) and diphosgene (0.8 eq, 3.5 mmol) in DCM (20 mL) at 0 °C. After the addition was completed, the resulting mixture was stirred at 0 °C for 45 min and additional 2 hours at room temperature. The organic phase was then washed with 0.5 M HCl (3 × 20 mL), 1 N NaOH (2 × 10 mL), and brine. Drying ($MgSO_4$) and removal of solvent afforded the corresponding isocyanate as a yellow solid. This material was used for the subsequent reaction without further purification

General procedure D: The substituted aniline (1 eq, 0.2 mmol) was added to a solution of isocyanate (1 eq, 0.2 mmol) in toluene (1 mL) under argon. The resulting mixture was stirred at 80 °C for 1.5 h. The solvent was removed by rotary evaporation, and the crude product was purified by flash chromatography to give the diaryl urea as colorless solid.

General procedure E: To a solution of the corresponding alcohol (1 eq, 0.25 mmol) in 4 mL DCM, 4-toluenesulfonyl chloride (60 mg, 1.2 eq, 0.30 mmol) and pyridine (1 mL) were added and the reaction mixture was stirred overnight at room temperature. The reaction was quenched by addition of 20 mL 1 M HCl solution. The aqueous solution was extracted with DCM (2 x 20 mL) and the combined organic phases were washed with $NaHCO_3$ (20 mL), brine (10 mL) and dried over $MgSO_4$. Evaporation of the solvent under reduced pressure afforded the corresponding tosylate as colorless solid.

General procedure F: A solution of tosylate (1 eq, 0.09 mmol) in THF (2 mL) was treated with a 1M TBAF solution in THF (180 µL, 2 eq, 0.18 mmol) and stirred overnight at room temperature. Saturated aqueous $NaHCO_3$ (5 mL) was added and the mixture was washed with EA (3 x 5 mL). The combined organic phases were dried ($MgSO_4$) and concentrated by rotary

evaporation. The remaining residue was purified by column chromatography (silica) to give the fluorinated derivative as colorless solid.

General procedure G: A mixture of amine (e.g. **12a**, 1 eq, 2.06 mmol) and benzoyl isothiocyanate (1.1 eq, 2.27 mmol) was refluxed in 10 mL DCM for 2 h. Elimination of the solvent under reduced pressure afforded a thick yellowish oil which was redissolved in a 2M LiOH/MeOH (3:1, 15 mL) and kept at 50 °C for 2 h. H_2O (20 mL) and EA (20 mL) were added with stirring, and the phases were separated in a separatory funnel. The organic phase was washed with aqueous saturated $NaHCO_3$ and NaCl solutions, dried over $MgSO_4$ and concentrated under reduced pressure to give the corresponding thiourea (e.g. 1-(2-[2-(*tert*-butyl)phenoxy]pyridin-3-yl)thiourea (**56**)) as tan solid, which was used without purification in the next step.

To a solution of the thiourea (1 eq, 1.65 mmol) obtained above and 3-bromo-1,1,1-trifluoropropan-2-one (1.3 eq, 21.5 mmol) in EtOH (15 mL), 2,6-lutidine (2 eq, 3.3 mmol) was added and the mixture was refluxed under argon for 24 h. The solvent was evaporated, 20 mL 2M HCl was added and the mixture was washed with EA (2 x 15 mL). The combined organic phases were washed 1 x 15 mL $NaHCO_3$ and 1 x 10 mL NaCl aqueous saturated solutions, dried over $MgSO_4$ and concentrated under reduced pressure to give a yellow solid which was further washed with 3 x 10 mL *n*-hexane. Upon solvent evaporation under reduced pressure, 2-aminothiazole (e.g. **26**, 82% over 3 steps) was obtained as a light grey solid.

General procedure H: To a solution of 2-aminothiazole (e.g. **26**, 1 eq, 0.52 mmol) in 10 mL AcOH/THF (1:5) at 0 °C, NBS (1.1 eq, 0.58 mmol) was added and the reaction was stirred for 2 h at 0 °C. EA (15 mL) was added and the organic solution was washed with 15 mL H_2O, concentrated aqueous $NaHCO_3$ and NaCl solutions dried over $MgSO_4$ and concentrated under reduced pressure. The resulting solid was purified by column chromatography (silica, EA/IH, 1:18) to give 5-bromo-2-amino-thiazole (e.g. **27**, 198 mg, 82%) as colorless solid.

General procedure I: Under argon, 5-bromo-2-amino-thiazole (e.g. **27**, 1 eq, 0.11 mmol), boronic acid (1.5 eq, 0.17 mmol), $[Pd(PPh_3)_4]$ (0.1 eq, 0.01 mmol) and Na_2CO_3 (3 eq, 0.33 mmol) were added to 5 mL toluene/EtOH (2:1) at rt and the mixture was refluxed (95 °C) overnight. The solvent was eliminated by rotary evaporation, and the resulting residue was purified by column chromatography on silica. Target compounds were obtained as colorless solids.

2-[2-(*tert*-Butyl)phenoxy]pyridin-3-amine (**12a**): colorless solid, 55% yield over 2 steps; TLC (silica gel, EA/IH, 2:8): R_f = 0.55.

^{1}H NMR (400 MHz, $CDCl_3$): δ = 7.59 (dd, *J* = 4.9, 1.7 Hz, 1H), 7.44 (dd, *J* = 7.8, 1.8 Hz, 1H), 7.25 – 7.16 (td, J = 7.6, 1.5 Hz, 1H), 7.11 (td, *J* = 7.6, 1.5 Hz, 1H), 7.04 (dd, *J* = 7.6, 1.6 Hz, 1H), 6.93 (dd, *J* = 7.9, 1.5 Hz, 1H), 6.83 (dd, *J* = 7.6, 4.9 Hz, 1H), 3.95 (s, 2H), 1.42 (s, 9H).

^{13}C NMR (100 MHz, $CDCl_3$): δ = 152.9, 152.0, 141.1, 136.2, 132.2, 127.4, 127.0, 124.3, 122.6, 122.0, 119.2, 30.5.

1-{2-[2-(*tert*-Butyl)phenoxy]pyridin-3-yl}-3-[4-(trifluoromethoxy)phenyl]urea (**7**): General procedure D (colorless solid, 95% yield)

HPLC: t_R = 26.1 min, >99 %.

M. p. = 152 °C.

TLC (silica gel, EA/IH, 3:7): R_f = 0.50.

^{1}H NMR (400 MHz, $CDCl_3$): δ = 8.53 (dd, *J* = 8.0, 1.7 Hz, 1H), 7.79 (dd, *J* = 4.9, 1.7 Hz, 1H), 7.49 (s, 1H), 7.46 – 7.37 (m, 1H), 7.32 (s, 1H), 7.30 – 7.22 (m, 2H), 7.22 – 7.05 (m, 4H), 6.94 (dd, *J* = 7.9, 4.9 Hz, 1H), 6.87 – 6.76 (m, 1H), 1.29 (s, 9H).

^{13}C NMR (100 MHz, $CDCl_3$): δ = 153.0, 152.9, 152.3, 145.8, 141.5, 140.6, 136.2, 127.8, 127.7, 127.3, 125.2, 124.2, 123.1, 122.7, 122.2, 122.1, 119.1, 34.75, 30.63.

^{19}F NMR (282 MHz, $CDCl_3$): δ = –58.56.

HRFT-MS (ESI+): *m*/*z* = 446.1686 (calcd. 446.1686 for $C_{23}H_{23}F_3N_3O_3$ $[M+H]^+$).

1-{2-[2-(*tert*-Butyl)phenoxy]pyridin-3-yl}-3-[4-(2-hydroxyethyl)phenyl]urea (**14**): General procedure D (colorless solid, 72% yield)

M. p. = 192 °C.

TLC (silica gel, EA/IH, 1:1): R_f = 0.38.

^{1}H NMR (400 MHz, $CDCl_3$): δ = 8.54 (dd, *J* = 8.0, 1.7 Hz, 1H), 7.66 (dd, *J* = 4.9, 1.7 Hz, 1H), 7.39 (dd, *J* = 7.6, 1.9 Hz, 1H), 7.34 – 7.22 (m, 2H), 7.15 – 7.07 (m, 4H), 6.92 (dd, *J* = 8.0, 4.9 Hz, 1H), 6.78 (dd, *J* = 7.7, 1.7 Hz, 1H), 3.71 (t, *J* = 6.7 Hz, 2H), 2.73 (t, *J* = 6.7 Hz, 2H), 1.30 (s, 9H).

^{13}C NMR (100 MHz, $CDCl_3$): δ = 153.7, 153.6, 152.7, 141.6, 139.4, 136.8, 136.7, 133.9, 129.6, 127.5, 127.3, 127.2, 125.1, 124.9, 123.0, 120.3, 119.0, 63.3, 38.4, 34.6, 30.5.

HRFT-MS (ESI+): *m*/*z* = 406.2125 (calcd. 406.2125 for $C_{24}H_{28}N_3O_3$ $[M+H]^+$).

4-{3-{2-[2-(*tert*-Butyl)phenoxy]pyridin-3-yl}ureido}phenethyl 4-methylbenzenesulfonate (**16**) General Procedure E (colorless solid, quantitative)

M. p. = 190 °C.

TLC (silica gel, EA/IH, 1:1): R_f = 0.80.

^{1}H NMR (400 MHz, $CDCl_3$): δ = 8.58 (dd, *J* = 8.0, 1.7 Hz, 1H), 7.78 (dd, *J* = 4.9, 1.7 Hz, 1H), 7.67 (d, *J* = 8.3 Hz, 2H), 7.41 (dd, *J* = 7.7, 1.9 Hz, 1H), 7.39 (s, 1H) 7.28 (s, 1H), 7.21 (d, *J* = 8.3 Hz, 2H) 7.20 – 7.10 (m, 2H), 7.03 (d, *J* = 8.4 Hz, 2H), 6.96 (dd, *J* = 8.0, 4.9 Hz, 1H), 6.91 (s, 1H), 6.82 (dd, *J* = 7.8, 1.6 Hz, 1H), 4.15 (t, *J* = 7.0 Hz, 2H), 2.88 (t, *J* = 7.0 Hz, 2H), 2.43 (s, 3H), 1.28 (s, 9H).

^{13}C NMR (100 MHz, $CDCl_3$): δ = 153.0, 152.7, 152.4, 144.9, 141.5, 140.3, 136.4, 133.0, 132.9, 130.0, 129.9, 127.9, 127.6, 127.4, 127.2, 125.1, 124.5, 123.2, 122.2, 119.1, 77.5, 77.1, 76.8, 70.5, 34.8, 34.7, 30.6, 21.7.

FT-MS (ESI+): *m*/*z* = 560.3 (calcd. 560.2 for $C_{31}H_{34}N_3O_5S$ $[M+H]^+$).

1-{2-[2-(*tert*-Butyl)phenoxy]pyridin-3-yl}-3-[4-(2-fluoroethyl)phenyl]urea (**18**) General Procedure F (colorless solid, 62% yield).

HPLC: t_R = 40.2 min, purity >99 % (Reprosil-Pur C18-AQ, 250 x 4.6 mm, gradient: 10-90-10% MeCN/20 mM NH_4OAc_{aq}; flow 1.0 mL/min, 60 min).

M. p. = 135 °C.

TLC (silica gel, EA/IH, 2:8): R_f = 0.35.

^{1}H NMR (400 MHz, $CDCl_3$): δ = 8.61 (dd, *J* = 7.9, 1.7 Hz, 1H), 7.79 (dd, *J* = 4.9, 1.7 Hz, 1H), 7.42 (dd, *J* = 7.7, 1.9 Hz, 1H), 7.36 – 7.26 (m, 3H), 7.24 – 7.09 (m, 4H), 6.99 (dd, *J* = 8.0, 4.9 Hz, 1H), 6.84 (dd, *J* = 7.8, 1.6 Hz, 1H), 6.59 (s, 1H), 4.58 (dt, *J* = 47.0, 6.5 Hz, 2H), 2.96 (dt, *J* = 23.7, 6.4 Hz, 2H), 1.28 (s, 9H).

^{13}C NMR (100 MHz, $CDCl_3$): δ = 153.1, 152.6, 152.5, 140.4, 135.9, 134.6, 130.4, 127.7, 127.5, 127.3, 125.1, 124.6, 123.2, 119.2, 85.1, 82.9, 36.6, 36.4, 30.7

^{19}F NMR (282 MHz, $CDCl_3$): δ = –216.10.

HRFT-MS (ESI+): *m*/*z* = 408.2082 (calcd. 408.2082 for $C_{24}H_{27}FN_3O_2$ $[M+H]^+$).

1-{2-[2-(*tert*-Butyl)phenoxy]pyridin-3-yl}-3-(4-methoxyphenyl)urea (**20**) General procedure D (colorless solid, 95%).

TLC (silica gel, EA/IH, 2:8): R_f = 0.32.

^{1}H NMR (400 MHz, $CDCl_3$): δ = 8.63 (dd, *J* = 8.0, 1.7 Hz, 1H), 7.77 (dd, *J* = 4.9, 1.7 Hz, 1H), 7.40 (dd, *J* = 7.7, 1.9 Hz, 1H), 7.25 – 7.07 (m, 4H), 6.97 (dd, *J* = 8.0, 4.9 Hz, 1H), 6.90 – 6.76 (m, 3H), 6.46 (s, 1H), 3.76 (s, 3H), 1.22 (s, 9H).

1-{2-[2-(*tert*-Butyl)phenoxy]pyridin-3-yl}-3-(4-hydroxyphenyl)urea (**21**) A solution of $AlCl_3$ (1.0 g, 6 eq, 7.7 mmol) in EtSH (30 mL) was added slowly to a solution of **20** (0.5 g, 1 eq, 1.3 mmol) in DCM (20 mL) at 0 °C under argon. The reaction was stirred for 2 hours at room temperature, quenched by addition of saturated aqueous $NaHCO_3$ solution (30 mL) and extracted with DCM (3 x 20 mL). The combined DCM solutions were washed once with saturated aqueous NaCl solution, dried over $MgSO_4$ and the solvent was evaporated to give **21** as gray solid (0.4 g, 1.1 mmol, 85%).

M. p. = 213 °C.

TLC (silica gel, EA/IH, 2:8): R_f = 0.10.

^{1}H NMR (400 MHz, $CDCl_3$): δ = 8.55 (dd, *J* = 8.0, 1.7 Hz, 1H), 7.66 (dd, *J* = 4.9, 1.7 Hz, 1H), 7.47 – 7.37 (m, 2H), 7.26 – 7.07 (m, 4H), 6.97 (dd, *J* = 8.0, 4.9 Hz, 1H), 6.80 (dd, *J* = 7.8, 1.5 Hz, 1H), 6.78 – 6.70 (m, 2H), 1.32 (s, 9H).

^{13}C NMR (100 MHz, $CDCl_3$): δ = 154.5, 153.0, 152.9, 141.7, 139.2, 127.6, 127.5, 127.2, 125.5, 125.0, 123.1, 119.1, 115.9, 34.7, 30.5.

HRFT-MS (ESI+): *m*/*z* = 378.1812 (calcd. 378.1812 for $C_{22}H_{24}N_3O_3$ $[M+H]^+$).

1-{2-[2-(*tert*-Butyl)phenoxy]pyridin-3-yl}-3-[4-(2,2,2-trifluoroethoxy)phenyl]urea (**23**): CF_3CH_2OTs (134 mg, 4 eq, 0.52 mmol) was reacted with **17** (50 mg, 1 eq, 0.13 mmol) in the presence of K_2CO_3 (55 mg, 3 eq, 0.40 mmol) in MeCN (5 mL) at 82 °C under argon for 16 hours. Saturated aqueous $NaHCO_3$ solution (10 mL) was added and the mixture was washed with EA (3 x 10 mL). The combined EA fractions were washed with H_2O (1 x 10 mL), saturated aqueous $NaHCO_3$ (1 x 10) mL and dried over $MgSO_4$. The solvent was removed by rotary evaporation and the remaining residue was purified by flash chromatography (silica, EA/IH 1:9) to give **23** (29 mg, 0.06 mmol, 48%) as colorless solid.

HPLC: t_R = 24.4 min, >99 %.

M. p. = 165 °C.

TLC (silica gel, EA/IH, 2:8) R_f = 0.55.

^{1}H NMR (400 MHz, $CDCl_3$): δ = 8.60 (d, *J* = 7.5 Hz, 1H), 7.79 (s, 1H), 7.41 (d, *J* = 7.4 Hz, 1H), 7.37 – 7.07 (m, 5H), 7.06 – 6.54 (m, 4H), 4.29 (q, *J* = 8.1 Hz, 2H), 1.26 (s, 9H).

^{13}C NMR (100 MHz, $CDCl_3$): δ = 155.4, 152.6, 152.4, 141.4, 140.3, 131.5, 127.6, 127.4, 127.3, 125.5, 125.0, 124.6, 124.6 (m, 1C), 123.1, 119.2, 116.2, 66.3 (d, *J* = 44.8 Hz, 1C), 34.7, 30.6.

^{19}F NMR (282 MHz, $CDCl_3$): δ = –74.39.

HRFT-MS (ESI+): *m*/*z* = 482.1662 (calcd. 482.1662 for $C_{24}H_{25}F_3N_3O_3$ $[M+H]^+$).

1-{2-[2-(*tert*-Butyl)phenoxy]pyridin-3-yl}-3-[4-(2-fluoroethoxy)phenyl]urea (**22**) was obtained by the same procedure as compound **23** with $Br(CH_2)_2F$ as alkylating reagent. (colorless solid, 82% yield).

HPLC: t_R = 23.3 min, >99 %.

M. p. = 179 °C.

TLC (silica gel, EA/IH, 2:8): R_f = 0.13.

^{1}H NMR (400 MHz, $CDCl_3$): δ = 8.60 (dd, *J* = 8.0, 1.7 Hz, 1H), 7.76 (dd, *J* = 4.9, 1.7 Hz, 1H), 7.41 (d, *J* = 1.6 Hz, 1H), 7.40 (dd, *J* = 7.7, 1.8 Hz, 1H), 7.21 (d, *J* = 8.9 Hz, 2H), 7.14 (tdd, *J* = 8.9, 6.2, 2.4 Hz, 2H), 6.95 (dd, *J* = 7.9, 4.9 Hz, 2H), 6.83 (d, *J* = 8.8 Hz, 2H), 6.85 – 6.79 (m, 1H), 4.84 – 4.57 (m, 2H), 4.24 – 4.03 (m, 2H), 1.25 (s, 9H).

^{13}C NMR (100 MHz, $CDCl_3$): δ = 156.5, 153.9, 152.6, 152.5, 141.4, 140.1, 130.4, 127.7, 127.3, 127.1, 125.6, 124.9, 124.7, 123.1, 119.1, 115.7, 83.1, 80.8, 81.9 (d, *J* = 171.0 Hz, 1C), 67.5 (d, *J* = 20.5 Hz, 1C). 34.6, 30.6.

^{19}F NMR (282 MHz, $CDCl_3$): δ = –224.30.

HRFT-MS (ESI+): *m*/*z* = 424.2031 (calcd. 424.2031 for $C_{24}H_{27}FN_3O_3$ $[M+H]^+$).

1-[4-(2-Hydroxyethyl)phenyl]-3-[2-(2-isopropylphenoxy)pyridin-3-yl]urea (**15**): To a solution of isocyanate (**13b**) (50 mg, 1 eq, 0.2 mmol) in toluene (1 mL) under argon, 2-(4-aminophenyl)ethanol (27.4 mg, 1 eq, 0.2 mmol) was added. The resulting mixture was stirred at 80 °C for 1.5 h. The solvent was removed by rotary evaporation, and the crude product was purified by column chromatography (silica, EA/IH, 3:17) to give **15** (53 mg, 0.13 mmol, 67%) as colorless solid.

TLC (silica gel, EA/IH, 1:1): R_f = 0.38.

^{1}H NMR (400 MHz, $CDCl_3$): δ = 8.54 (dd, *J* = 7.9, 1.6 Hz, 1H), 7.75 (s, 1H), 7.68 (dd, *J* = 4.9, 1.7 Hz, 1H), 7.57 (s, 1H), 7.38 – 7.29 (m, 1H), 7.24 – 7.11 (m, 4H), 7.06 (s, 2H), 6.97 – 6.82 (m, 2H), 3.75 (t, *J* = 6.3 Hz, 2H), 3.21 – 2.87 (m, 1H), 2.73 (t, *J* = 6.3 Hz, 1H), 1.11 (d, *J* = 6.9 Hz, 6H).

^{13}C NMR (100 MHz, $CDCl_3$): δ = 153.5, 152.8, 150.6, 140.8, 139.6, 136.2, 134.7, 129.8, 126.9, 126.9, 125.9, 124.0, 122.2, 121.5, 118.9, 63.5, 38.5, 27.2, 23.1.

HRFT-MS (ESI+): *m*/*z* = 392.1969 (calcd. 392.1969 for $C_{23}H_{26}N_3O_3$ $[M+H]^+$).

4-{3-[2-(2-Isopropylphenoxy)pyridin-3-yl]ureido}phenethyl 4-methylbenzenesulfonate (**17**) was obtained according to general procedure E (95% yield, colorless solid).

M. p. = 128 °C.

TLC (silica gel, EA/IH, 2:8): R_f = 0.12.

^{1}H NMR (400 MHz, $CDCl_3$): δ = 8.56 (dd, *J* = 7.9, 1.7 Hz, 1H), 7.68 (m, 4H), 7.53 (s, 1H), 7.33 (dd, *J* = 7.2, 2.2 Hz, 1H), 7.30 – 7.23 (m, 4H), 7.23 – 7.13 (m, 2H), 7.01 (d, *J* = 8.4 Hz, 2H), 6.92 (dt, *J* = 6.9, 3.6 Hz, 2H), 4.21 – 4.07 (t, *J* = 6.9 Hz, 2H), 3.11 – 2.95 (m, 1H), 2.86 (t, *J* = 6.9 Hz, 2H), 2.42 (s, 3H), 1.10 (d, *J* = 6.9 Hz, 6H).

^{13}C NMR (100 MHz, $CDCl_3$): δ = 152.9, 150.6, 144.9, 141.0, 139.6, 137.1, 132.9, 131.8, 129.9, 129.7, 127.9, 127.1, 127.0, 126.7, 125.8, 124.0, 122.3, 120.8, 118.9, 70.7, 34.8, 27.2, 23.1, 21.7.

HRFT-MS (ESI+): *m*/*z* = 546.2056 (calcd. 387.9231 for $C_{30}H_{32}N_3O_5S$ $[M+H]^+$).

1-[4-(2-Fluoroethyl)phenyl]-3-[2-(2-isopropylphenoxy)pyridin-3-yl]urea (**19**) was obtained according to general procedure F as colorless solid, 82% yield.

HPLC: t_R = 23.8 min, >99 %.

M. p. = 124 °C.

TLC (silica gel, EA/IH, 2:8): R_f = 0.12.

^{1}H NMR (400 MHz, $CDCl_3$): δ = 8.58 (dd, *J* = 7.9, 1.7 Hz, 1H), 7.73 (dd, *J* = 4.9, 1.7 Hz, 1H), 7.41 (s, 1H), 7.39 – 7.29 (m, 3H), 7.21 (m, 3H), 7.02 – 6.90 (m, 2H), 6.83 (s, 1H), 4.58 (dt, *J* = 47.0, 6.5 Hz, 2H), 3.08 – 2.97 (m, 1H), 3.02 –2.91 (dt, *J* = 15.4, 4.9 Hz, 2H), 1.14 (d, *J* = 6.9 Hz, 2H).

^{13}C NMR (100 MHz, $CDCl_3$): δ = 152.9, 152.7, 150.5, 140.8, 139.9, 136.3, 130.1, 127.1, 127.0, 126.9, 125.9, 123.9, 122.3, 122.1, 119.0, 84.9, 83.2, 36.4 (d, *J* = 20.3 Hz), 27.3, 23.1, 20.7.

^{19}F NMR (282 MHz, $CDCl_3$): δ = –216.00 (sep).

HRFT-MS (ESI+): *m*/*z* = 394.1925 (calcd. 394.1925 for $C_{23}H_{25}FN_3O_2$ $[M+H]^+$).

1-{2-[2-(*tert*-Butyl)phenoxy]pyridin-3-yl}-3-[2-fluoro-4-(trifluoromethoxy)phenyl]urea (**24**) was obtained according to general procedure D as colorless solid, quantitative yield.

HPLC: t_R = 27.2 min, >99 %.

M. p. = 68 °C.

TLC (silica gel, EA/IH, 2:8): R_f = 0.50.

^{1}H NMR (400 MHz, $CDCl_3$): δ = 8.52 (dd, *J* = 7.9, 1.7 Hz, 1H), 8.05 (d, *J* = 8.8 Hz, 1H), 7.82 (dd, *J* = 4.9, 1.7 Hz, 1H), 7.49 (s, 1H), 7.47 – 7.40 (m, 1H), 7.25 – 7.10 (m, 3H), 7.08 – 6.93 (m, 3H), 6.84 (dd, *J* = 7.7, 1.7 Hz, 1H), 1.34 (s, 9H).

^{13}C NMR (100 MHz, $CDCl_3$): δ = 152.9, 152.4, 152.2, 141.5, 140.8, 127.8, 127.3, 125.5, 125.3, 124.1, 123.2, 122.9, 119.15, 117.5, 117.4, 109.4, 109.1, 34.8, 30.7.

^{19}F NMR (282 MHz, $CDCl_3$): δ = –58.76 (3F), –126.41 (1F).

HRFT-MS (ESI+): *m*/*z* = 464.1592 (calcd. 464.1592 for $C_{23}H_{22}F_4N_3O_3$ $[M+H]^+$).

1-[2-Fluoro-4-(trifluoromethoxy)phenyl]-3-[2-(2-isopropylphenoxy)pyridin-3-yl]urea (**25**) was obtained according to general procedure D (colorless solid, quantitative).

HPLC: t_R = 26.5 min, >99 %.

M. p. = 67 °C.

TLC (silica gel, EA/IH, 1:9): R_f = 0.18.

^{1}H NMR (400 MHz, $CDCl_3$): δ = 8.51 (dd, *J* = 7.9, 1.7 Hz, 1H), 8.11 (t, *J* = 9.0 Hz, 1H), 7.75 (dd, *J* = 4.9, 1.7 Hz, 1H), 7.62 (s, 1H), 7.36 – 7.31 (m, 3H), 7.24 – 7.13 (m, 2H), 7.06 – 6.85 (m, 4H), 3.15 – 2.93 (m, 1H), 1.14 (d, *J* = 6.9 Hz, 2H).

^{13}C NMR (100 MHz, $CDCl_3$): δ = 153.7, 152.9, 152.2, 151.3, 150.4, 140.9, 140.2, 127.3, 127.1, 127.0, 126.1, 125.5 (d, *J* = 10.4 Hz), 123.5, 122.4, 122.1, 118.9, 117.4, 109.2, 109.0, 27.2, 23.1.

^{19}F NMR (282 MHz, $CDCl_3$): δ = –58.78 (s), –126.88 (s).

HRFT-MS (ESI+): *m*/*z* = 450.1435 (calcd. 450.1435 for $C_{22}H_{20}F_4N_3O_3$ $[M+H]^+$).

1-[1,2-dicarba-*closo*-dodecaboran(12)yl]-3[2-(2-isopropylphenoxy)pyridin-3-yl]urea (**32**) was obtained according to general procedure D within 24 hours (colorless solid, quantitative).

HPLC: t_R = 28.7 min, >97 %.

TLC (silica gel, EA/IH, 1:9): R_f = 0.22.

^{1}H NMR (400 MHz, $CDCl_3$): δ = 8.38 (dd, *J* = 7.9, 1.7 Hz, 1H), 7.84 (dd, *J* = 4.9, 1.7 Hz, 1H), 7.47 (m, 1H), 7.32 (s, 1H), 7.24 – 7.18 (m, 2H), 6.99 (dd, *J* = 7.9, 1.7 Hz, 1H), 6.84 (dd, *J* = 4.9, 1.7 Hz, 1H), 6.65 (s, 1H, N*H*), 4.27 (s, 1H, $C_{cluster}H$), 3.5 – 1.25 (m, 10H, $B_{10}H_{10}$), 1.36 (s, 9H).

^{13}C NMR (100 MHz, $CDCl_3$): δ = 153.0, 152.3, 151.6, 141.5, 141.3, 127.9, 127.8, 127.4, 125.4, 123.2, 119.0, 77.0, 61.4, 34.7, 30.7.

HRFT-MS (ESI+): *m*/*z* = 428.3344 (calcd. 428.3336 for $C_{18}H_{30}B_{10}N_3O_2$ $[M+H]^+$).

***N*-{2-[2-(*tert*-Butyl)phenoxy]pyridin-3-yl}-4-(trifluoromethyl)thiazol-2-amine** (**20**):

A mixture of **12** (500 mg, 1 eq, 2.06 mmol) and benzoyl isothiocyanate (306 µL, 1.1 eq, 2.27 mmol) was refluxed in 10 mL DCM for 2 h. Elimination of the solvent under reduced pressure afforded a thick yellowish oil which was redissolved in a 2M LiOH/MeOH (3:1, 15 mL) and kept at 50 °C for 2 h. H_2O (20 mL) and EA (20 mL) were added with stirring, and the phases were separated in a separatory funnel. The organic phase was washed with aqueous saturated $NaHCO_3$ and NaCl solutions, dried over $MgSO_4$ and concentrated under reduced pressure to give the corresponding thiourea as tan solid, which was used without purification in the next step. 3-Bromo-1,1,1-trifluoropropan-2-one (221 µL, 1.3 eq, 21.5 mmol) and 2,6-lutidine (287 µL, 2 eq, 3.3 mmol) were added to the thiourea intermediate (500 mg, 1 eq, 1.65 mmol) obtained above in EtOH (15 mL) and the mixture was refluxed under argon for 24 h. The solvent was evaporated, 20 mL 2M HCl was added and the mixture was washed with EA (2 x 15 mL). The combined organic phases were washed with 1 x 15 mL $NaHCO_3$ and 1 x 10 mL NaCl aqueous saturated solutions, dried over $MgSO_4$ and concentrated under reduced pressure to give a yellow solid which was further washed with 3 x 10 mL *n*-hexane. Upon solvent evaporation under reduced pressure, **20** (650 mg, 82% over 3 steps) was obtained as a light grey solid.

M. p. = 65 °C.

TLC (silica gel, EA/IH, 1:9): R_f = 0.55.

^{1}H NMR (400 MHz, $CDCl_3$): δ= 8.60 (dd, *J* = 7.9, 1.6 Hz, 1H), 7.83 (dd, *J* = 4.9, 1.7 Hz, 2H), 7.48 (dd, *J* = 7.7, 1.9 Hz, 1H), 7.33 – 7.14 (m, 3H), 7.07 (dd, *J* = 7.9, 4.9 Hz, 1H), 6.94 (dd, *J* = 7.8, 1.6 Hz, 1H), 1.40 (s, 9H).

^{13}C NMR (100 MHz, $CDCl_3$): δ = 164.2, 152.2, 152.1, 141.6, 140.1, 127.7, 127.3, 125.5, 125.3, 125.0, 123.3, 119.1, 110.9 (dd, *J* = 7.9, 3.9 Hz), 34.8, 30.8.

^{19}F NMR (282 MHz, $CDCl_3$): δ= –65.51.

***N*-{2-[2-(*tert*-Butyl)phenoxy]pyridin-3-yl}-5-(6-fluoropyridin-3-yl)-4-(trifluoromethyl)thiazol-2-amine** (**21**): To a solution of **20** (200 mg, 1 eq, 0.52 mmol) in 10 mL AcOH/THF (1:5) at 0 °C, NBS (103 mg, 1.1 eq, 0.58 mmol) was added and the reaction was stirred for 2 h at 0 °C. EA (15 mL) was added and the organic solution was washed with 15 mL

H_2O, concentrated aqueous $NaHCO_3$ and NaCl solutions, dried over $MgSO_4$ and concentrated under reduced pressure. The resulting solid was purified by flash chromatography (silica, EA/IH, 1:18) to give the corresponding 5-bromo-2-aminothiazole intermediate (198 mg, 82%) as colorless solid. Under argon, the so obtained 5-bromo-2-aminothiazole intermediate (50 mg, 1 eq, 0.11 mmol), 2-fluoropyridin-5-boronic acid (23 mg, 1.5 eq, 0.17 mmol), $[Pd(PPh_3)_4]$ (13 mg, 0.1 eq, 0.01 mmol) and Na_2CO_3 (34 mg, 3 eq, 0.33 mmol) were added to 5 mL toluene/EtOH (2:1) at rt and the mixture was refluxed (95 °C) overnight. The solvent was eliminated by rotary evaporation and the resulting residue was purified by flash chromatography (EA/IH, 1:39). Compound **21** (38 mg, 0.8 mmol, 78%) was obtained as colorless solid.

M. p. = 197 °C.

TLC (silica gel, EA/IH, 1:9): R_f = 0.24.

^{1}H NMR (400 MHz, $CDCl_3$): δ = 8.56 (dd, *J* = 7.9, 1.6 Hz, 1H), 8.32 (d, *J* = 2.3 Hz, 1H), 7.91 – 7.84 (m, 3H), 7.48 (dd, *J* = 7.7, 1.8 Hz, 1H), 7.31 – 7.15 (m, 2H), 7.08 (dd, *J* = 7.9, 5.0 Hz, 1H), 7.03 (dd, *J* = 8.4, 3.0 Hz, 1H), 6.94 (dd, *J* = 7.8, 1.4 Hz, 1H), 1.39 (s, 9H).

^{13}C NMR (100 MHz, $CDCl_3$): δ = 165.1, 162.7, 162.3, 152.3, 152.1, 148.5, 148.3, 142.6 (d, *J* = 1.4 Hz), 142.5 (d, *J* = 1.4 Hz), 141.6, 140.5, 127.8, 127.3, 125.4, 125.2, 125.1, 123.3 (d, *J* = 5.9 Hz), 119.1, 109.8, 109.6, 34.8, 30.8.

^{19}F NMR (282 MHz, $CDCl_3$): δ = –60.40 (3F), –66.73 (1F).

HRFT-MS (ESI+): *m*/*z* = 489.1367 (calcd. 489.1367 for $C_{24}H_{21}F_4N_4OS$ $[M+H]^+$).

***N*-{2-[2-(*tert*-Butyl)phenoxy]pyridin-3-yl}-4-(trifluoromethyl)thiazol-2-amine** (**26**) was obtained according to general procedure G in 82% yield over two steps.

M. p. = 65 °C.

TLC (silica gel, EA/IH, 1:9): R_f = 0.55.

^{1}H NMR (400 MHz, $CDCl_3$): δ = 8.60 (dd, *J* = 7.9, 1.6 Hz, 1H), 7.83 (dd, *J* = 4.9, 1.7 Hz, 2H), 7.48 (dd, *J* = 7.7, 1.9 Hz, 1H), 7.33 – 7.14 (m, 3H), 7.07 (dd, *J* = 7.9, 4.9 Hz, 1H), 6.94 (dd, *J* = 7.8, 1.6 Hz, 1H), 1.40 (s, 9H).

^{13}C NMR (100 MHz, $CDCl_3$): δ = 164.2, 152.2, 152.1, 141.6, 140.1, 127.7, 127.3, 125.5, 125.3, 125.0, 123.3, 119.1, 110.9 (dd, *J* = 7.9, 3.9 Hz), 34.8, 30.8.

^{19}F NMR (282 MHz, $CDCl_3$): δ = –65.51 (s).

FT-MS (ESI+): *m*/*z* = 394.1 (calcd. 394.1 for $C_{19}H_{19}F_3N_3OS$ $[M+H]^+$).

5-Bromo-*N*-{2-[2-(*tert*-butyl)phenoxy]pyridin-3-yl}-4-(trifluoromethyl)thiazol-2-amine (**27**) was obtained according to general procedure H in 82% yield.

M. p. = 114 °C.

TLC (silica gel, EA/IH, 1:9): R_f = 0.56.

^{1}H NMR (400 MHz, $CDCl_3$): δ = 8.44 (dd, *J* = 7.9, 1.6 Hz, 1H), 7.84 (dd, *J* = 4.9, 1.6 Hz, 1H), 7.74 (s, 1H), 7.48 (dd, *J* = 7.6, 1.9 Hz, 1H), 7.27 – 7.16 (m, 2H), 7.05 (dd, *J* = 7.9, 4.9 Hz, 1H), 6.93 (dd, *J* = 7.6, 1.8 Hz, 1H), 1.38 (s, 9H).

^{13}C NMR (100 MHz, $CDCl_3$): δ = 162.7, 152.3, 152.1, 141.6, 140.6, 127.8, 127.3, 125.4, 125.2, 124.9, 123.3, 119.1, 119.1, 34.8, 30.8.

^{19}F NMR (282 MHz, $CDCl_3$): δ = –62.57 (s).

FT-MS (ESI+): *m*/*z* = 474.1 (calcd. 474.0 for $C_{19}H_{18}BrF_3N_3OS$ $[M+H]^+$).

***N*-{2-[2-(*tert*-Butyl)phenoxy]pyridin-3-yl}-5-(6-fluoropyridin-3-yl)-4-(trifluoromethyl)thiazol-2-amine** (**28**) was obtained according to general procedure I (colorless solid, 78% yield).

HPLC: t_R = 27.3 min, >99 %.

M. p. = 197 °C.

TLC (silica gel, EA/IH, 1:9): R_f = 0.24.

^{1}H NMR (400 MHz, $CDCl_3$): δ = 8.56 (dd, *J* = 7.9, 1.6 Hz, 1H), 8.32 (d, *J* = 2.3 Hz, 1H), 7.91 – 7.84 (m, 3H), 7.48 (dd, *J* = 7.7, 1.8 Hz, 1H), 7.31 – 7.15 (m, 2H), 7.08 (dd, *J* = 7.9, 5.0 Hz, 1H), 7.03 (dd, *J* = 8.4, 3.0 Hz, 1H), 6.94 (dd, *J* = 7.8, 1.4 Hz, 1H), 1.39 (s, 9H).

^{13}C NMR (100 MHz, $CDCl_3$): δ = 165.1, 162.7, 162.3, 152.3, 152.1, 148.5, 148.3, 142.6 (d, *J* = 1.4 Hz), 142.5 (d, *J* = 1.4 Hz), 141.6, 140.5, 127.8, 127.3, 125.4, 125.2, 125.1, 123.3 (d, *J* = 5.9 Hz), 119.1, 109.8, 109.6, 34.8, 30.8.

^{19}F NMR (282 MHz, $CDCl_3$): δ = –60.40 (s), –66.73 (d, *J* = 9.7 Hz).

HRFT-MS (ESI+): *m*/*z* = 489.1367 (calcd. 489.1367 for $C_{24}H_{21}F_4N_4OS$ $[M+H]^+$).

***N*-{2-[2-(*tert*-Butyl)phenoxy]pyridin-3-yl}-5-(2-fluoropyridin-3-yl)-4-(trifluoromethyl)thiazol-2-amine** (**29**) was obtained according to general procedure I in 71% yield as colorless solid.

HPLC: t_R = 26.6 min, >99 %.

M. p. = 169 °C.

TLC (silica gel, EA/IH, 1:9): R_f = 0.21.

^{1}H NMR (400 MHz, $CDCl_3$): δ = 8.55 (dd, *J* = 7.9, 1.6 Hz, 1H), 8.31 (d, *J* = 4.8 Hz, 1H), 7.96 – 7.77 (m, 3H), 7.48 (dd, *J* = 7.6, 1.9 Hz, 1H), 7.36 – 7.12 (m, 3H), 7.07 (dd, *J* = 7.9, 4.9 Hz, 1H), 6.94 (dd, *J* = 7.7, 1.7 Hz, 1H), 1.39 (s, 9H).

^{13}C NMR (100 MHz, $CDCl_3$): δ = 163.2, 152.3, 152.2, 149.1, 148.9, 142.9, 141.6, 140.5, 127.8, 127.3, 125.4, 125.2, 125.1, 123.3, 121.5, 121.5, 119.1, 34.8, 30.8.

^{19}F NMR (282 MHz, $CDCl_3$): δ = –61.95 (d, *J* = 2.7 Hz), –66.30 (d, *J* = 8.8 Hz).

HRFT-MS (ESI+): *m*/*z* = 489.1366 (calcd. 489.1367 for $C_{24}H_{21}F_4N_4OS$ $[M+H]^+$).

***N*-{2-[2-(*tert*-Butyl)phenoxy]pyridin-3-yl}-5-(4-fluorophenyl)-4-(trifluoromethyl)thiazol-2-amine** (**30**) was obtained according to general procedure I in 81% yield as colorless solid.

HPLC: t_R = 30.5 min, >95 %.

M. p. = 126 °C.

TLC (silica gel, EA/IH, 1:9): R_f = 0.54.

^{1}H NMR (400 MHz, $CDCl_3$): δ = 8.48 (dd, *J* = 7.9, 1.3 Hz, 1H), 7.75 (dd, *J* = 4.9, 1.4 Hz, 1H), 7.69 (s, 1H), 7.42 – 7.34 (m, 3H), 7.18 – 7.01 (m, 5H), 6.86 (dd, *J* = 7.7, 1.4 Hz, 1H), 1.32 (s, 9H).

^{13}C NMR (100 MHz, $CDCl_3$): δ = 165.0, 161.7, 161.4, 152.2, 141.6, 140.1, 131.9 (d, *J* = 1.6 Hz), 131.8 (d, *J* = 1.6 Hz), 127.8, 127.3, 125.4, 125.4, 124.8, 123.2, 119.1, 116.0, 115.7, 34.8, 30.8.

^{19}F NMR (282 MHz, $CDCl_3$): δ = –60.63 (s), –112.16 (sep).

HRFT-MS (ESI+): *m*/*z* = 488.1414 (calcd. 488.1414 for $C_{25}H_{22}F_4N_3OS$ $[M+H]^+$).

2-[2-(*tert*-Butyl)phenoxy]-6-fluoro-3-nitropyridine (**34**) was obtained according to general procedure A as yellow oil, 43% yield.

TLC (silica gel, EA/IH, 1:18): R_f = 0.18.

^{1}H NMR (400 MHz, $CDCl_3$): δ = 8.57 (dd, *J* = 8.6, 6.7 Hz, 1H), 7.47 (dd, *J* = 7.3, 2.3 Hz, 1H), 7.27 – 7.20 (m, 2H), 6.95 (dd, *J* = 7.4, 2.0 Hz, 1H), 6.70 (dd, *J* = 8.6, 3.5 Hz, 1H), 1.37 (s, 9H).

^{13}C NMR (100 MHz, $CDCl_3$): δ = 164.1, 161.6, 156.0 (d, *J* = 15.4 Hz), 150.8, 141.6, 141.2 (d, *J* = 10.2 Hz), 127.8, 127.1, 126.1, 123.3, 103.4 (d, *J* = 38.3 Hz), 34.7, 30.3.

^{19}F NMR (282 MHz, $CDCl_3$): δ = –56.75 (s).

FT-MS (ESI+): *m*/*z* = 313.1 (calcd. 313.1 for $C_{15}H_{15}N_2NaO_3$ $[M+Na]^+$).

6-[2-(*tert*-Butyl)phenoxy]-2-fluoro-3-nitropyridine (**35**) was obtained according to general procedure A as colorless solid, 35% yield.

M. p. = 98 °C.

TLC (silica gel, EA/IH, 1:18): R_f = 0.20.

^{1}H NMR (400 MHz, $CDCl_3$): δ = 8.54 (t, *J* = 8.9 Hz, 1H), 7.48 (dd, *J* = 7.5, 2.2 Hz, 1H), 7.26 (tdt, *J* = 11.0, 7.4, 3.8 Hz, 2H), 6.98 (dd, *J* = 7.5, 1.9 Hz, 1H), 6.88 (d, *J* = 8.7 Hz, 1H), 1.34 (s, 9H).

^{13}C NMR (100 MHz, $CDCl_3$): δ = 165.1 (d, *J* = 14.0 Hz), 156.6, 154.1, 151.2, 141.6, 140.1, 128.0, 127.5, 126.4, 123.1, 108.7 (d, *J* = 5.5 Hz), 34.7, 30.4.

^{19}F NMR (282 MHz, $CDCl_3$): δ = –69.06 (d, *J* = 8.6 Hz).

FT-MS (ESI+): *m*/*z* = 313.1 (calcd. 313.1 for $C_{15}H_{15}N_2NaO_3$ $[M+Na]^+$).

2-[2-(*tert*-Butyl)phenoxy]-6-fluoropyridin-3-amine (**57**) was obtained according to general procedure B as colorless solid, 92% yield.

M. p. = 135 °C.

TLC (silica gel, EA/IH, 1:9): R_f = 0.35.

^{1}H NMR (400 MHz, $CDCl_3$): δ = 7.42 (dd, *J* = 7.8, 1.8 Hz, 1H), 7.25 – 7.06 (m, 3H), 6.94 (dd, *J* = 7.9, 1.5 Hz, 1H), 6.46 (dd, *J* = 8.1, 3.0 Hz, 1H), 3.36 (s, 2H), 1.40 (s, 9H).

^{13}C NMR (100 MHz, $CDCl_3$): δ = 155.4, 153.1, 152.4, 148.7 (d, *J* = 13.0 Hz), 141.0, 129.0 (d, *J* = 5.2 Hz), 127.2 (d, *J* = 35.5 Hz), 126.9 (d, *J* = 6.9 Hz), 124.7, 122.5, 102.5 (d, *J* = 37.6 Hz), 34.8, 30.6.

^{19}F NMR (282 MHz, $CDCl_3$): δ = –82.53 (d, *J* = 6.5 Hz).

FT-MS (ESI+): *m*/*z* = 283.1 (calcd. 283.1 for $C_{15}H_{17}N_2NaO$ $[M+Na]^+$).

6-[2-(*tert*-Butyl)phenoxy]-2-fluoropyridin-3-amine (**58**) was obtained according to general procedure B as yellow-brown oil, 92% yield.

TLC (silica gel, EA/IH, 1:9): R_f = 0.30.

^{1}H NMR (400 MHz, $CDCl_3$): δ = 7.39 (dd, *J* = 7.8, 1.8 Hz, 1H), 7.21 – 7.12 (m, 2H), 7.08 (td, *J* = 7.5, 1.5 Hz, 1H), 6.87 (dd, *J* = 7.8, 1.6 Hz, 1H), 6.54 (d, *J* = 8.2 Hz, 1H), 3.56 (s, 2H), 1.39 (s, 9H).

^{13}C NMR (100 MHz, $CDCl_3$): δ = 154.0, 153.2 (d, *J* = 12.0 Hz), 151.6, 149.3, 141.1, 129.1 (d, *J* = 5.4 Hz), 127.3 (d, *J* = 28.1 Hz), 124.4, 124.2, 121.5, 108.81 (d, *J* = 5.2 Hz), 34.82, 30.33.

^{19}F NMR (282 MHz, $CDCl_3$): δ = –86.51 (d, *J* = 10.8 Hz).

FT-MS (ESI+): *m*/*z* = 283.1 (calcd. 283.1 for $C_{15}H_{17}N_2NaO$ $[M+Na]^+$).

1-{2-[2-(*tert*-Butyl)phenoxy]-6-fluoropyridin-3-yl}-3-[4-(trifluoromethoxy)phenyl]urea (**36**) was obtained according to general procedure D in colorless solid, 91% yield.

HPLC: t_R = 26.2 min, >99 %.

M. p. = 145 °C.

TLC (silica gel, EA/IH, 1:9): R_f = 0.36.

^{1}H NMR (400 MHz, $CDCl_3$): δ = 8.58 (dd, *J* = 8.5, 7.3 Hz, 1H), 7.41 (dd, *J* = 7.3, 2.3 Hz, 1H), 7.35 – 7.24 (m, 3H), 7.18 (m, 3H), 7.10 (d, *J* = 6.0 Hz, 2H), 6.82 (dd, *J* = 7.5, 2.0 Hz, 1H), 6.57 (dd, *J* = 8.5, 3.1 Hz, 1H), 1.29 (s, 9H).

^{13}C NMR (100 MHz, $CDCl_3$): δ = 157.9, 155.5, 153.0, 151.9, 150.8 (d, *J* = 13.4 Hz), 145.9, 141.3, 136.1, 133.3 (d, *J* = 7.2 Hz), 127.7, 127.3, 125.5, 122.9 (d, *J* = 13.5 Hz), 122.1, 121.8, 121.0 (d, *J* = 5.7 Hz), 119.3, 102.8 (d, *J* = 36.7 Hz), 34.7, 30.6.

^{19}F NMR (282 MHz, $CDCl_3$): δ = –58.56 (s), –75.57 (s).

HRFT-MS (ESI+): *m*/*z* = 464.1592 (calcd. 464.1592 for $C_{23}H_{22}F_4N_3O_3$ $[M+H]^+$).

1-{2-[2-(*tert*-Butyl)phenoxy]-6-fluoropyridin-3-yl}-3-[4-(*tert*-butyl)phenyl]urea (**37**) was obtained according to general procedure D as colorless solid, quantitative.

HPLC: t_R = 28.1 min, >97 %.

M. p. = 192 °C.

TLC (silica gel, EA/IH, 1:9): R_f = 0.38.

^{1}H NMR (400 MHz, $CDCl_3$): δ = 8.66 (dd, *J* = 8.5, 7.3 Hz, 1H), 7.39 (dd, *J* = 7.6, 2.0 Hz, 1H), 7.36 – 7.27 (m, 3H), 7.24 – 7.06 (m, 4H), 6.83 (dd, *J* = 7.7, 1.7 Hz, 1H), 6.77 (s, 1H), 6.57 (dd, *J* = 8.5, 3.1 Hz, 1H), 1.27(s, 9H), 1.25 (s, 9H)

^{13}C NMR (100 MHz, $CDCl_3$): δ = 158.0, 154.8, 153.5, 152.0, 150.5, 150.3, 148.9, 141.2, 134.3, 132.9 (d, *J* = 7.2 Hz), 127.5, 127.2, 126.7, 125.2, 123.0, 122.9, 121.5 (d, *J* = 5.7 Hz), 102.7 (d, *J* = 36.7 Hz), 34.6, 34.5, 31.4, 30.6.

^{19}F NMR (282 MHz, $CDCl_3$): δ = –76.34 (d, *J* = 7.3 Hz).

HRFT-MS (ESI+): *m*/*z* = 436.2395 (calcd. 436.2395 for $C_{26}H_{31}FN_3O_2$ $[M+H]^+$).

1-{2-[2-(*tert*-Butyl)phenoxy]-6-fluoropyridin-3-yl}-3-[4-(2-hydroxyethyl)phenyl]urea (**38**) was obtained according to general procedure D (colorless solid, 68% yield).

HPLC: t_R = 22.0 min, >99 %.

M. p. = 160 °C.

TLC (silica gel, EA/IH, 1:1): R_f = 0.32.

^{1}H NMR (400 MHz, $CDCl_3$): δ = 8.59 (dd, *J* = 8.5, 7.4 Hz, 1H), 7.38 (dd, *J* = 7.5, 2.1 Hz, 1H), 7.27 (d, *J* = 8.4 Hz, 2H), 7.21 – 7.01 (m, 4H), 6.79 (dd, *J* = 7.7, 1.7 Hz, 1H), 6.54 (dd, *J* = 8.5, 3.1 Hz, 1H), 3.72 (t, *J* = 6.8 Hz, 2H), 2.73 (t, *J* = 6.7 Hz, 2H), 1.29 (s, 9H).

^{13}C NMR (100 MHz, $CDCl_3$): δ = 157.7, 154.5, 153.5, 152.3, 150.5 (d, *J* = 13.4 Hz), 141.5, 136.7, 133.9, 132.7, 132.6, 129.6, 127.5, 127.2, 125.1, 122.9, 121.8 (d, *J* = 5.7 Hz), 120.3, 102.4 (d, *J* = 36.5 Hz), 63.3, 38.4, 34.6, 30.5.

^{19}F NMR (282 MHz, $CDCl_3$): δ = –77.49 (d, *J* = 7.3 Hz).

FT-MS (ESI+): *m*/*z* = 446.3 (calcd. 446.2 for $C_{24}H_{26}FN_3NaO_3$ $[M+Na]^+$).

1-[(3*s*,5*s*,7*s*)-Adamantan-1-yl]-3-{2-[2-(*tert*-butyl)phenoxy]-6-fluoropyridin-3-yl}urea (**39**) was obtained according to general procedure D as colorless solid, 82% yield.

HPLC: t_R = 30.6 min, >97 %.

M. p. = 222 °C.

TLC (silica gel, EA/IH, 1:9): R_f = 0.22.

^{1}H NMR (400 MHz, $CDCl_3$): δ = 8.56 (dd, *J* = 8.5, 7.4 Hz, 1H), 7.43 (dd, *J* = 7.6, 2.0 Hz, 1H), 7.25 – 7.06 (m, 2H), 6.85 (dd, *J* = 7.7, 1.7 Hz, 1H), 6.66 (s, 1H), 6.56 (dd, *J* = 8.5, 3.1 Hz, 1H), 4.55 (s, 1H), 2.06 (s, 3H), 2.01 (s, 6H), 1.68 (s, 6H), 1.37 (s, 9H).

^{13}C NMR (100 MHz, $CDCl_3$): δ = 157.6, 154.4, 153.8, 152.3, 150.1 (d, *J* = 13.3 Hz), 141.3, 132.5 (d, *J* = 6.8 Hz), 127.5 (d, *J* = 24.7 Hz), 125.2, 122.9, 122.3 (d, *J* = 5.6 Hz), 102.6 (d, *J* = 36.6 Hz), 51.8, 42.4, 36.4, 34.8, 30.7, 29.6.

^{19}F NMR (282 MHz, $CDCl_3$): δ = –77.49 (dd, *J* = 7.3, 3.0 Hz).

HRFT-MS (ESI+): *m*/*z* = 438.2551 (calcd. 438.2551 for $C_{26}H_{33}FN_3O_2$ $[M+H]^+$).

1-{2-[2-(*tert*-Butyl)phenoxy]-6-fluoropyridin-3-yl}-3-cyclohexylurea (**40**) was obtained according to general procedure D as colorless solid, 76% yield.

HPLC: t_R = 25.2 min, >99 %.

M. p. = 192 °C.

TLC (silica gel, EA/IH, 1:9): R_f = 0.20.

^{1}H NMR (400 MHz, $CDCl_3$): δ = 8.58 (dd, *J* = 8.5, 7.4 Hz, 1H), 7.43 (dd, *J* = 7.6, 2.0 Hz, 1H), 7.25 – 7.10 (m, 2H), 6.86 (dd, *J* = 7.6, 1.8 Hz, 1H), 6.83 (s, 1H), 6.56 (dd, *J* = 8.5, 3.1 Hz, 1H), 4.79 (d, *J* = 7.8 Hz), 3.69 – 3.43 (m, 1H), 2.02 – 1.87 (m, 2H), 1.81 – 1.51 (m, 2H), 1.47 – 1.00 (m, 6H), 1.36 (s, 9H).

^{13}C NMR (100 MHz, $CDCl_3$): δ = 157.6, 154.5, 154.4, 152.1, 150.1 (d, *J* = 13.3 Hz), 141.3, 132.6 (d, *J* = 7.0 Hz), 127.5 (d, *J* = 25.4 Hz), 125.3, 122.9, 122.1 (d, *J* = 5.6 Hz), 102.7 (d, *J* = 36.6 Hz), 49.7, 34.8, 33.7, 30.7, 25.6, 25.0.

^{19}F NMR (282 MHz, $CDCl_3$): δ = –77.26 (dd, *J* = 7.3, 2.9 Hz).

HRFT-MS (ESI+): *m*/*z* = 386.2238 (calcd. 386.2238 for $C_{22}H_{29}FN_3O_2$ $[M+H]^+$).

1-{2-[2-(*tert*-Butyl)phenoxy]-6-fluoropyridin-3-yl}-3-cyclopentylurea (**41**) was quantitatively obtained according to general procedure D as colorless solid,.

HPLC: t_R = 24.2 min, >99 %.

M. p. = 213 °C.

TLC (silica gel, EA/IH, 2:8): R_f = 0.24.

^{1}H NMR (400 MHz, $CDCl_3$): δ = 8.59 (dt, *J* = 10.5, 5.2 Hz, 1H), 7.43 (dd, *J* = 7.7, 1.9 Hz, 1H), 7.25 – 7.10 (m, 2H), 6.91 (s, 1H), 6.85 (dd, *J* = 7.8, 1.6 Hz, 1H), 6.56 (dd, *J* = 8.5, 3.1 Hz, 1H), 4.92 (d, *J* = 6.7 Hz, 1H), 4.02 (dd, *J* = 13.3, 6.6 Hz, 1H), 1.97 (qd, *J* = 6.3, 4.8 Hz, 2H), 1.73 – 1.49 (m, 4H), 1.47 – 1.32 (m, 2H), 1.36 (s, 9H).

^{13}C NMR (100 MHz, $CDCl_3$): δ = 157.3, 154.9, 152.1, 150.1 (d, *J* = 13.3 Hz), 141.3, 132.5 (d, *J* = 7.1 Hz), 127.6, 127.3, 125.3, 122.9, 122.1 (d, *J* = 5.6 Hz), 102.7 (d, *J* = 36.5 Hz), 52.6, 34.8, 33.6, 30.7, 23.7.

^{19}F NMR (282 MHz, $CDCl_3$): δ = –77.22 (d, *J* = 4.8 Hz).

HRFT-MS (ESI+): *m*/*z* = 394.1901 (calcd. 394.1901 for $C_{21}H_{26}FN_3NaO_2$ $[M+H]^+$).

1-{6-[2-(*tert*-Butyl)phenoxy]-2-fluoropyridin-3-yl}-3-[4-(trifluoromethoxy)phenyl]urea (**42**) was quantitatively obtained according to general procedure D as colorless solid,.

HPLC: t_R = 26.7 min, >99 %.

M. p. = 65 °C.

TLC (silica gel, EA/IH, 2:8): R_f = 0.30.

^{1}H NMR (400 MHz, $CDCl_3$): δ = 8.38 (dd, *J* = 10.0, 8.6 Hz, 1H), 7.47 (s, 1H), 7.41 (dd, *J* = 6.6, 3.0 Hz, 1H), 7.33 (d, *J* = 9.0 Hz, 2H), 7.25 – 7.04 (m, 5H), 6.87 (dd, *J* = 6.8, 2.7 Hz, 1H), 6.64 (d, *J* = 8.6 Hz, 1H), 1.32 (s, 9H).

^{13}C NMR (100 MHz, $CDCl_3$): δ = 157.2 (d, *J* = 12.8 Hz), 153.9, 153.0 (d, *J* = 27.5 Hz), 150.7, 145.4 (d, *J* = 2.0 Hz), 141.6, 136.5, 136.0 (d, *J* = 3.5 Hz), 127.6 (d, *J* = 28.7 Hz), 125.2, 122.3, 122.0, 121.8, 115.9 (d, *J* = 24.5 Hz), 108.3 (d, *J* = 5.1 Hz), 34.8, 30.3

^{19}F NMR (282 MHz, $CDCl_3$): δ = –58.60 (s), –83.25 (d, *J* = 9.7 Hz).

HRFT-MS (ESI+): *m*/*z* = 464.1592 (calcd. 464.1592for $C_{23}H_{22}F_4N_3O_3$ $[M+H]^+$).

1-{6-[2-(*tert*-Butyl)phenoxy]-2-fluoropyridin-3-yl}-3-[4-(2-hydroxyethyl)phenyl]urea (**43**) was obtained according to general procedure D as colorless solid, 65% yield.

HPLC: t_R = 22.7 min, >99 %.

M. p. = 171 °C.

TLC (silica gel, EA/IH, 1:1): R_f = 0.38.

^{1}H NMR (400 MHz, $CDCl_3$): δ = 8.50 (dd, *J* = 10.1, 8.6 Hz, 1H), 8.00 (s, 1H), 7.39 (dd, *J* = 7.7, 1.9 Hz, 1H), 7.26 (d, *J* = 8.5 Hz, 2H), 7.21 – 7.03 (m, 4H), 6.87 (dd, *J* = 7.7, 1.7 Hz, 1H), 6.61 (d, *J* = 8.6 Hz, 1H), 3.76 (t, *J* = 6.5 Hz, 2H), 2.76 (t, *J* = 6.5 Hz, 2H), 1.34 (s).

^{13}C NMR (100 MHz, $CDCl_3$): δ = 155.9 (d, *J* = 12.8 Hz), 153.3, 153.1, 153.0, 149.8, 141.4, 136.8, 136.7, 134.5, 134.4 (d, *J* = 3.6 Hz), 133.7, 129.6, 127.4 (d, *J* = 23.6 Hz), 124.8, 122.1, 120.1, 119.9, 117.1 (d, *J* = 24.1 Hz), 63.4, 38.5, 34.7, 30.1.

^{19}F NMR (282 MHz, $CDCl_3$): δ = –84.69 (m).

HRFT-MS (ESI+): *m*/z = 424.2031 (calcd. 424.2031 for $C_{24}H_{27}FN_3O_3$ $[M+H]^+$).

***N*-{2-[2-(*tert*-Butyl)phenoxy]-6-fluoropyridin-3-yl}-4-(trifluoromethyl)thiazol-2-amine** (**45**) was obtained according to general procedure G, as colorless solid, 89% yield.

M. p. = 136 °C.

TLC (silica gel, EA/IH, 1:9): R_f = 0.55.

^{1}H NMR (400 MHz, $CDCl_3$): δ = 8.73 (dd, *J* = 8.5, 7.0 Hz, 1H), 7.61 (s, 1H), 7.46 (dd, *J* = 7.7, 1.9 Hz, 1H), 7.33 – 7.11 (m, 3H), 6.94 (dd, *J* = 7.8, 1.6 Hz, 1H), 6.68 (dd, *J* = 8.5, 3.1 Hz, 1H), 1.37 (s, 9H).

^{13}C NMR (100 MHz, $CDCl_3$): δ = 164.9, 157.7, 155.3, 151.8, 150.3 (d, *J* = 13.5 Hz), 141.5, 131.2 (d, *J* = 7.3 Hz), 127.8, 127.4, 125.7, 123.1, 122.6 (d, *J* = 5.6 Hz), 110.9, 103.0, 102.6, 34.9, 30.8.

^{19}F NMR (282 MHz, $CDCl_3$): δ = –65.56 (s), –74.31 (m).

FT-MS (ESI+): *m*/*z* = 412.2 (calcd. 421.1 for $C_{19}H_{18}F_4N_3OS$ $[M+H]^+$).

5-Bromo-*N*-{2-[2-(*tert*-butyl)phenoxy]-6-fluoropyridin-3-yl}-4-(trifluoromethyl)thiazol-2-amine (46) was quantitatively obtained according to general procedure H, as colorless solid,.

M. p. = 155 °C.

TLC (silica gel, EA/IH, 1:9): R_f = 0.66.

^{1}H NMR (400 MHz, $CDCl_3$): δ = 8.58 (dd, *J* = 8.5, 7.0 Hz, 1H), 7.54 (s, 1H), 7.48 (dd, *J* = 7.7, 1.9 Hz, 1H), 7.29 – 7.12 (m, 2H), 7.07 (dd, *J* = 7.9, 4.9 Hz, 1H), 6.66 (dd, *J* = 8.5, 3.1 Hz, 1H), 1.35 (s, 9H).

^{13}C NMR (100 MHz, $CDCl_3$): δ = 163.4, 158.4, 155.3, 151.6, 141.4, 138.6, 131.7, 131.6, 127.8, 127.3, 125.7, 123.1, 121.9 (d, *J* = 5.7 Hz), 102.8 (d, *J* = 37.0 Hz), 34.7, 30.7.

^{19}F NMR (282 MHz, $CDCl_3$): δ = –62.60 (s), –74.85 (dd, *J* = 6.9, 3.0 Hz).

FT-MS (ESI+): *m*/*z* = 492.1 (calcd. 492.0 for $C_{19}H_{17}BrF_4N_4OS$ $[M+H]^+$).

***N*-{2-[2-(*tert*-Butyl)phenoxy]-6-fluoropyridin-3-yl}-5-phenyl-4-(trifluoromethyl)thiazol-2-amine** (**47**) was obtained according to general procedure I as colorless solid, 78% yield.

HPLC: t_R = 30.4 min, >95 %.

M. p. = 151 °C.

TLC (silica gel, EA/IH, 1:9): R_f = 0.65.

^{1}H NMR (400 MHz, $CDCl_3$): δ = 8.73 (dd, *J* = 8.5, 7.0 Hz, 1H), 7.55 (s, 1H), 7.74 – 7.36 (m, 6H), 7.36 – 7.12 (m, 2H), 6.95 (dd, *J* = 7.6, 1.9 Hz, 1H), 6.68 (dd, *J* = 8.5, 3.0 Hz, 1H), 1.38 (s, 9H).

^{13}C NMR (100 MHz, $CDCl_3$): δ = 161.9, 158.0, 151.8, 141.4, 130.9 (d, *J* = 7.5 Hz), 130.0, 129.9, 129.8, 129.4, 128.8, 128.7, 127.8, 127.3, 125.6, 123.1, 122.6 (d, *J* = 5.5 Hz), 102.7 (d, *J* = 37.0 Hz), 34.8, 30.8.

^{19}F NMR (282 MHz, $CDCl_3$): δ = –60.25 (s), –76.01 (s).

HRFT-MS (ESI+): *m*/*z* = 488.1414 (calcd. 488.1414 for $C_{25}H_{22}F_4N_3OS$ $[M+H]^+$).

***N*-{2-[2-(*tert*-Butyl)phenoxy]-6-fluoropyridin-3-yl}-5-(pyridin-4-yl)-4-(trifluoromethyl)thiazol-2-amine** (**48**) was obtained according to general procedure I, as colorless solid, 83% yield.

HPLC: t_R = 28.4 min, >99 %.

M. p. = 159 °C.

TLC (silica gel, EA/IH, 2:8): R_f = 0.11.

^{1}H NMR (400 MHz, $CDCl_3$): δ = 8.72 – 8.66 (m, 3H), 7.83 (s, 1H), 7.47 (dd, *J* = 7.5, 1.2, Hz, 1H), 7.35 (d, *J* = 6 Hz, 2H), 7.26 – 7.19 (m, 3H), 6.94 (dd, *J* = 7.8, 1.8 Hz, 1H), 6.69 (dd, *J* = 8.4, 3 Hz, 1H), 1.36 (s, 9H)

^{13}C NMR (100 MHz, $CDCl_3$): δ = 163.1, 158.4, 155.2, 151.7, 150.7 (d, *J* = 13.8 Hz), 150.2, 141.4, 137.1, 131.6 (d, *J* = 7.5 Hz), 127.8, 127.4, 125.7, 124.1, 123.1, 122.2 (d, *J* = 5.7 Hz), 102.8 (d, *J* = 36.9 Hz), 34.8, 30.7.

^{19}F NMR (282 MHz, $CDCl_3$): δ = –60.27 (s), –75.01 (dd, *J* = 6.7, 2.8 Hz).

HRFT-MS (ESI+): *m*/*z* = 489.1367 (calcd. 489.1367 for $C_{24}H_{21}F_4N_4OS$ $[M+H]^+$).

***N*-{2-[2-(*tert*-Butyl)phenoxy]-6-fluoropyridin-3-yl}-5-(pyridin-3-yl)-4-(trifluoromethyl)thiazol-2-amine** (**49**) was obtained according to general procedure I as colorless solid, 84% yield.

HPLC: t_R = 27.1 min, >99 %.

M. p. = 234 °C.

TLC (silica gel, EA/IH, 2:8): R_f = 0.18.

^{1}H NMR (400 MHz, $CDCl_3$): δ = 8.81 – 8.56 (m, 3H), 7.78 (dt, *J* = 7.9, 1.7 Hz, 1H), 7.62 (s, 1H), 7.46 (dd, *J* = 7.6, 2.0 Hz, 1H), 7.38 (ddd, *J* = 7.9, 4.9, 0.8 Hz, 1H), 7.30 – 7.09 (m, 3H), 6.95 (dd, *J* = 7.7, 1.7 Hz, 1H), 6.70 (dd, *J* = 8.5, 3.1 Hz, 1H), 1.38 (s, 9H).

^{13}C NMR (100 MHz, $CDCl_3$): δ = 162.8, 158.2, 155.0, 151.7, 150.6, 150.3, 150.1 (d, *J* = 1.6 Hz), 141.4, 137.3 (dt, *J* = 3.2, 1.5 Hz), 131.3, 131.3, 127.8, 127.4, 125.7, 125.4, 123.4, 123.1, 122.3 (d, *J* = 5.6 Hz), 122.3 (d, *J* = 5.6 Hz), 102.8 (d, *J* = 37.0 Hz), 34.8, 30.7.

^{19}F NMR (282 MHz, $CDCl_3$): δ = –60.38 (s), –75.42 (dd, *J* = 6.9, 3.1 Hz).

HRFT-MS (ESI+): *m*/*z* = 489.1367 (calcd. 489.1367 for $C_{24}H_{21}F_4N_4OS$ $[M+H]^+$).

***N*-{6-[2-(*tert*-Butyl)phenoxy]-2-fluoropyridin-3-yl}-4-(trifluoromethyl)thiazol-2-amine** (**51**) was obtained according to general procedure G, as orange solid, 67% yield.

M. p. = 50 °C.

TLC (silica gel, EA/IH, 1:9): R_f = 0.12.

^{1}H NMR (400 MHz, $CDCl_3$): δ = 8.61 (dd, *J* = 10.2, 8.6 Hz, 1H), 7.44 (dd, *J* = 7.6, 1.9 Hz, 1H), 7.32 (s, 1H), 7.23 – 7.10 (m, 3H), 6.96 – 6.93 (m, 1H), 6.75 (d, *J* = 8.6 Hz, 1H), 1.38 (9H).

^{13}C NMR (100 MHz, $CDCl_3$): δ = 152.9, 141.6, 133.6, 129.3, 127.7, 127.3, 125.1, 122.6, 122.4, 110.7 (d, *J* = 18.5 Hz), 108.4 (d, *J* = 5.3 Hz), 34.8, 30.4.

^{19}F NMR (282 MHz, $CDCl_3$): δ = –66.60 (s).

FT-MS (ESI+): *m*/*z* = 412.2 (calcd. 421.1 for $C_{19}H_{18}F_4N_3OS$ $[M+H]^+$).

5-Bromo-*N*-{6-[2-(*tert*-butyl)phenoxy]-2-fluoropyridin-3-yl}-4-(trifluoromethyl)thiazol-2-amine (52) was quantitatively obtained according to general procedure H, as an thick oil,.

TLC (silica gel, EA/IH, 1:9): R_f = 0.22.

^{1}H NMR (400 MHz, $CDCl_3$): δ = 8.60 (dd, *J* = 10.2, 8.7 Hz, 1H), 7.43 (dd, *J* = 7.5, 1.8 Hz, 1H), 7.26 (s, 1H), 7.21 – 7.15 (m, 3H), 6.95 (dd, *J* = 7.8, 1.8 Hz, 1H), 6.75 (d, *J* = 8.4 Hz, 1H), 1.37 (s, 9H).

^{13}C NMR (100 MHz, $CDCl_3$): δ = 165.2 (s), 156.9 (d, *J* = 12.7 Hz), 153.1, 152.9, 149.9, 141.6, 133.7 (d, *J* = 2.4 Hz), 127.7, 127.3, 125.1, 122.5, 122.0, 117.7 (d, *J* = 24.7 Hz), 110.8 (dd, *J* = 8.1, 4.0 Hz), 108.4 (d, *J* = 5.2 Hz), 34.8, 30.4.

^{19}F NMR (282 MHz, $CDCl_3$): δ = –65.57 (s), –82.63 (s).

FT-MS (ESI+): *m*/*z* = 492.1 (calcd. 492.0 for $C_{19}H_{17}BrF_4N_4OS$ $[M+H]^+$).

***N*-{6-[2-(*tert*-Butyl)phenoxy]-2-fluoropyridin-3-yl}-5-[4-(trifluoromethoxy)phenyl]-4-(trifluoromethyl)thiazol-2-amine** (**53**) was obtained according to general procedure I as colorless solid, 45% yield.

HPLC: t_R = 26.6 min, >99 %.

M. p. = 159 °C.

TLC (silica gel, EA/IH, 1:9): R_f = 0.18.

^{1}H NMR (400 MHz, $CDCl_3$): δ = 8.59 (dd, *J* = 10.2, 8.6 Hz, 1H), 7.48 – 7.42 (m, 3H), 7.32 – 7.23 (m, 1H), 7.23 – 7.12 (m, 2H), 7.08 (s, 1H), 6.95 (dd, *J* = 7.7, 1.7 Hz, 1H), 6.76 (d, *J* = 8.6 Hz, 1H), 1.38 (s, 9H).

^{13}C NMR (100 MHz, $CDCl_3$): δ = 162.4, 152.9, 141.6, 135.9, 133.5, 133.5, 131.6, 127.7, 127.4, 127.3, 125.1, 122.4, 121.0, 108.5, 34.8, 30.4.

^{19}F NMR (282 MHz, $CDCl_3$): δ = –58.20 (s), –60.39 (s), –82.58 (dd, *J* = 10.3, 4.9 Hz).

HRFT-MS (ESI+): *m*/*z* = 594.1057 (calcd. 594.1057 for $C_{26}H_{20}F_7N_3NaO_2S$ $[M+Na]^+$).

***N*-{6-[2-(*tert*-Butyl)phenoxy]-2-fluoropyridin-3-yl}-5-phenyl-4-(trifluoromethyl)thiazol-2-amine** (**54**) was obtained according to general procedure I as an colorless solid, 31% yield.

HPLC: t_R = 23.3 min, >99 %.

M. p. = 165 °C.

TLC (silica gel, EA/IH, 1:9): R_f = 0.15.

^{1}H NMR (400 MHz, $CDCl_3$): δ = 8.60 (dd, *J* = 10.2, 8.6 Hz, 1H), 7.60 – 7.36 (m, 6H), 7.25 – 7.11 (m, 2H), 7.08 (s, 1H), 6.95 (dd, *J* = 7.8, 1.6 Hz, 1H), 6.76 (d, *J* = 8.5 Hz, 1H), 1.38 (s, 9H).

^{13}C NMR (100 MHz, $CDCl_3$): δ = 162.2, 156.9, 152.9, 133.3, 133.3, 130.0, 129.4, 128.8, 128.7, 127.7, 127.4, 127.3, 125.1, 122.4, 108.5 (d, *J* = 5.3 Hz), 34.8, 30.4.

^{19}F NMR (282 MHz, $CDCl_3$): δ = –60.32 (s), –82.78 (d, J = 10.2 Hz).

HRFT-MS (ESI+): m/z = 488.1414 (calcd. 488.1414 for $C_{25}H_{22}F_4N_3OS$ $[M+H]^+$).

In vitro Pharmacology

Cellular and nuclear receptor functional $P2Y_1R$ assay was performed by Cerep (France, Item 4293 and 4294 respectively) with human recombinant 1321N1 cells using 2MeSATP (1 nM) as stimulus at room temperature. Intracellular $[Ca^{2+}]$ was detected by fluorimetry. The agonistic effect was investigated using the $P2Y_1R$ agonist **55** (MRS2365, [[(1*R*,2*R*,3*S*,4*R*,5*S*)-4-[6-amino-2-(methylthio)-9*H*-purin-9-yl]-2,3-dihydroxybicyclo[3.1.0]hex-1-yl]methyl] diphosphoric acid mono-ester trisodium salt) as reference compound. The antagonistic effect was investigated using compound **3** as reference antagonist (IC_{50} = 11 nM).

Radiochemistry

General

No-carrier-added [^{18}F]fluoride was produced *via* the [^{18}O(p,n)^{18}F] nuclear reaction by irradiation of an [^{18}O]H_2O target (Hyox 18 enriched water, Rotem Industries Ltd, Israel) on a Cyclone 18/9 (iba RadioPharma Solutions, Belgium) with fixed energy proton beam using Nirta [^{18}F]fluoride XL target.

Radio thin-layer chromatography (radio-TLC) was performed on silica gel (Polygram® SIL G/UV_{254}) pre-coated plates with a mixture of EA/*n*-hexane 1:1 (v/v) as eluent. The plates were exposed to storage phosphor screens (BAS-TR2025, FUJIFILM Co., Tokyo, Japan) and recorded using a bio-imaging analyzer system (BAS-1800 II, FUJIFILM). Images were evaluated with the BASReader and AIDA 2.31 software (raytest Isotopenmessgeräte GmbH, Straubenhardt, Germany).

Analytical chromatographic separations were performed on a JASCO LC-2000 system, incorporating a PU-2080*Plus* pump, AS-2055*Plus* auto injector (100 µL sample loop), and a UV-2070*Plus* detector coupled with a gamma radioactivity HPLC detector (Gabi Star, raytest Isotopenmessgeräte GmbH). Data analysis was performed with the Galaxie chromatography software (Agilent Technologies) using the chromatograms obtained at 254 nm. A Reprosil-Pur C18-AQ column (250 x 4.6 mm; 5 µm; Dr. Maisch HPLC GmbH; Germany) with MeCN/20 mM NH_4OAc_{aq} (pH 6.8) as eluent mixture and a flow of 1.0 mL/min was used (gradient: eluent

A 10% MeCN/20 mM NH_4OAc_{aq}; eluent B 90% MeCN/20 mM NH_4OAc_{aq}; 0–10' 100% A, 10–40' up to 100% B, 40–50' 100% B , 50–51 up to 100% A, 51–60' 100% A).

Semi-preparative HPLC separations were performed on a JASCO LC-2000 system, incorporating a PU-2080-20 pump, an UV/VIS-2075 detector coupled with a gamma radioactivity HPLC detector whose measurement geometry was slightly modified (Gabi Star, raytest Isotopenmessgeräte GmbH) and a fraction collector (Advantec CHF-122SC). A Reprosil-Pur C18-AQ column (150 x 10 mm) coupled with a precolumn (50 x 10 mm; 10 µm; Dr. Maisch HPLC GmbH; Germany) with 62% MeCN/20 mM NH_4OAc_{aq} (pH 6.8) as eluent at a flow of 4.0 mL/min were used.

The ammonium acetate and the SDS concentrations stated as 20 mM NH_4OAc_{aq} and 100 mM SDS_{aq}, respectively, correspond to the concentration in the aqueous component of an eluent mixture.

Radiosynthesis

No carrier added [^{18}F]fluoride (100 - 500 µL) was transferred into a 4 mL V vial and $TBAHCO_3$ (20 µL of a 0.075 M aqueous solution from ABX advanced biochemical compounds, Radeberg, Germany) in 1 mL CH_3CN was added. The aqueous [^{18}F]fluoride was azeotropically dried under vacuum and nitrogen flow within 7-10 min using a single mode microwave (75 W, at 50–60 °C, power cycling mode). Two aliquots of anhydrous CH_3CN (2 x 1.0 mL) were added during the drying procedure and the final [^{18}F]TBAF was dissolved in 500 µL of anhydrous *tert*-BuOH ready for labeling. Thereafter, a solution of 1.8− 2.0 mg of precursor in 300 µL of anhydrous *tert*-BuOH was added, and the ^{18}F-labeling was performed under thermal heating at 90 °C for 10 min. To analyze the reaction mixture and to determine radiochemical yields of the labeling, samples were taken for radio-HPLC and radio-TLC. Moreover, the stability of the tosylate precursor was investigated under the labeling conditions by using UV-HPLC analysis.

After cooling, 2.0 mL of a mixture of CH_3CN /water (35/75 v/v) was added and the solution was applied to an isocratic semi-preparative RP-HPLC system for isolation of [^{18}F]**18**. The collected radiotracer fraction (25-29 min) was diluted with 40 mL of H_2O to perform final purification by sorption on a preconditioned Sep-Pak® C18 light cartridge (Waters, Milford, MA, USA) and successive elution with 0.75 mL of ethanol. The solvent was reduced under a gentle argon stream at 70 °C and the desired radiotracer formulated in sterile isotonic saline containing 10% EtOH (v/v). The identity and radiochemical purity of [^{18}F]**18** was confirmed by radio-

HPLC and radio-TLC. Molar activity was determined on the basis of a UV/mass calibration curve carried out under isocratic HPLC conditions (62% CH_3CN /20 mM NH_4OAc_{aq}, pH 6.8) using chromatograms obtained at 260 nm.

Determination of the logD value

The partition coefficient of [^{18}F]**18** was experimentally determined for the *n*-octanol/PBS system by the shake-flask method. Small tracer amounts (~ 800 kBq) were added to a mixture of 3.0 mL of *n*-octanol and 3.0 mL of PBS. After shaking for 20 min at room temperature, the samples were centrifuged (10,000 rpm, 5 min) and 1 mL aliquots of the organic as well as the aqueous layer were taken and measured in a γ-counter (PerkinElmer Wallac Wizard 1480 Gamma Counter, manufactured by WALLAC, Turku, Finland). Another 1 mL aliquote of the organic layer was mixed with 2.0 mL *n*-octanol and 3.0 mL of PBS and subjected to the same procedure until constant partition coefficient values had been obtained. All measurements were done in quadruplicate.

Metabolism studies

Experiments followed the international guidelines of animal care and the study protocols were approved by the Landesdirektion Leipzig, the local authority for animal care (Reg.-Nr.: TVV 08/13; Reference number: 24-9168.11/18/8).

Mouse blood samples were taken at 30 min after intravenous injection of ~65 MBq of [^{18}F]**18** (n = 2). Plasma was obtained by centrifugation of blood at 12,000 rpm at room temperature for 1 minute.

MLC: For preparation of the MLC injection samples, mouse plasma (20 – 50 µL, 30 min p.i.) was dissolved in 100 – 300 µL of 100 mM aqueous SDS. Homogenized brain material (200 µL, 30 min p.i.) was dissolved in 400 µL of 200 mM aqueous SDS, stirred at 75 °C for 5 min and injected into the MLC system after cooling to room temperature. To proof the integrity of the radiotracer under this conditions, 50 kBq of the radiotracer were stirred at 75 °C for 5 min in 500 µl of 200 mM aqueous SDS and analyzed *via* MLC. The MLC system was built up of a JASCO PU-980 pump, an AS-2055*Plus* auto injector with a 2000 µL sample loop, and a UV-1575 detector coupled with a gamma radioactivity HPLC detector (Gabi Star, raytest Isotopenmessgeräte GmbH). Data analysis was performed with the Galaxie chromatography software (Agilent Technologies). A Reprosil-Pur C18-AQ column (250 x 4.6 mm, particle size: 10 µm) coupled with a pre-column of 10 mm length was used. Separations were performed by

using an eluent mixture of 1-PrOH/100 mM aqueous SDS/10mM Na_2HPO_{4aq} in gradient mode (0 – 15' at 3% 1-PrOH, 15 – 30' up to 30% 1-PrOH, 30 – 45' at 30% 1-PrOH, 45 – 50' up to 3% 1-PrOH; 50 – 60' at 3% 1-PrOH/ 100 mM SDS_{aq}, 10 mM Na_2HPO_{4aq}) at a flow rate of 0.75 mL/min.

RP-HPLC: For protein precipitation and extraction two different solvent systems were tested by adding an ice-cold mixture of (i) acetone/water (4/1; v/v) and (ii) MeOH/water (9/1; v/v) in a ratio of 4 : 1 of solvent to plasma or brain homogenate, respectively. The samples were vortexed for 2 min, equilibrated on ice for 15 min, and centrifuged for 5 min at 10,000 rpm. The precipitates were washed with 200 µL of the solvent mixture and subjected to the same procedure. The combined supernatants (total volume between 1.0 –1.5 mL) were concentrated at 65 °C under nitrogen flow to a final volume of approximately 100 µL and analyzed by analytical radio-HPLC. To determine the percentage of radioactivity in the supernatants compared to total activity, aliquots of each step as well as the precipitates were quantified by γ counting. Using the acetone/water system, the obtained recoveries were lower with 44% for plasma and 26% for the brain homogenate compared to the MeOH/water system with 70% and 57%, respectively. To analyze the worked-up samples, the same HPLC method was used as described in the radiochemistry part.

HILIC: For HILIC chromatography the brain samples were prepared as described for RP-HPLC using MeOH/water as extraction solvent. The separations were performed with a NUCLEODUR®HILIC column (250 x 4.6 mm, particle size: 5 µm) from Macherey-Nagel (Düren, Germany) under isocratic conditions (70 – 82% CH_3CN/20 mM NH_4OAc_{aq}) at a flow of 1 mL/min.

ORCID

Rareş-Petru Moldovan: 0000-0003-3119-7945

Evamarie Hey-Hawkins: 0000-0003-4267-0603

Wilma Neumann: 0000-0002-1728-5140

Peter Brust: 0000-0001-5555-7058

Supporting Information: ^{1}H NMR spectra of target compounds, HRMS of compound **32**, crystallographic data of compound **36**, HPLC chromatograms of target compounds.

Acknowledgments: The authors are grateful for financial support by the Life Science Stiftung (Project-Nr.1011170009 to R.-P.M, B.W., R.T., W.D.-C, P.B.), HZDR-Innovationsfonds (R.-

P.M, B.W., R.T., W.D.-C, P.B.), by the Sino German Center for Research Promotion (GZ1236 to U.K. and P.R.), and Fonds der Chemischen Industrie (doctoral grant for W.N.). We thank the staff of the Institute of Analytical Chemistry, Department of Chemistry and Mineralogy of Leipzig University, for obtaining the MS and NMR spectra. We are very thankful to Dr. K. Franke, Dr. S. Fischer and Dr. A. Mansel for providing [^{18}F]fluoride.

Conflicts of Interest: A patent application has been filed with the registration file number 2018060718590600DE.

References

1. Burnstock, G. Introduction to purinergic signalling in the brain. In *Glioma Signaling*, Barańska, J., Ed. Springer Netherlands: Dordrecht, 2013; pp 1-12.
2. Abbracchio, M. P.; Burnstock, G.; Verkhratsky, A.; Zimmermann, H. Purinergic signalling in the nervous system: an overview. *Trends Neurosci.* **2009,** 32, 19-29.
3. Burnstock, G. Introductory overview of purinergic signalling. *Front. Biosci. (Elite Ed.)* **2011,** 3, 896-900.
4. Nörenberg, W.; Illes, P. Neuronal P2X receptors: Localisation and functional properties. *Naunyn. Schmiedebergs Arch. Pharmacol.* **2000,** 362, 324-339.
5. von Kugelgen, I.; Hoffmann, K. Pharmacology and structure of P2Y receptors. *Neuropharmacology* **2016,** 104, 50-61.
6. North, R. A. Molecular physiology of P2X receptors. *Physiol. Rev.* **2002,** 82, 1013-1067.
7. Kaczmarek-Hájek, K.; Lörinczi, É.; Hausmann, R.; Nicke, A. Molecular and functional properties of P2X receptors—recent progress and persisting challenges. *Purinergic Signal.* **2012,** 8, 375-417.
8. Dal Ben, D.; Buccioni, M.; Lambertucci, C.; Marucci, G.; Thomas, A.; Volpini, R. Purinergic P2X receptors: structural models and analysis of ligand-target interaction. *Eur. J. Med. Chem.* **2015,** 89, 561-580.
9. <http://www.nobelprize.org/nobel_prizes/chemistry/laureates/2012/press.html>.
10. Jacobson, K. A.; Müller, C. E. Medicinal chemistry of adenosine, P2Y and P2X receptors. *Neuropharmacology* **2016,** 104, 31-49.
11. Rodrigues, R. J.; Tomé, A. R.; Cunha, R. A. ATP as a multi-target danger signal in the brain. *Front. Neurosci.* **2015,** 9.
12. Burnstock, G.; Krügel, U.; Abbracchio, M. P.; Illes, P. Purinergic signalling: From normal behaviour to pathological brain function. *Prog. Neurobiol.* **2011,** 95, 229-274.
13. Krügel, U. Purinergic receptors in psychiatric disorders. *Neuropharmacology* **2016,** 104, 212-225.
14. Rafehi, M.; Müller, C. E. Tools and drugs for uracil nucleotide-activated P2Y receptors. *Pharmacol. Ther.* **2018**, In Press, Accepted Manuscript.

15. Conroy, S.; Kindon, N.; Kellam, B.; Stocks, M. J. Drug-like antagonists of P2Y receptors—from lead identification to drug development. *J. Med. Chem.* **2016,** 59, 9981–10005.
16. Baranska, J.; Czajkowski, R.; Pomorski, P. $P2Y_1$ Receptors - Properties and functional activities. *Adv. Exp. Med. Biol.* **2017**, 1-19.
17. Simon, J.; Webb, T. E.; Barnard, E. A. Characterization of a P2Y purinoceptor in the brain. *Pharmacol. Toxicol.* **1995,** 76, 302-307.
18. Burnstock, G. Purinergic signalling and neurological diseases: An update. *CNS Neurol. Disord. Drug Targets* **2017,** 16, 257-265.
19. Delekate, A.; Fuchtemeier, M.; Schumacher, T.; Ulbrich, C.; Foddis, M.; Petzold, G. C. Metabotropic $P2Y_1$ receptor signalling mediates astrocytic hyperactivity in vivo in an Alzheimer's disease mouse model. *Nat. Commun.* **2014,** 5, 5422.
20. Moore, D.; Iritani, S.; Chambers, J.; Emson, P. Immunohistochemical localization of the $P2Y_1$ purinergic receptor in Alzheimer's Disease. *Neuroreport* **2000,** 11, 3799-3803.
21. Alves, M.; Gomez-Villafuertes, R.; Delanty, N.; Farrell, M. A.; O'Brien, D. F.; Miras-Portugal, M. T.; Hernandez, M. D.; Henshall, D. C.; Engel, T. Expression and function of the metabotropic purinergic P2Y receptor family in experimental seizure models and patients with drug-refractory epilepsy. *Epilepsia* **2017,** 58, 1603-1614.
22. Alvarez-Ferradas, C.; Morales, J. C.; Wellmann, M.; Nualart, F.; Roncagliolo, M.; Fuenzalida, M.; Bonansco, C. Enhanced astroglial Ca^{2+} signaling increases excitatory synaptic strength in the epileptic brain. *Glia* **2015,** 63, 1507-1521.
23. Shinozaki, Y.; Shibata, K.; Yoshida, K.; Shigetomi, E.; Gachet, C.; Ikenaka, K.; Tanaka, K. F.; Koizumi, S. Transformation of astrocytes to a neuroprotective phenotype by microglia *via* $P2Y_1$ receptor downregulation. *Cell. Rep.* **2017,** 19, 1151-1164.
24. Chin, Y.; Kishi, M.; Sekino, M.; Nakajo, F.; Abe, Y.; Terazono, Y.; Hiroyuki, O.; Kato, F.; Koizumi, S.; Gachet, C.; Hisatsune, T. Involvement of glial $P2Y_1$ receptors in cognitive deficit after focal cerebral stroke in a rodent model. *J. Neuroinflammation* **2013,** 10, 95.
25. Franke, H.; Illes, P. Nucleotide signaling in astrogliosis. *Neurosci. Lett.* **2014,** 565, 14-22.
26. Guzman, S. J.; Gerevich, Z. P2Y receptors in synaptic transmission and plasticity: Therapeutic potential in cognitive dysfunction. *Neural plasticity* **2016,** 2016, 1207393.
27. Koch, H.; Bespalov, A.; Drescher, K.; Franke, H.; Krügel, U. Impaired cognition after stimulation of $P2Y_1$ receptors in the rat medial prefrontal cortex. *Neuropsychopharmacology* **2015,** 40, 305-314.
28. Boeynaems, J.-M.; Robaye, B.; Janssens, R.; Suarez-Huerta, N.; Communi, D. Overview of P2Y receptors as therapeutic targets. *Drug Dev. Res.* **2001,** 52, 187-189.
29. Jacobson, K. A.; Deflorian, F.; Mishra, S.; Costanzi, S. Pharmacochemistry of the platelet purinergic receptors. *Purinergic Signal.* **2011,** 7, 305-324.
30. Webb, T. E.; Simon, J.; Barnard, E. A. Regional distribution of [^{35}S]2'-deoxy 5'-O-(1-thio) ATP binding sites and the $P2Y_1$ messenger RNA within the chick brain. *Neuroscience* **1998,** 84, 825-837.

31. Simon, J.; Webb, T. E.; Barnard, E. A. Distribution of [^{35}S]dATPaS binding sites in the adult rat neuraxis. *Neuropharmacology* **1997,** 36, 1243-1251.
32. http://mouse.brain-map.org/. http://human.brain-map.org/
33. Moore, D.; Chambers, J.; Waldvogel, H.; Faull, R.; Emson, P. Regional and cellular distribution of the $P2Y_1$ purinergic receptor in the human brain: striking neuronal localisation. *J. Comp. Neurol.* **2000,** 421, 374-384.
34. Krugel, U.; Kittner, H.; Franke, H.; Illes, P. Stimulation of P2 receptors in the ventral tegmental area enhances dopaminergic mechanisms *in vivo*. *Neuropharmacology* **2001,** 40, 1084-1093.
35. Seidel, B.; Bigl, M.; Franke, H.; Kittner, H.; Kiess, W.; Illes, P.; Krügel, U. Expression of purinergic receptors in the hypothalamus of the rat is modified by reduced food availability. *Brain Res.* **2006,** 1089, 143-152.
36. Chao, H.; Turdi, H.; Herpin, T. F.; Roberge, J. Y.; Liu, Y.; Schnur, D. M.; Poss, M. A.; Rehfuss, R.; Hua, J.; Wu, Q.; Price, L. A.; Abell, L. M.; Schumacher, W. A.; Bostwick, J. S.; Steinbacher, T. E.; Stewart, A. B.; Ogletree, M. L.; Huang, C. S.; Chang, M.; Cacace, A. M.; Arcuri, M. J.; Celani, D.; Wexler, R. R.; Lawrence, R. M. Discovery of 2-(phenoxypyridine)-3-phenylureas as small molecule $P2Y_1$ antagonists. *J. Med. Chem.* **2013,** 56, 1704-1714.
37. Felix, R. A.; Martin, S.; Pinion, S.; Crawford, D. J. Development of a comprehensive set of P2 receptor pharmacological research compounds. *Purinergic Signal.* **2012,** 8, 101-112.
38. Houston, D.; Costanzi, S.; Jacobson, K. A.; Harden, T. K. Development of selective high affinity antagonists, agonists, and radioligands for the $P2Y_1$ receptor. *Comb. Chem. High Throughput Screen.* **2008,** 11, 410-419.
39. Bourdon, D. M.; Mahanty, S. K.; Jacobson, K. A.; Boyer, J. L.; Harden, T. K. (*N*)-methanocarba-2MeSADP (MRS2365) is a subtype-specific agonist that induces rapid desensitization of the $P2Y_1$ receptor of human platelets. *J. Thromb. Haemost.* **2006,** 4, 861-868.
40. Lipinski, C. A. Drug-like properties and the causes of poor solubility and poor permeability. *J. Pharmacol. Toxicol. Methods* **2000,** 44, 235-249.
41. Di, L.; Kerns, E. H.; Carter, G. T. Drug-like property concepts in pharmaceutical design. *Curr. Pharm. Des.* **2009,** 15, 2184-2194.
42. Brust, P.; van den Hoff, J.; Steinbach, J. Development of ^{18}F-labeled radiotracers for neuroreceptor imaging with positron emission tomography. *Neurosci. Bull.* **2014,** 30, 777-811.
43. Thalji, R. K.; Aiyar, N.; Davenport, E. A.; Erhardt, J. A.; Kallal, L. A.; Morrow, D. M.; Senadhi, S.; Burns-Kurtis, C. L.; Marino, J. P., Jr. Benzofuran-substituted urea derivatives as novel $P2Y_1$ receptor antagonists. *Bioorg. Med. Chem. Lett.* **2010,** 20, 4104-4107.
44. Costanzi, S.; Santhosh Kumar, T.; Balasubramanian, R.; Kendall Harden, T.; Jacobson, K. A. Virtual screening leads to the discovery of novel non-nucleotide $P2Y_1$ receptor antagonists. *Bioorg. Med. Chem. Lett.* **2012,** 20, 5254-5261.
45. Pfefferkorn, J. A.; Choi, C.; Winters, T.; Kennedy, R.; Chi, L.; Perrin, L. A.; Lu, G.; Ping, Y. W.; McClanahan, T.; Schroeder, R.; Leininger, M. T.; Geyer, A.; Schefzick, S.;

Atherton, J. $P2Y_1$ receptor antagonists as novel antithrombotic agents. *Bioorg. Med. Chem. Lett.* **2008,** 18, 3338-3343.

46. Zhang, D.; Gao, Z. G.; Zhang, K.; Kiselev, E.; Crane, S.; Wang, J.; Paoletta, S.; Yi, C.; Ma, L.; Zhang, W.; Han, G. W.; Liu, H.; Cherezov, V.; Katritch, V.; Jiang, H.; Stevens, R. C.; Jacobson, K. A.; Zhao, Q.; Wu, B. Two disparate ligand-binding sites in the human $P2Y_1$ receptor. *Nature* **2015,** 520, 317-321.

47. Gao, Z. G.; Jacobson, K. A. Distinct signaling patterns of allosteric antagonism at the P2Y1 receptor. *Mol. Pharmacol.* **2017**, mol.117.109660.

48. Mañé, N.; Jiménez-Sábado, V.; Jiménez, M. BPTU, an allosteric antagonist of $P2Y_1$ receptor, blocks nerve mediated inhibitory neuromuscular responses in the gastrointestinal tract of rodents. *Neuropharmacology* **2016,** 110, 376-385.

49. Yuan, S.; Chan, H. C. S.; Vogel, H.; Filipek, S.; Stevens, R. C.; Palczewski, K. The molecular mechanism of $P2Y_1$ receptor activation. *Angew. Chem. Int. Ed.* **2016,** 55, 10331-10335.

50. Zhang, X.; Lu, F.; Chen, Y. K. Discovery of potential orthosteric and allosteric antagonists of $P2Y_1R$ from chinese herbs by molecular simulation methods. *Evid. Based Complement. Alternat. Med.* **2016,** 2016, ID 4320201.

51. Wang, T. C.; Qiao, J. X.; Clark, C. G.; Jua, J.; Price, L. A.; Wu, Q.; Chang, M.; Zheng, J.; Huang, C. S.; Everlof, G.; Schumacher, W. A.; Wong, P. C.; Seiffert, D. A.; Stewart, A. B.; Bostwick, J. S.; Crain, E. J.; Watson, C. A.; Rehfuss, R.; Wexler, R. R.; Lam, P. Y. Discovery of diarylurea $P2Y_1$ antagonists with improved aqueous solubility. *Bioorg. Med. Chem. Lett.* **2013,** 23, 3239-3243.

52. Pi, Z.; Sutton, J.; Lloyd, J.; Hua, J.; Price, L.; Wu, Q.; Chang, M.; Zheng, J.; Rehfuss, R.; Huang, C. S.; Wexler, R. R.; Lam, P. Y. 2-Aminothiazole based $P2Y_1$ antagonists as novel antiplatelet agents. *Bioorg. Med. Chem. Lett.* **2013,** 23, 4206-4209.

53. Kuchar, M.; Mamat, C. Methods to increase the metabolic stability of ^{18}F-radiotracers. *Molecules* **2015,** 20, 16186-16220.

54. Neumann, W.; Xu, S.; Sárosi, M. B.; Scholz, M. S.; Crews, B. C.; Ghebreselasie, K.; Banerjee, S.; Marnett, L. J.; Hey□Hawkins, E. nido□Dicarbaborate induces potent and selective inhibition of cyclooxygenase□2. *ChemMedChem* **2016,** 11, 175-178.

55. Scholz, M.; Blobaum, A. L.; Marnett, L. J.; Hey-Hawkins, E. *ortho*-Carbaborane derivatives of indomethacin as cyclooxygenase (COX)-2 selective inhibitors. *Bioorg. Med. Chem.* **2012,** 20, 4830-4837.

56. Laube, M.; Neumann, W.; Scholz, M.; Lönnecke, P.; Crews, B.; Marnett, L. J.; Pietzsch, J.; Kniess, T.; Hey-Hawkins, E. 2-Carbaborane-3-phenyl-1*H*-indoles - synthesis *via* McMurry reaction and cyclooxygenase (COX) inhibition activity. *ChemMedChem* **2013,** 8, 329-335.

57. Miyaura, N.; Suzuki, A. Stereoselective synthesis of arylated (*E*)-alkenes by the reaction of alk-1-enylboranes with aryl halides in the presence of palladium catalyst. *J. Chem. Soc. Chem. Comm.* **1979**, 866-867.

58. Miyaura, N.; Yamada, K.; Suzuki, A. A new stereospecific cross-coupling by the palladium-catalyzed reaction of 1-alkenylboranes with 1-alkenyl or 1-alkynyl halides. *Tet. Lett.* **1979,** 20, 3437-3440.
59. Kasar, R. A.; Knudsen, G. M.; Kahl, S. B. Synthesis of 3-amino-1-carboxy-o-carborane and an improved, general method for the synthesis of all three *C*-amino-*C*-carboxycarboranes. *Inorg. Chem.* **1999,** 38, 2936-2940.
60. Petrus, H.; Knut, I. Hydrophilic interaction chromatography. *J. Sep. Sci*. **2006,** 29, 1784-1821.
61. K.C. Lee, S.-Y. L., Y.S. Choe, D.I.Chi Metabolic stability of [^{18}F]fluoroalkylbiphenyls *Bull. Korean. Chem. Soc* **2004,** 25, 1225-1230.
62. King, R. S. Biotransformations in Drug Metabolism. In *Drug Metabolism Handbook: Concepts and Applications*, Ala F. Nassar, P. F. H., JoAnn Scatina, Ed. John Wiley & Sons, Inc.: NJ, USA, 2008; pp 17-40.
63. Guengerich, F. P. Common and uncommon cytochrome P450 reactions related to metabolism and chemical toxicity. *Chem. Res. Toxicol.* **2001,** 14, 611-650.
64. Testa, B.; Kramer, S. D. The biochemistry of drug metabolism--an introduction: Part 2. Redox reactions and their enzymes. *Chem. Biodivers.* **2007,** 4, 257-405.
65. Ferguson, C. S.; Tyndale, R. F. Cytochrome P450 enzymes in the brain: emerging evidence of biological significance. *Trends Pharmacol. Sci.* **2011,** 32, 708-714.
66. Coenen, H. H.; Laufer, P.; Stöcklin, G.; Wienhard, K.; Pawlik, G.; Böcher-Schwarz, H. G.; Heiss, W. D. 3-*N*-(2-[^{18}F]-fluoroethyl)-spiperone: A novel ligand for cerebral dopamine receptor studies with PET. *Life Sci.* **1987,** 40, 81-88.
67. Welch, M. J.; Katzenellenbogen, J. A.; Mathias, C. J.; Brodack, J. W.; Carlson, K. E.; Chi, D. Y.; Dence, C. S.; Kilbourn, M. R.; Perlmutter, J. S.; Raichle, M. E.; et al. *N*-(3-[^{18}F]fluoropropyl)-spiperone: the preferred ^{18}F labeled spiperone analog for positron emission tomographic studies of the dopamine receptor. *Int. J. Rad. Appl. Instrum. B* **1988,** 15, 83-97.
68. Wenzel, B.; Mollitor, J.; Deuther-Conrad, W.; Dukic-Stefanovic, S.; Kranz, M.; Vraka, C.; Teodoro, R.; Günther, R.; Donat, C. K.; Ludwig, F.-A.; Fischer, S.; Smits, R.; Wadsak, W.; Mitterhauser, M.; Steinbach, J.; Hoepping, A.; Brust, P. Development of a novel nonpeptidic ^{18}F-labeled radiotracer for in vivo imaging of oxytocin receptors with positron emission tomography. *J. Med. Chem.* **2016,** 59, 1800-1817.
69. Kirchmair, J.; Goller, A. H.; Lang, D.; Kunze, J.; Testa, B.; Wilson, I. D.; Glen, R. C.; Schneider, G. Predicting drug metabolism: experiment and/or computation? *Nat. Rev. Drug Discov.* **2015,** 14, 387-404.

Highlights

- A series of fluorinated, non-nucleotidic $P2Y_1R$ ligands was developed
- Derivative **18** was identified with an 18-fold higher antagonistic potency than the lead compound **7**
- [^{18}F]**18** was obtained in high radiochemical purity, yield and molar activities

Supporting Information

Studies towards the development of a PET radiotracer for imaging of the $P2Y_1$ receptors in the brain: synthesis, ^{18}F-labeling and preliminary biological evaluation

Rareş-Petru Moldovan[a,], Barbara Wenzel[a], Rodrigo Teodoro[a], Wilma Neumann[c], Sladjana Dukic-Stefanovic[a], Werner Kraus[b], Peijing Rong[e],*

Winnie Deuther-Conrad[a], Evamarie Hey-Hawkins[c], Ute Krügel[d§] and Peter Brust[a§]

[a] Institute of Radiopharmaceutical Cancer Research, Helmholtz-Zentrum Dresden-Rossendorf e. V., Permoserstraße 15, 04318 Leipzig, Germany

[b] BAM Federal Institute for Materials Research and Testing, Richard-Willstätter-Str. 11, 12489 Berlin, Germany

[c] Institute of Inorganic Chemistry, Faculty of Chemistry and Mineralogy, Leipzig University, 04103 Leipzig, Germany

[d] Rudolf Boehm Institute of Pharmacology and Toxicology, Medical Faculty, Leipzig University, 04107 Leipzig, Germany

[e] Institute of Acupuncture and Moxibustion, China Academy of Chinese Medical Sciences, 100700 Beijing, China

Corresponding author.

R.-P. Moldovan*: phone, 0049 341 234179 4634; e-mail, r.moldovan@hzdr.de.

Supporting Information: ^1H NMR spectra of target compounds, HRMS of compound **32**, crystallographic data of compound **36**, HPLC chromatograms of target compounds.

^{1}H NMR (400 MHz, $CDCl_3$) cpd. **7**

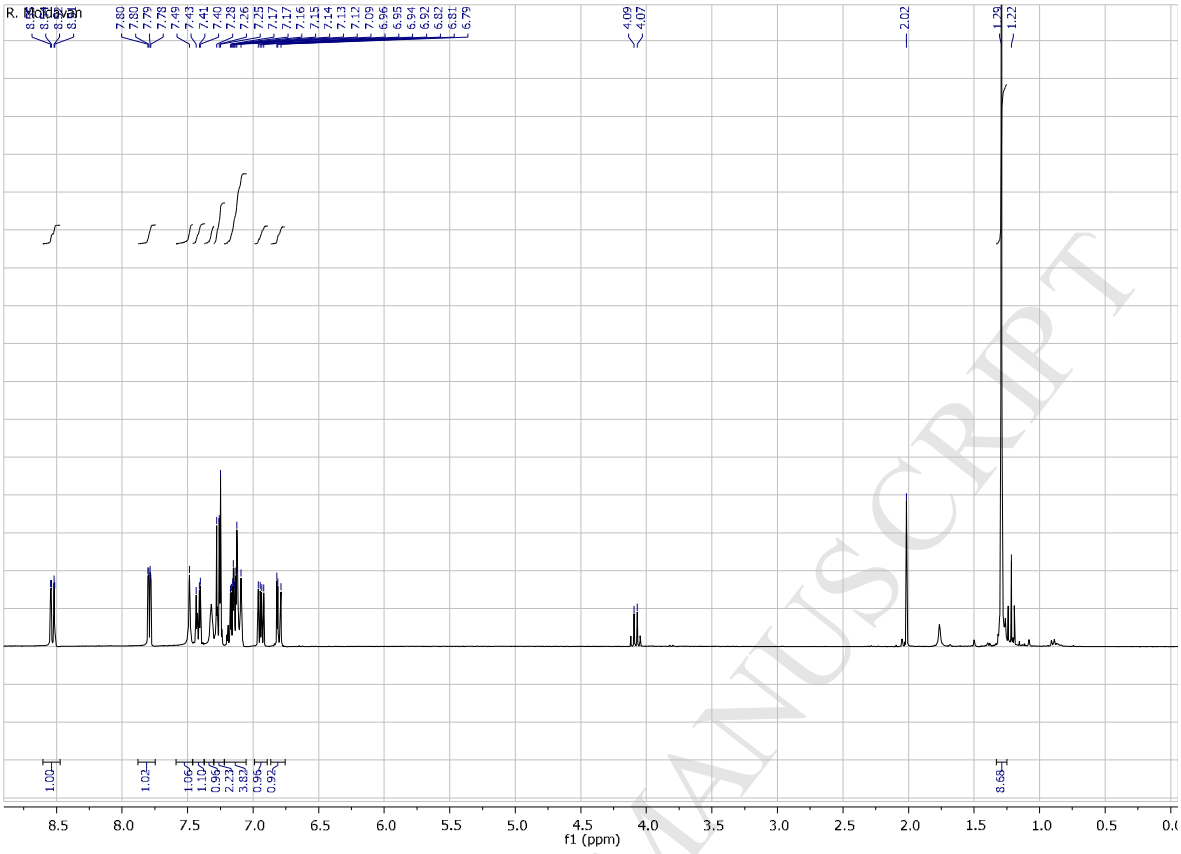

^{1}H NMR (400 MHz, $CDCl_3$) cpd. **18**

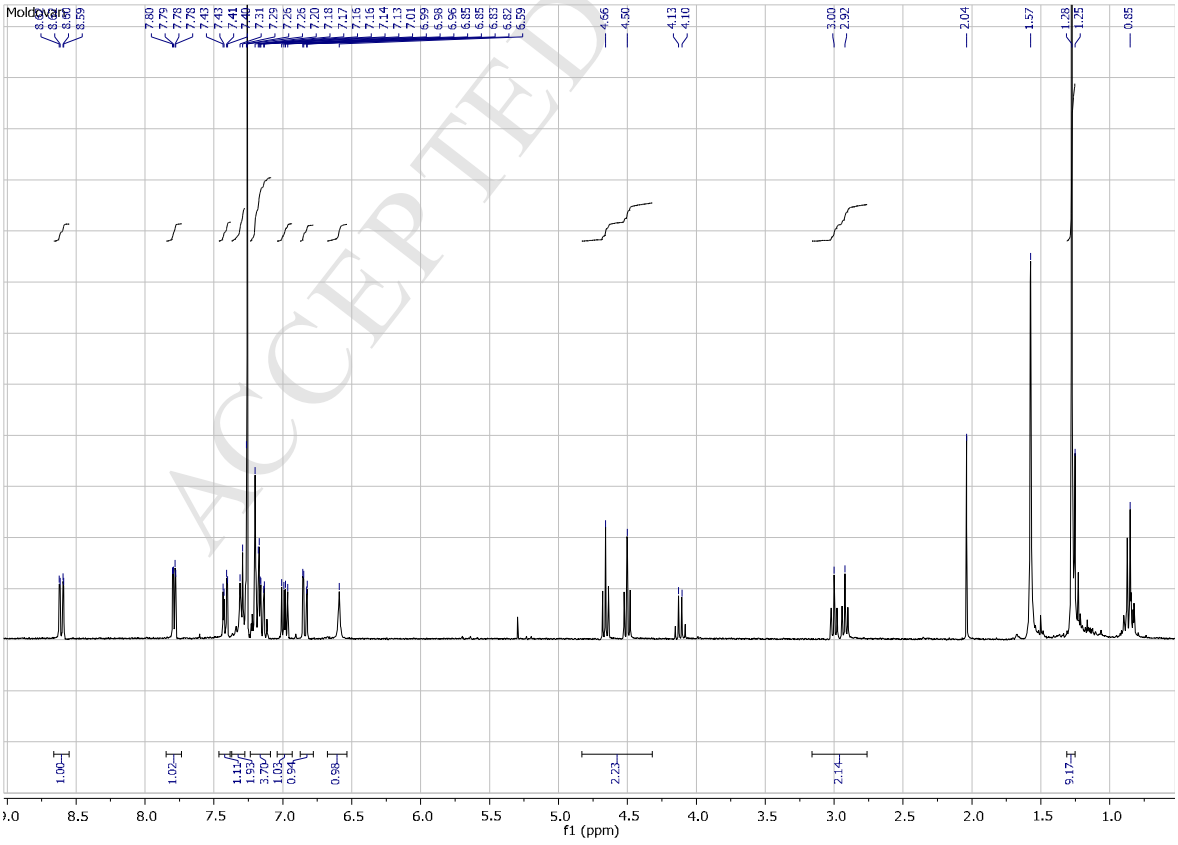

^{1}H NMR (400 MHz, $CDCl_3$) cpd. **19**

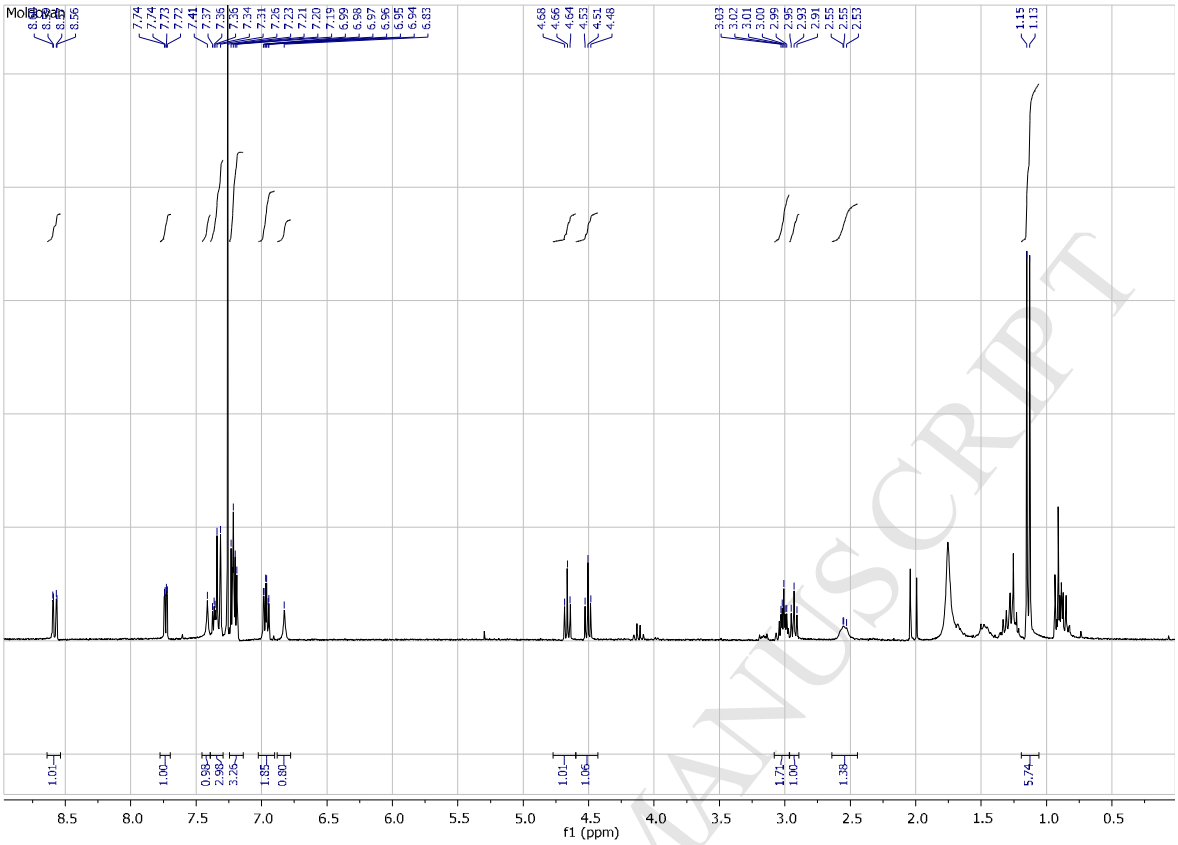

^{1}H NMR (400 MHz, $CDCl_3$) cpd. **22**

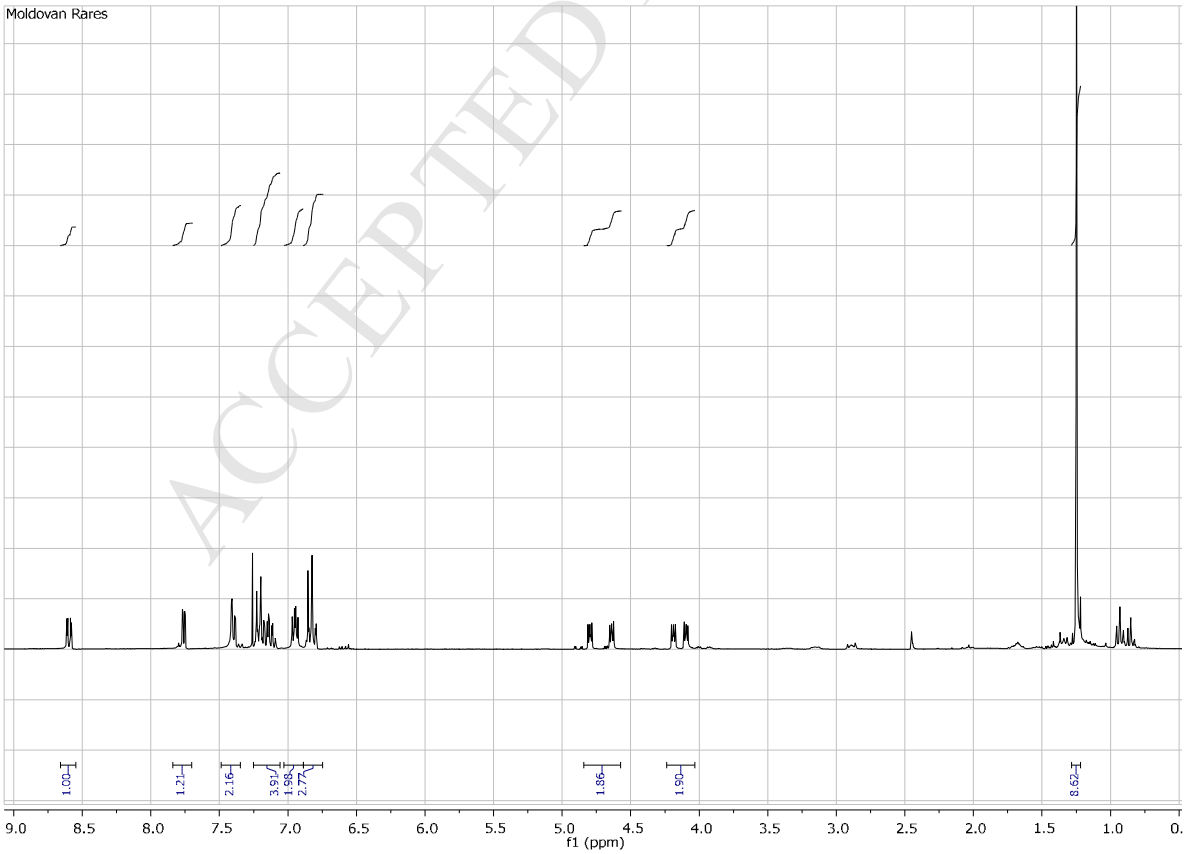

^{1}H NMR (400 MHz, $CDCl_3$) cpd. **23**

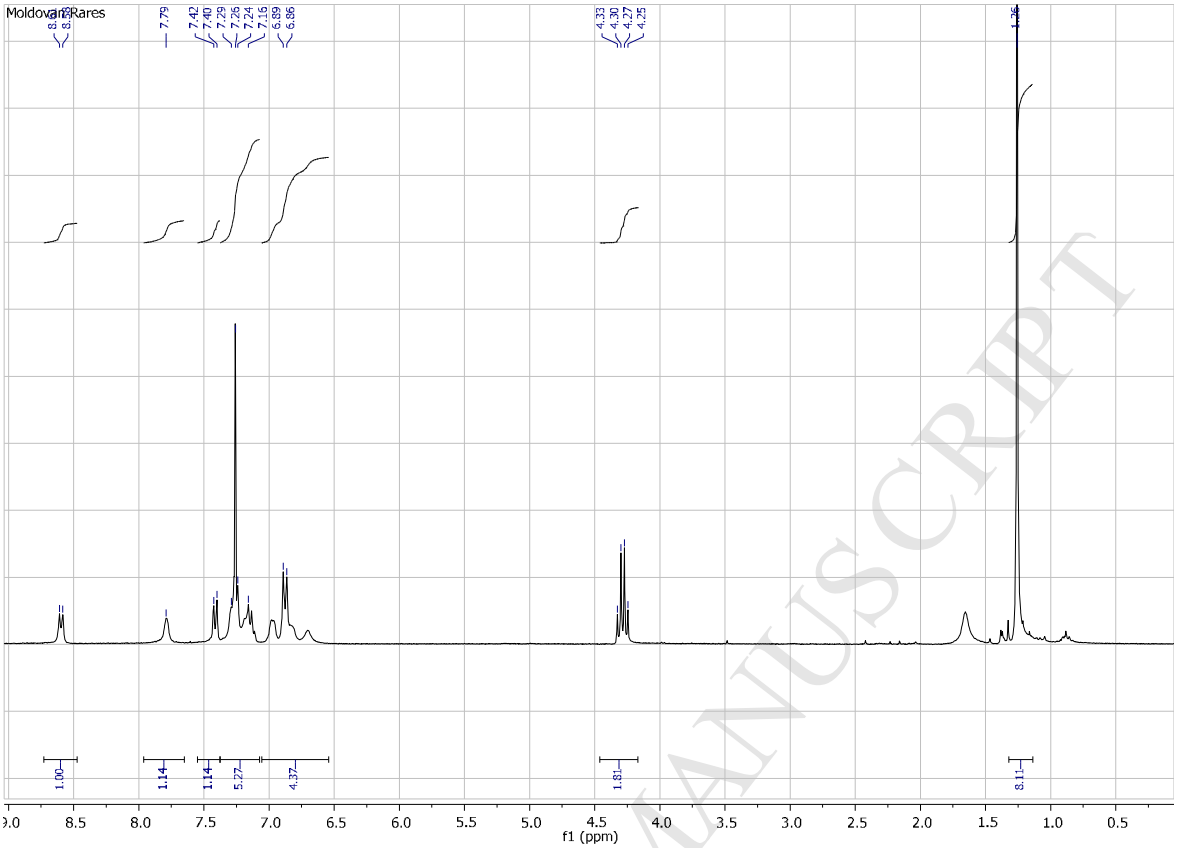

^{1}H NMR (400 MHz, $CDCl_3$) cpd. **24**

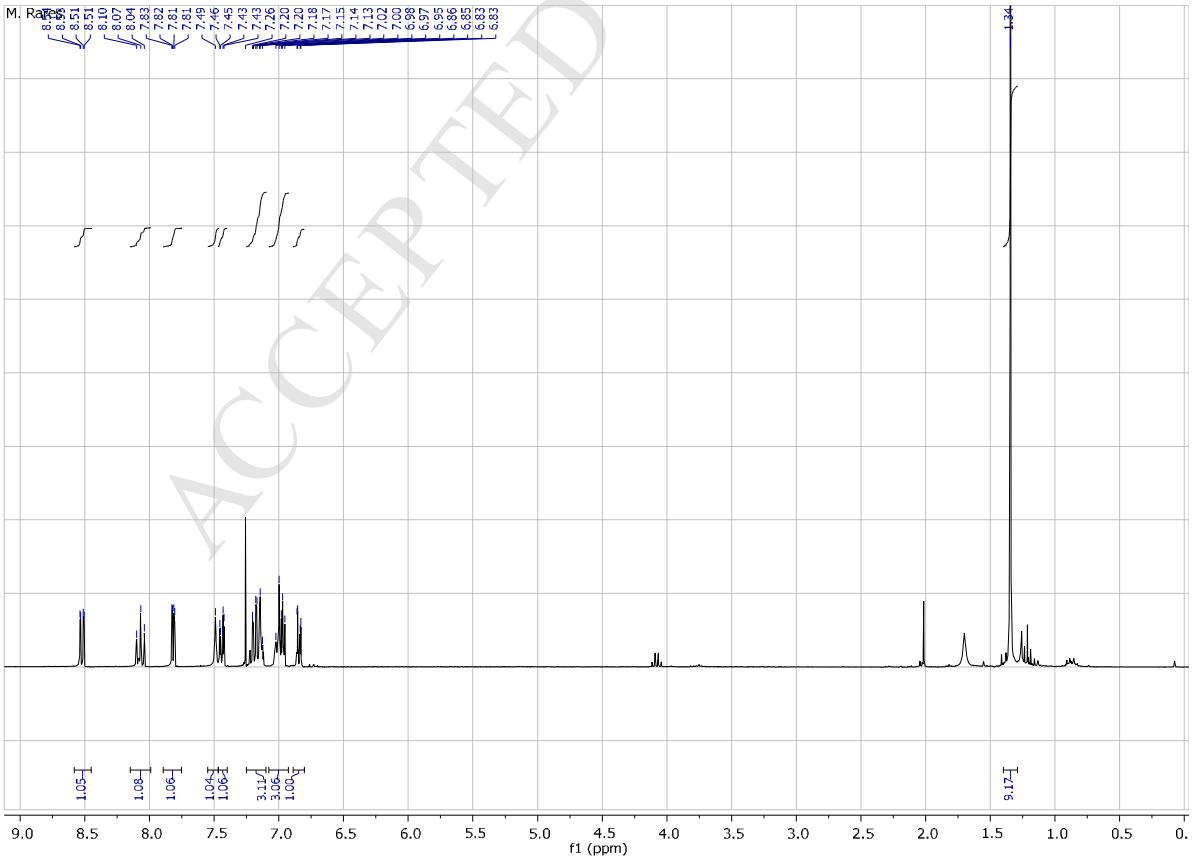

^{1}H NMR (400 MHz, $CDCl_3$) cpd. **25**

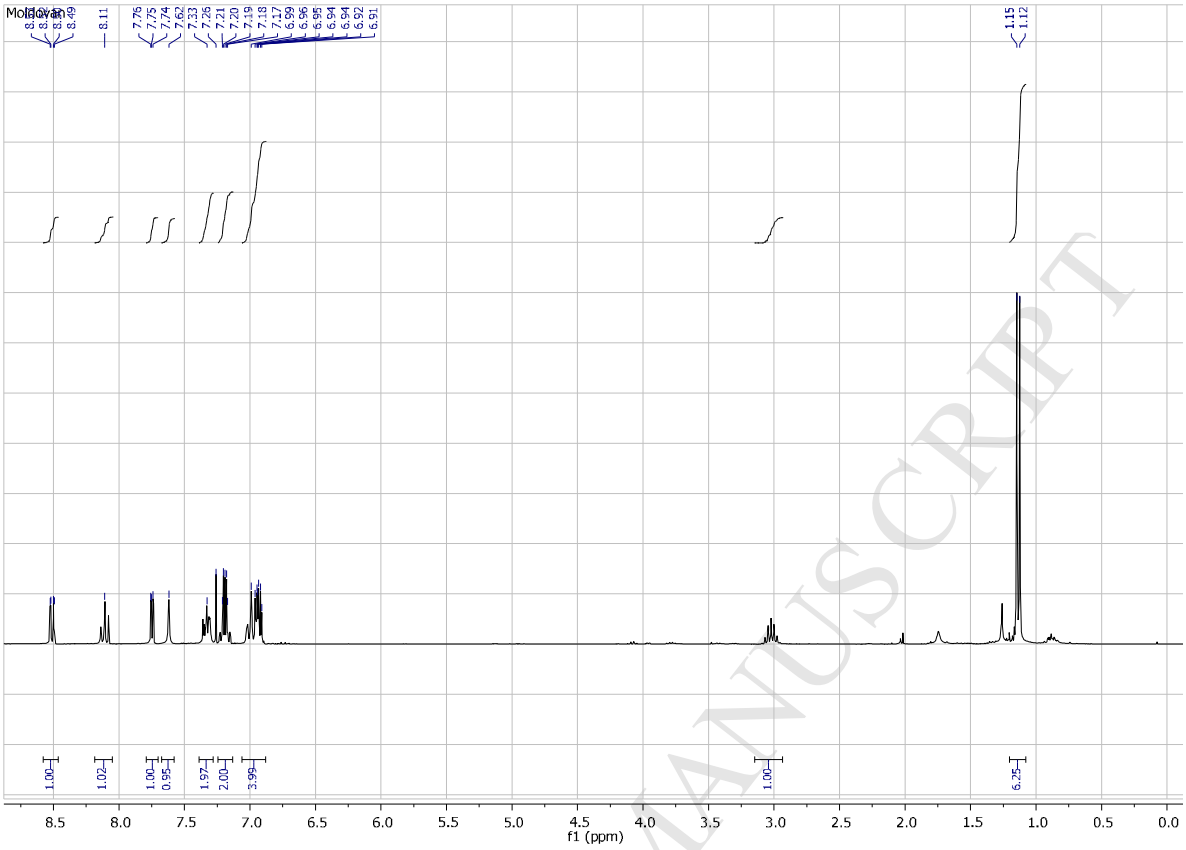

^{1}H NMR (400 MHz, $CDCl_3$) cpd. **28**

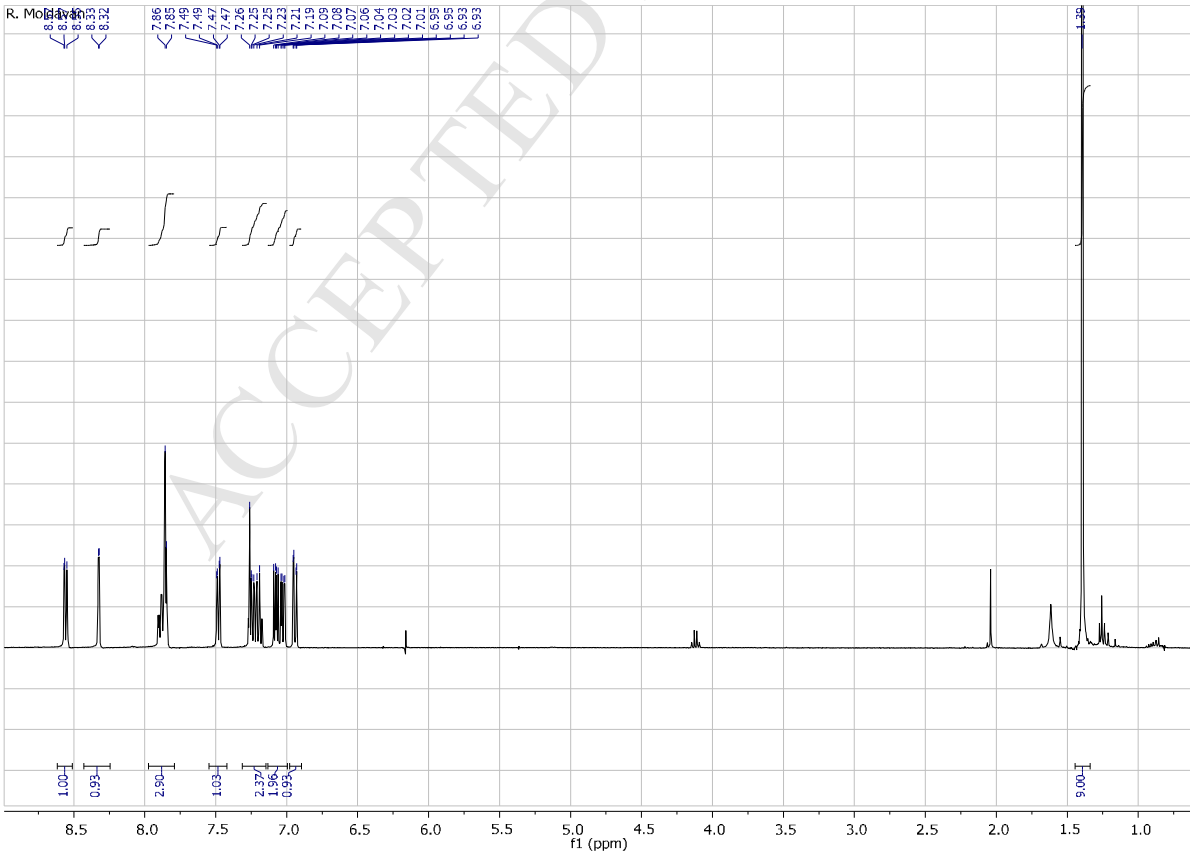

^{1}H NMR (400 MHz, $CDCl_3$) cpd. **29**

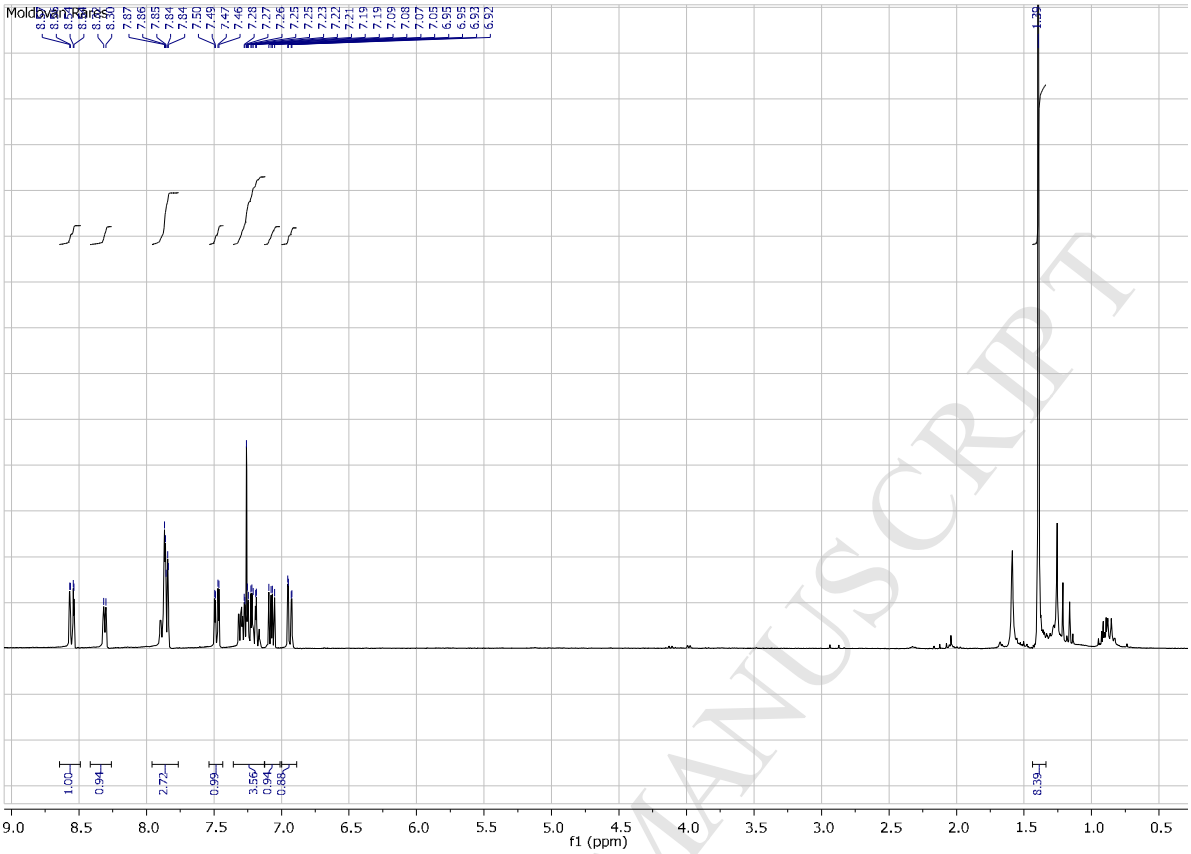

^{1}H NMR (400 MHz, $CDCl_3$) cpd. **30**

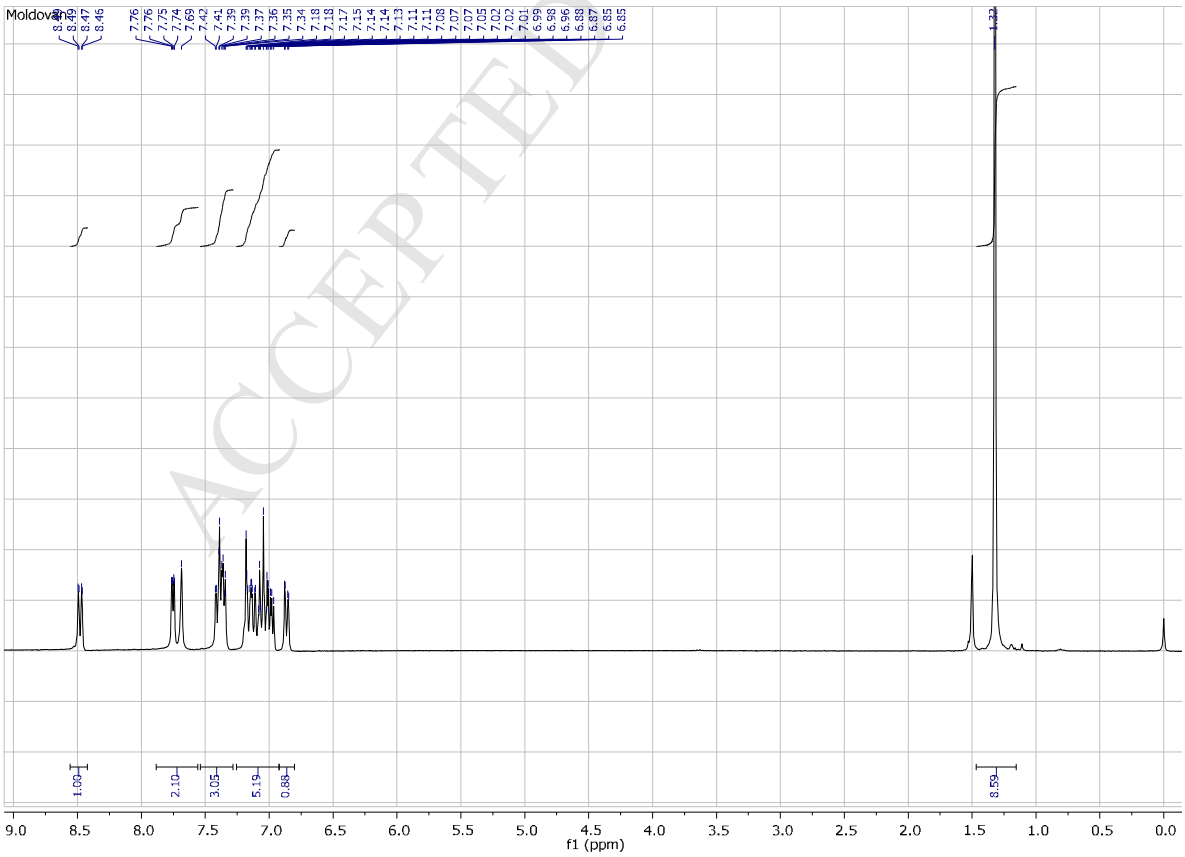

^{1}H NMR (400 MHz, $CDCl_3$) cpd. **32**

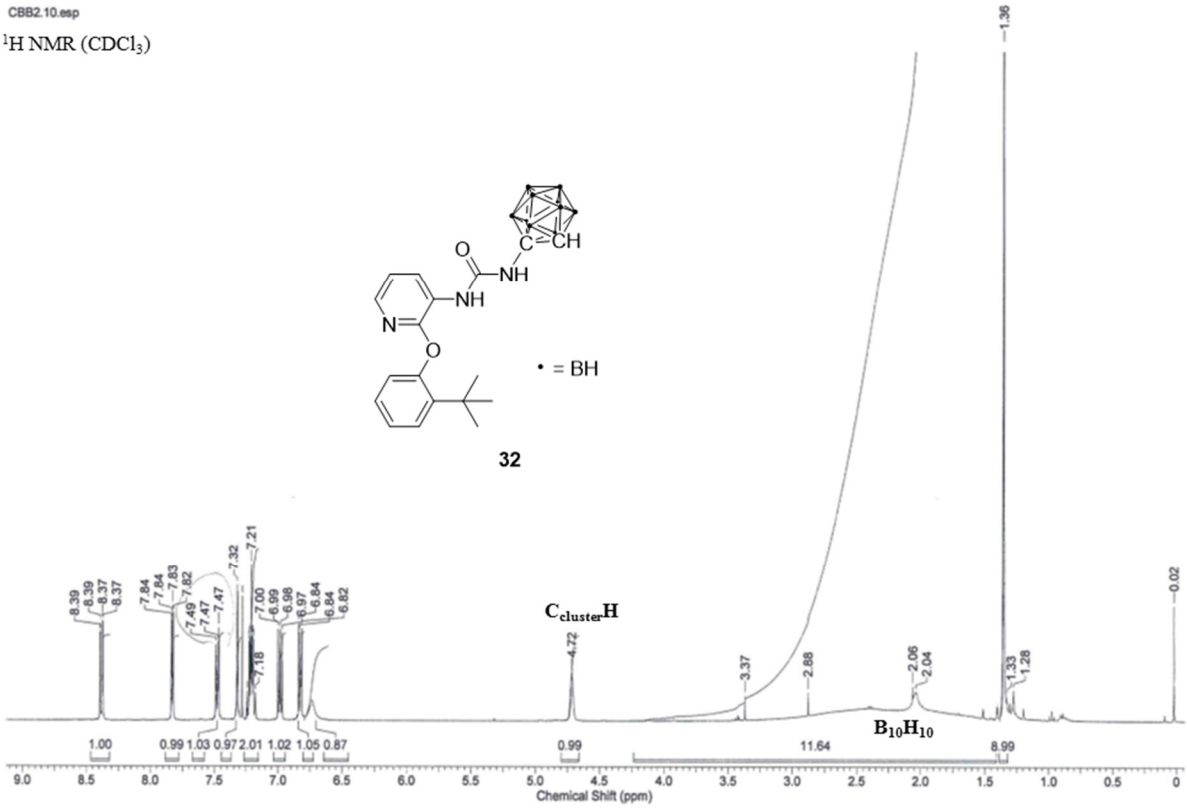

^{1}H NMR (400 MHz, $CDCl_3$) cpd. **36**

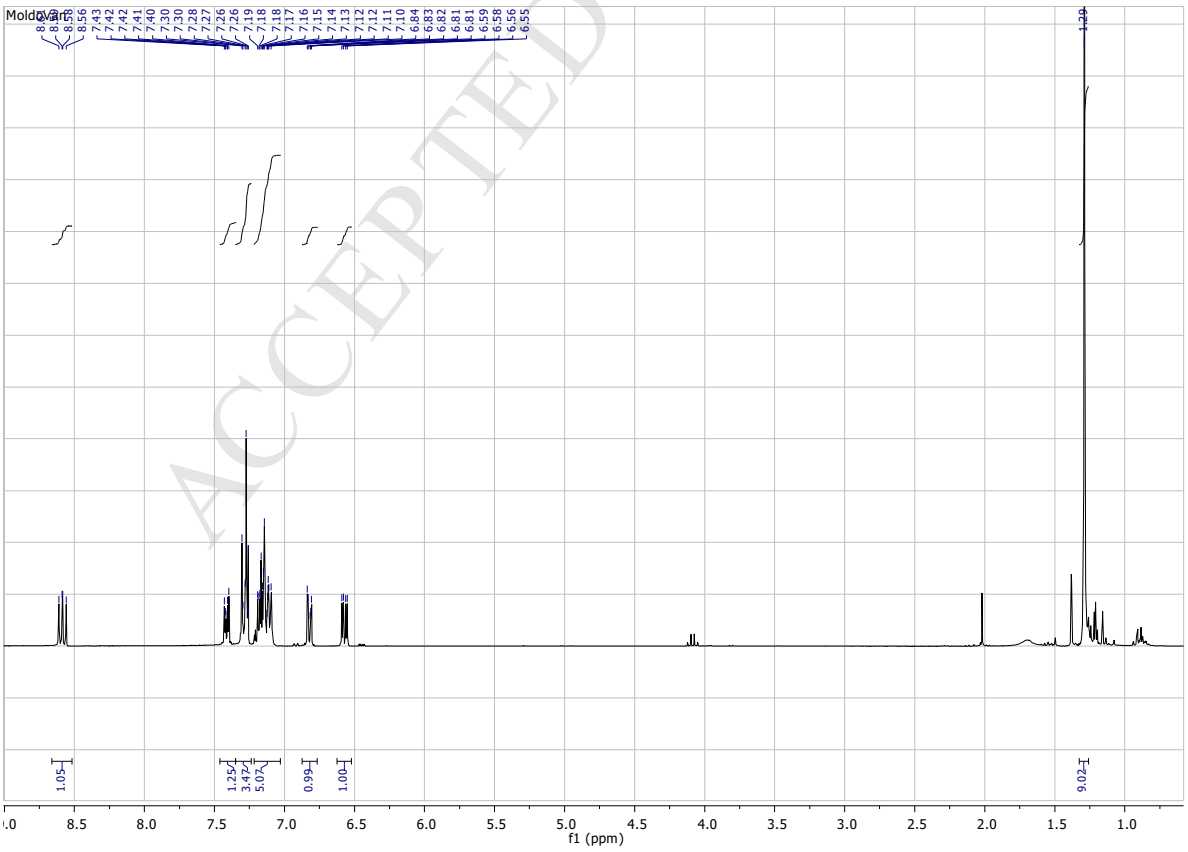

^{1}H NMR (400 MHz, $CDCl_3$) cpd. **37**

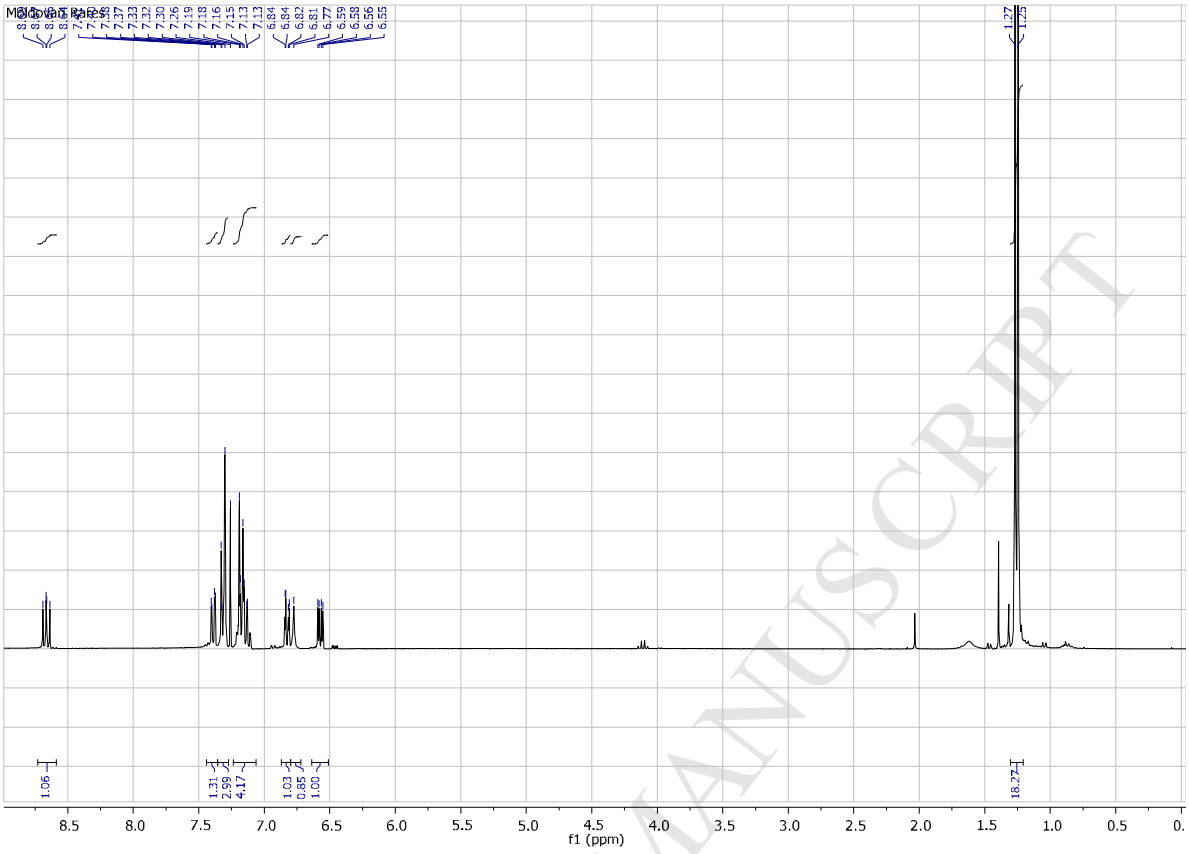

^{1}H NMR (400 MHz, $CDCl_3$) cpd. **38**

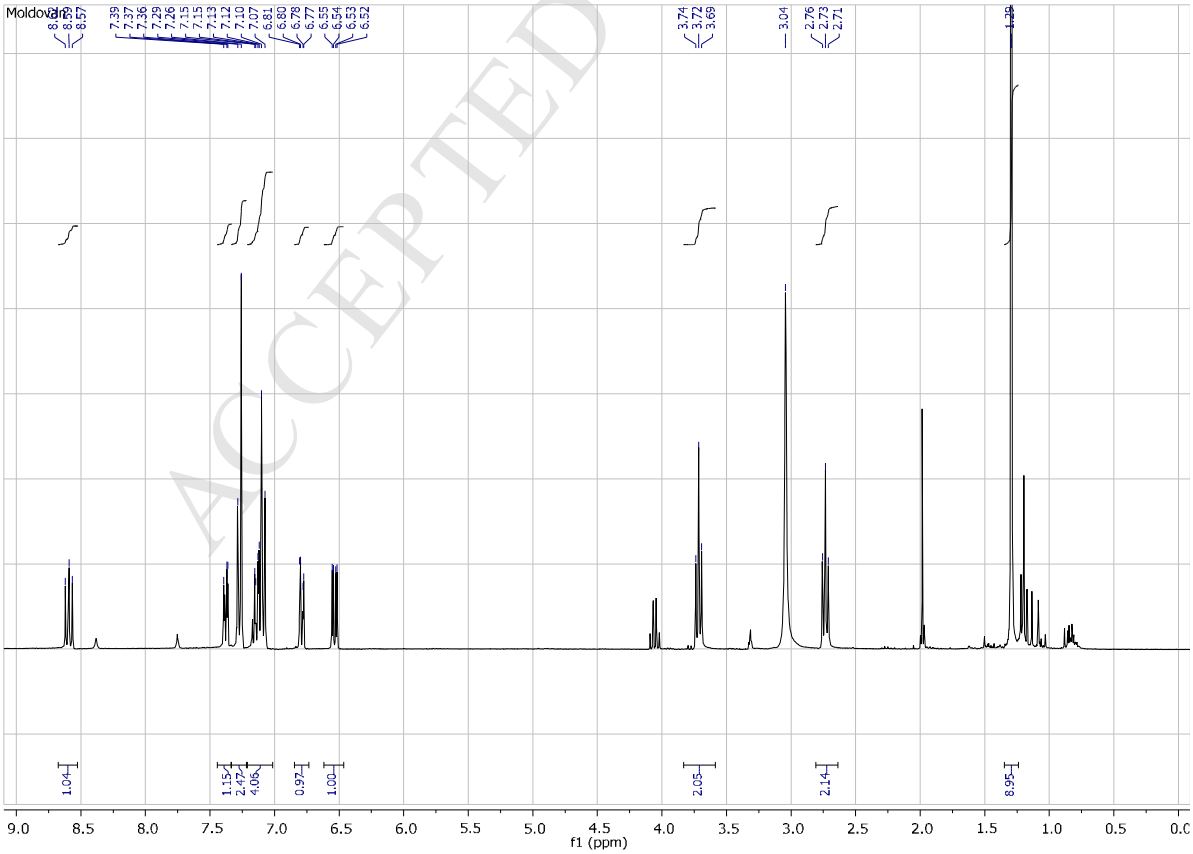

^{1}H NMR (400 MHz, $CDCl_3$) cpd. **39**

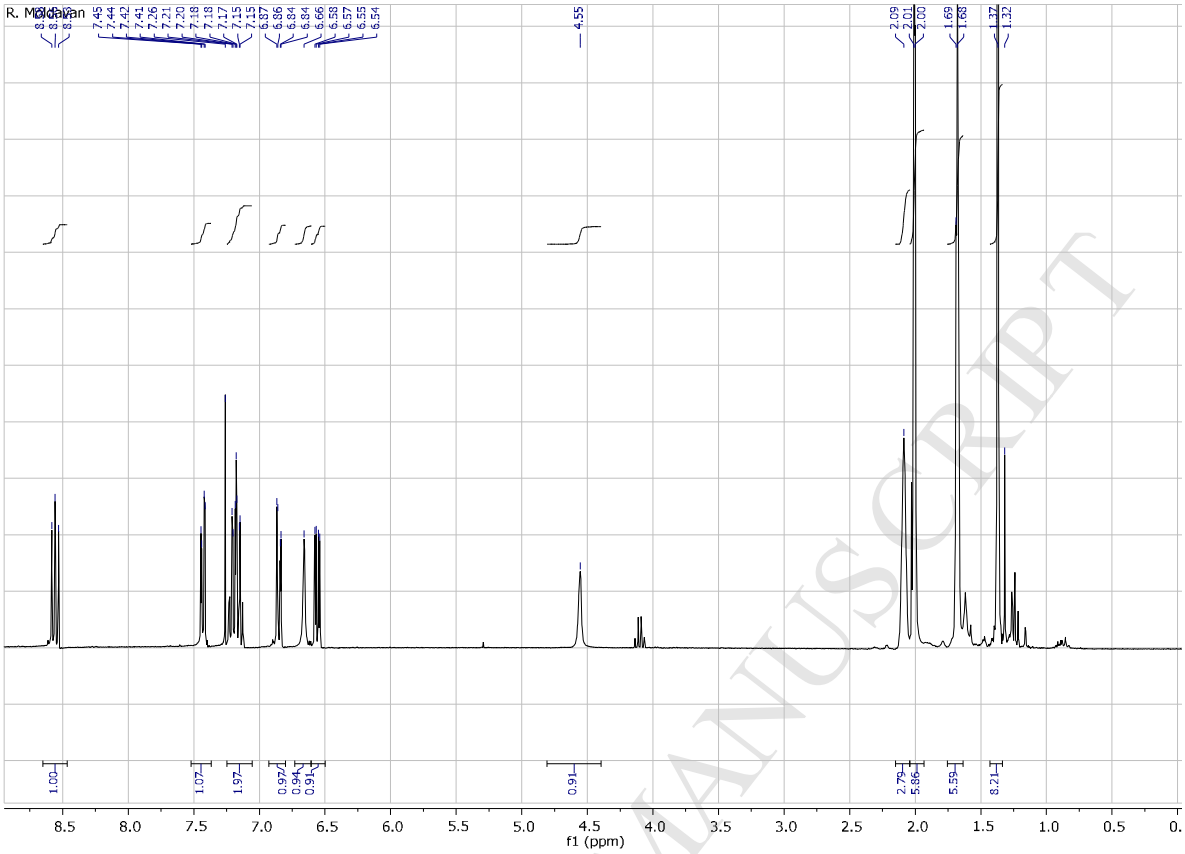

^{1}H NMR (400 MHz, $CDCl_3$) cpd. **40**

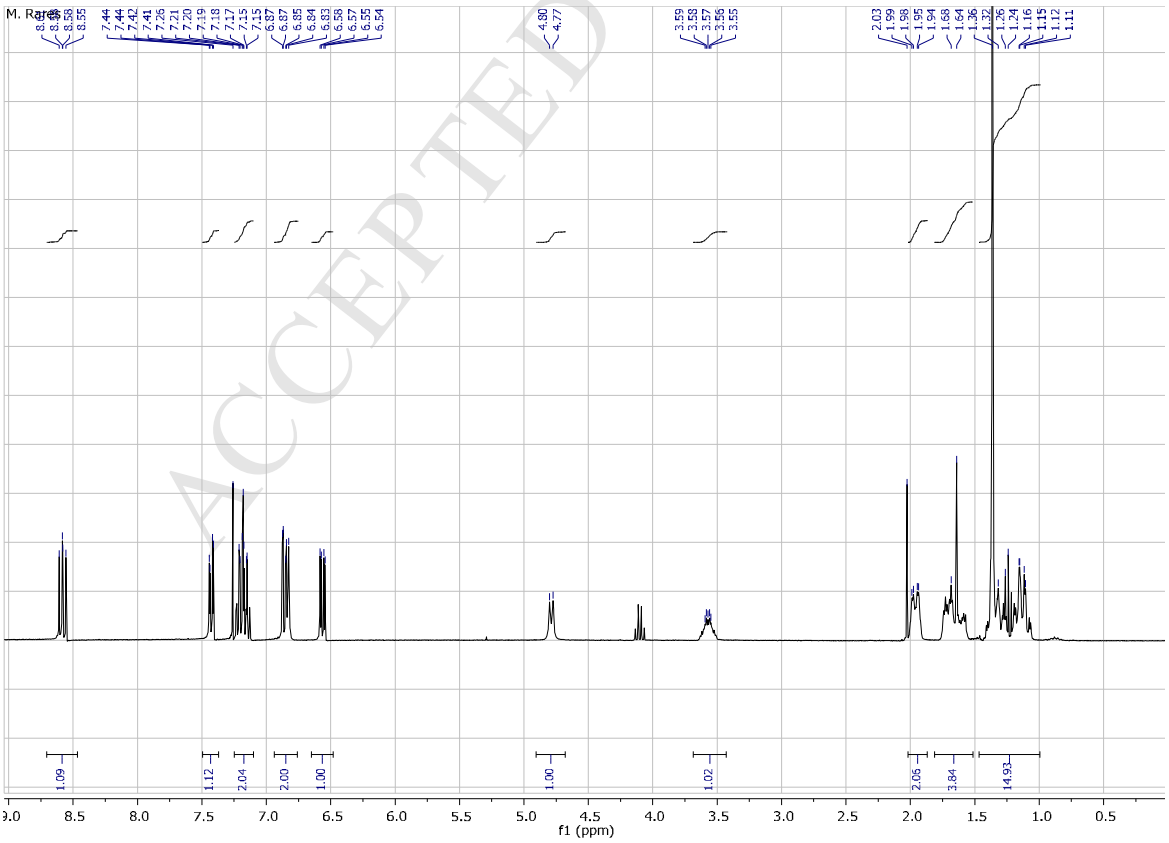

^{1}H NMR (400 MHz, $CDCl_3$) cpd. **41**

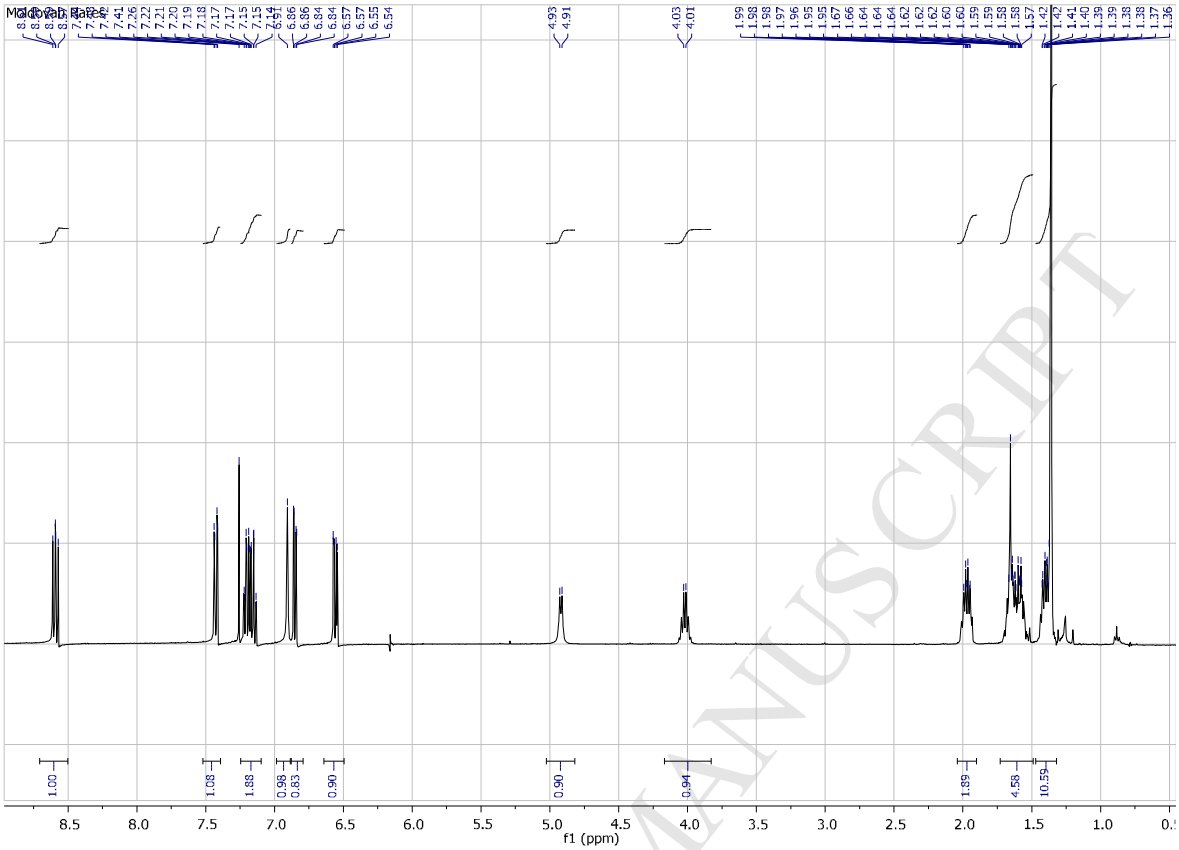

^{1}H NMR (400 MHz, $CDCl_3$) cpd. **42**

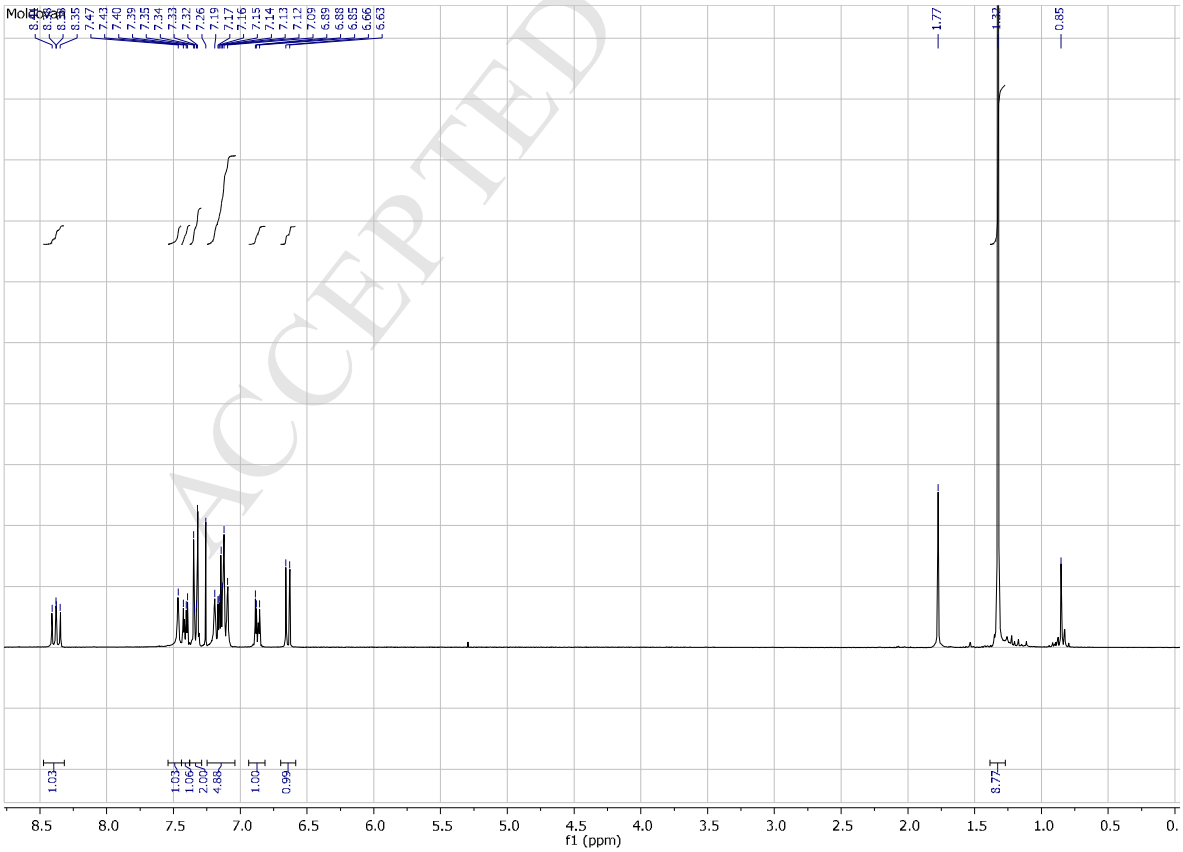

^{1}H NMR (400 MHz, $CDCl_3$) cpd. **43**

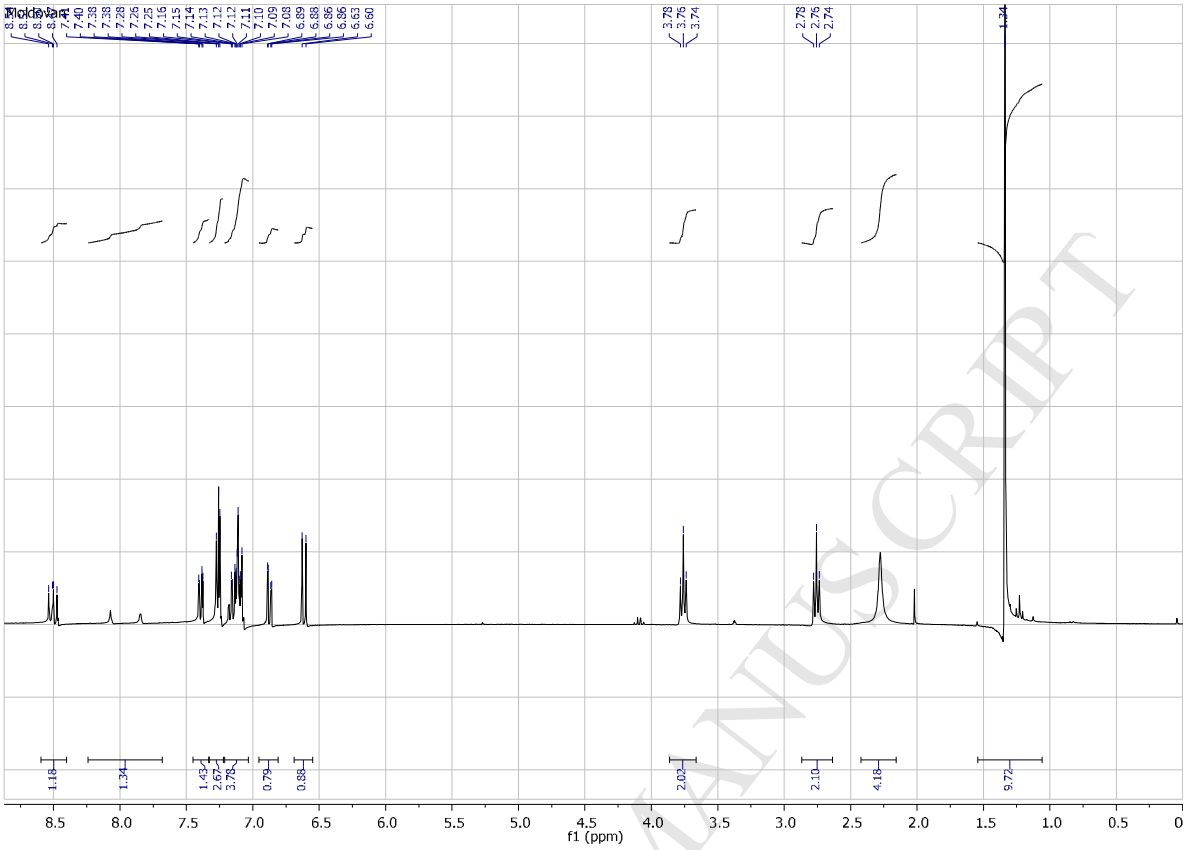

^{1}H NMR (400 MHz, $CDCl_3$) cpd. **45**

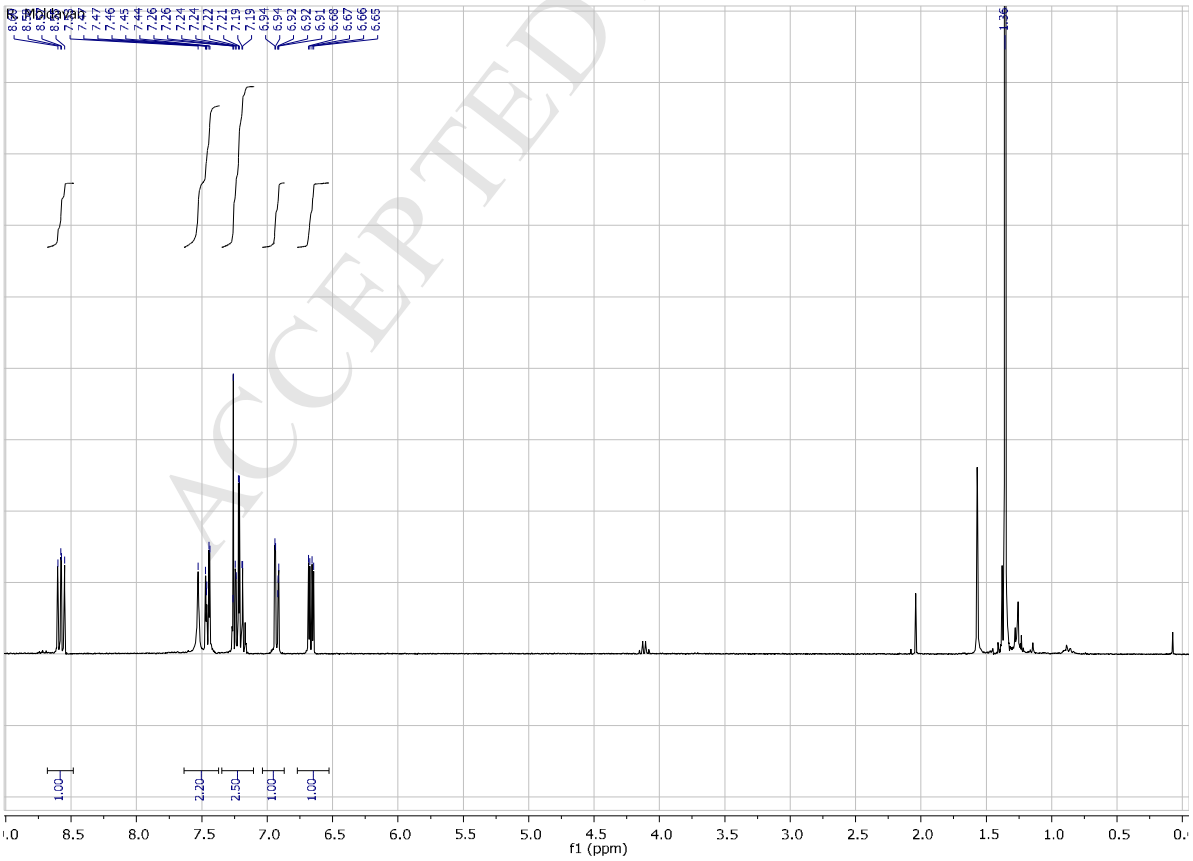

^{1}H NMR (400 MHz, $CDCl_3$) cpd. **47**

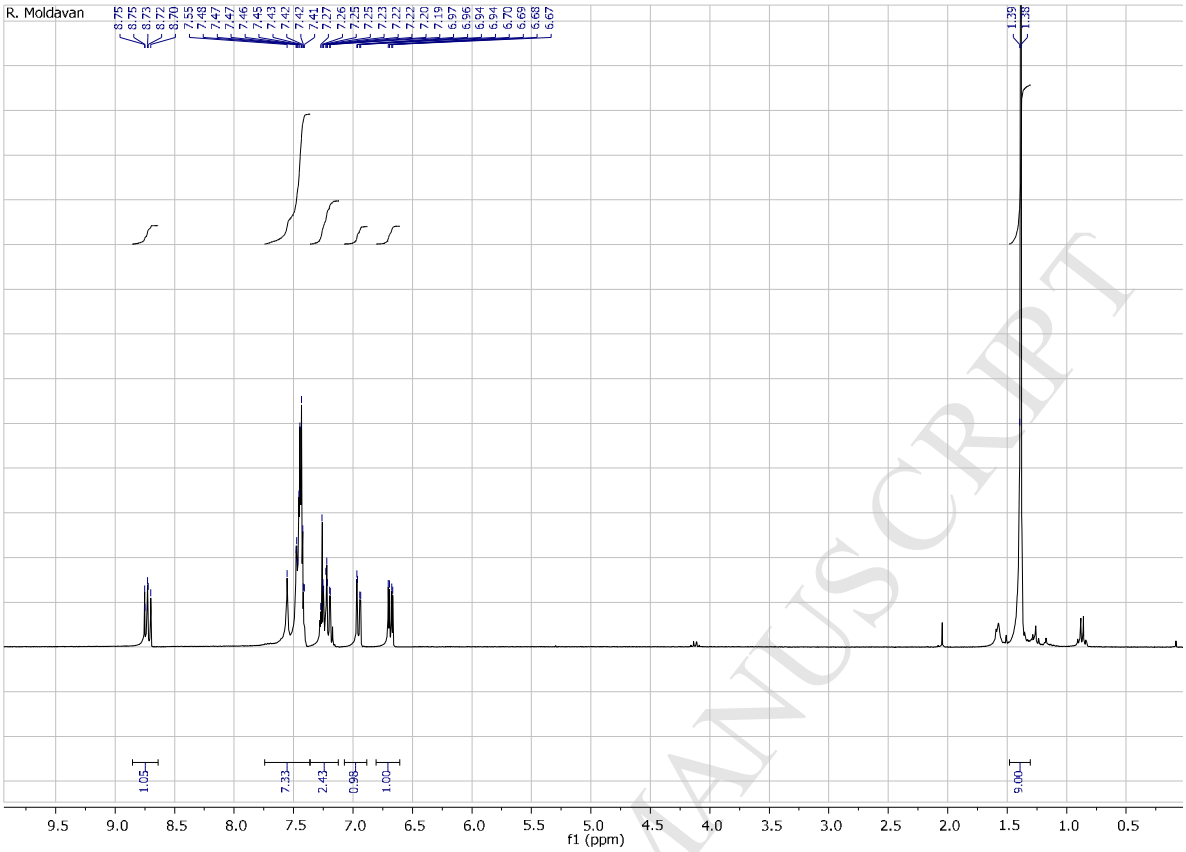

^{1}H NMR (400 MHz, $CDCl_3$) cpd. **49**

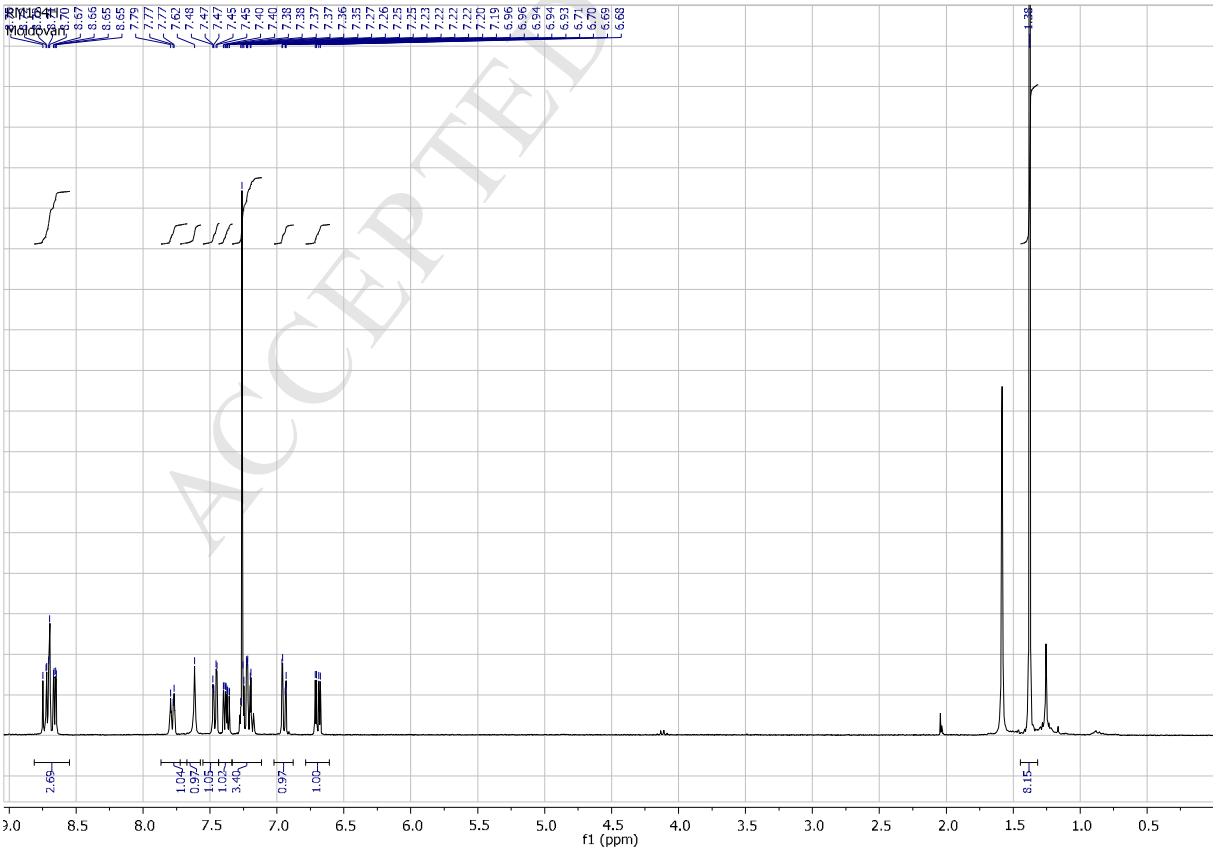

^{1}H NMR (400 MHz, $CDCl_3$) cpd. **53**

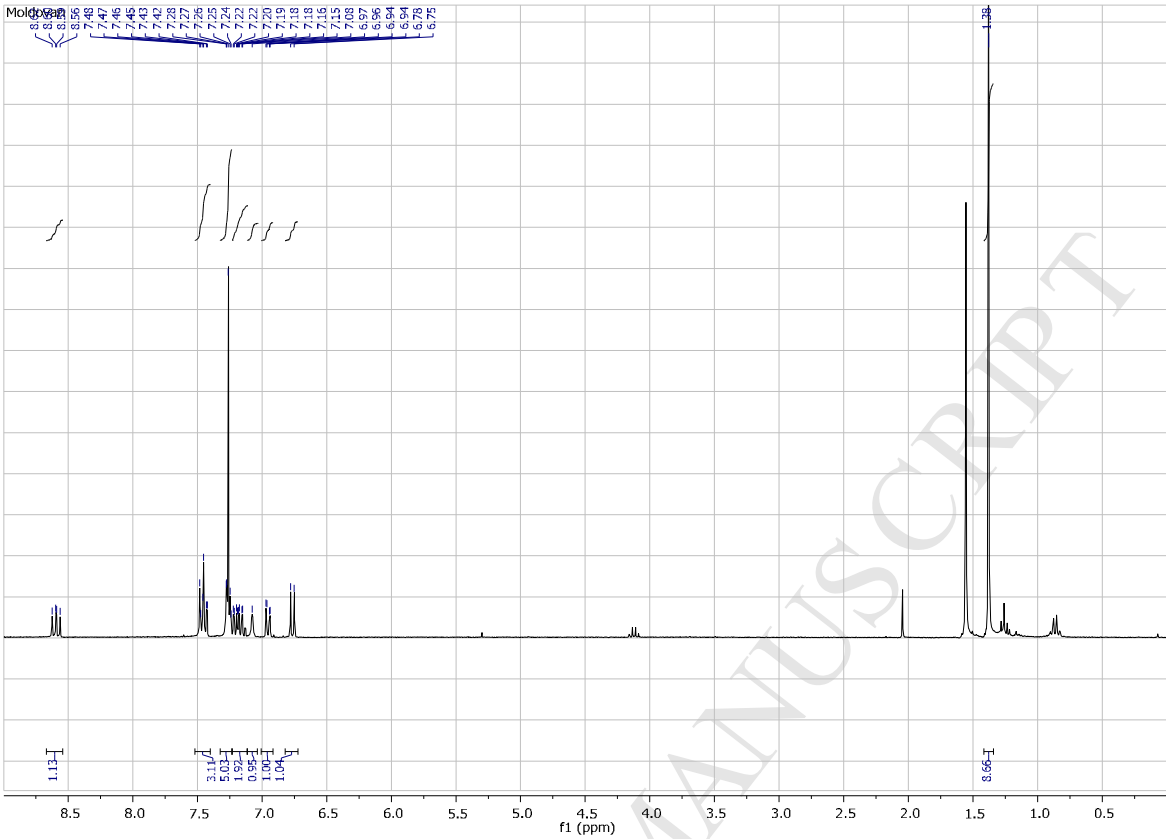

^{1}H NMR (400 MHz, $CDCl_3$) cpd. **54**

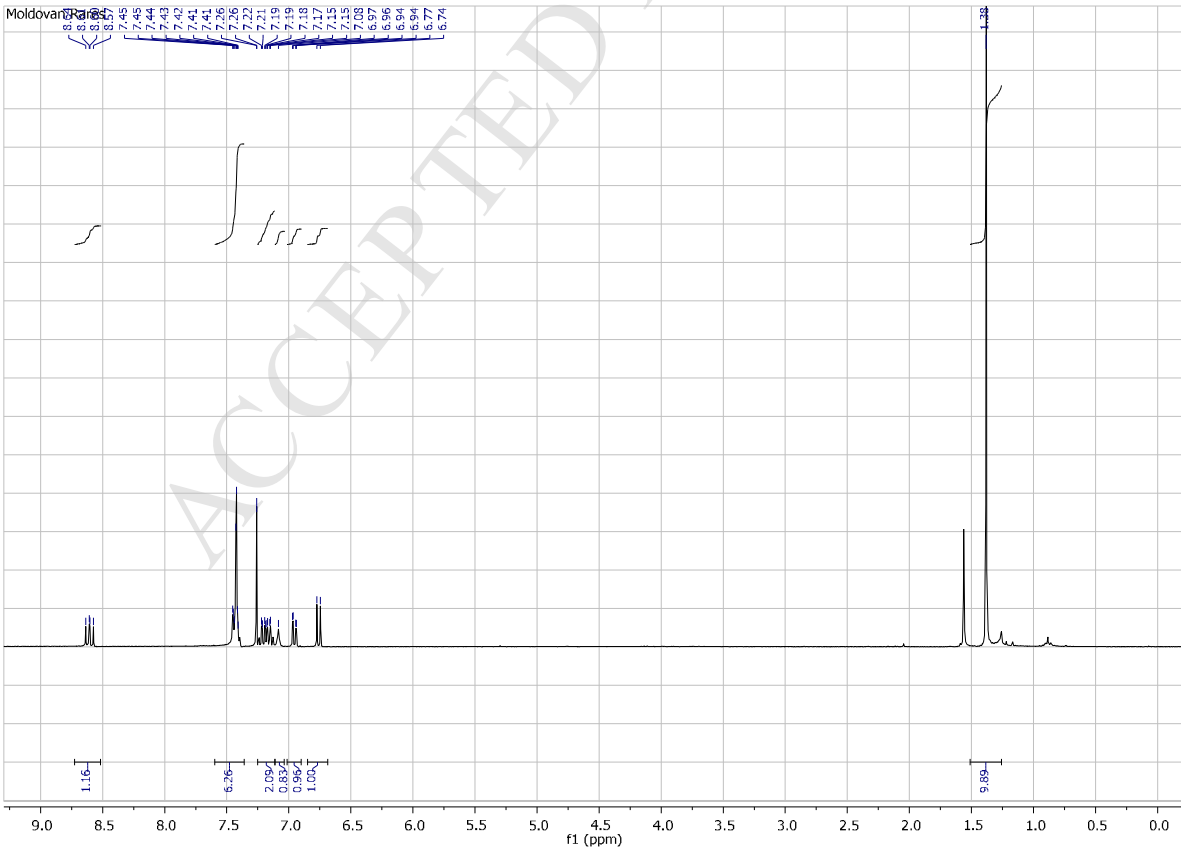

HRFTMS (ESI+) cpd. **32**

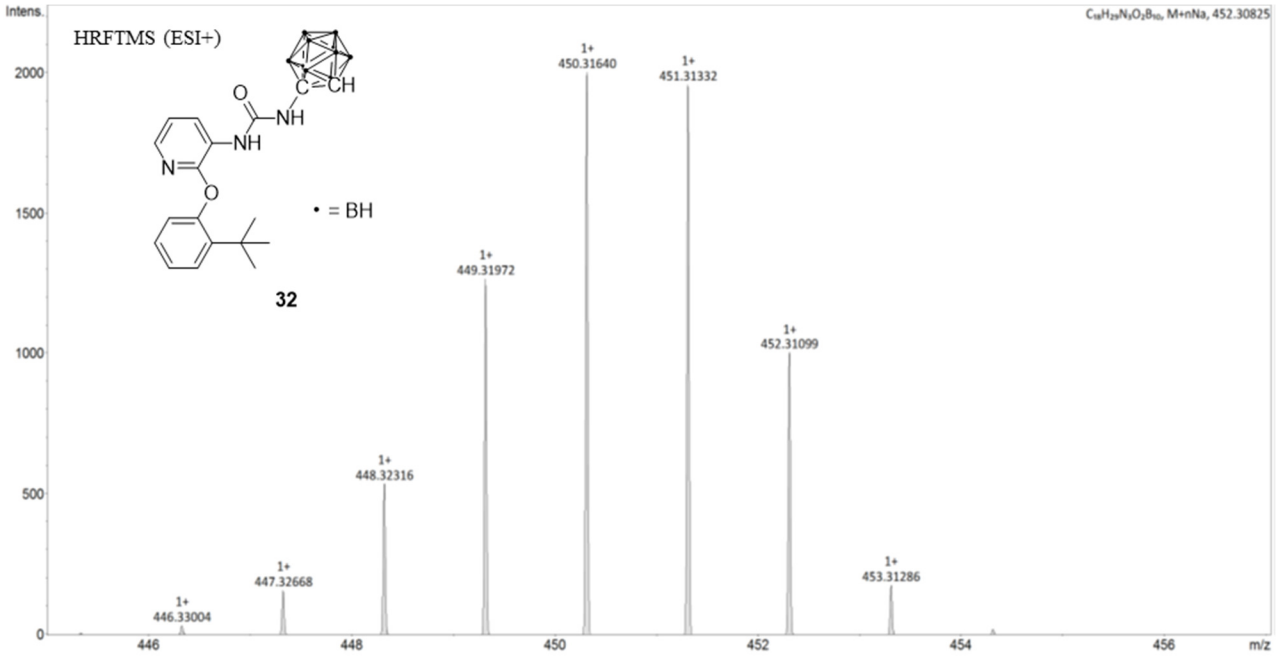

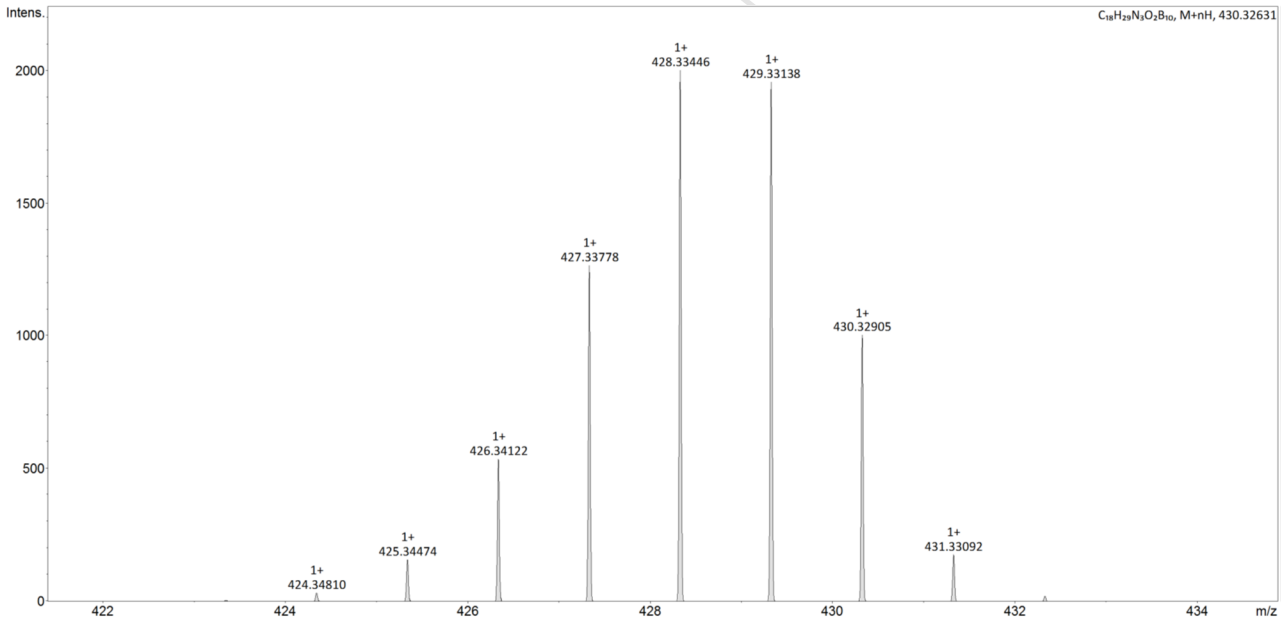

X-Ray Diffraction

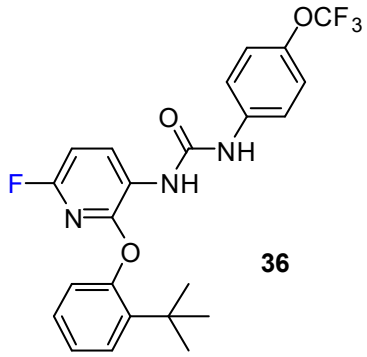

36

Experimental

The single crystal X-ray data collection was carried out on a Bruker AXS SMART diffractometer at room temperature using Mo Kα radiation (λ=0.71073 Å) monochromatised by a graphite crystal. Data reduction was performed by using the Bruker AXS SAINT and SADABS packages. The structures were solved by direct methods and refined by full-matrix least squares calculation using SHELX.[1] Anisotropic thermal parameters were employed for non-hydrogen atoms. The hydrogen atoms were treated isotropically with Uiso = 1.2 times the Ueq value of the parent atom. The hydrogen atoms included were introduced in ideal positions. Crystal data and structure refinement details are summarized in Table 1. The crystallographic data for the structures have been deposited with the Cambridge Crystallographic Data Centre. The CCDC number listed in Table 2. Copies of the data can be obtained, free of charge, on application to CCDC, 12 Union Road, Cambridge CB2 1EZ, UK, fax: +44 1223 336033 or e-mail: deposit@ccdc.cam.ac.uk.

X-ray structure analysis

The molecular structure of **36** is determined by single-crystal diffraction analysis. The molecular configuration is shown in Figure 1. Selected crystallographic data and structure refinement parameters are listed in Table 1.

Compound **36** crystallizes in the monoclinic space group $P2_1/n$ with two molecules in the asymmetric unit and eight molecules in the unit cell. The two molecules of the asymmetric unit

have different conformations, see Figure 1. Significant differences between the two conformations are the opposite direction (position) of the *t*-butylbenzene group and the dihedral between the two aromatic rings (phenyl and pyridine) alongside the carbamide (urea) group with 11.4°, respectively 65.5° (Figure 2).

These two molecules connected via a hydrogen bond in the crystal lattice with a distance of $d_{N1\text{-}O5}$=2.873 Å. Additional interactions are two π-π interactions between the phenyl ring from the t-butylbenzene of the first molecule to the pyridine ring of the second molecule and vice versa, with a plane-to-plane distance of 3.80 Å and a dihedral angle of 12.07° between the planes, respectively 3.95 Å and 14.35° (Figure 3).

The crystal lattice contains no solvent accessible voids.

Table 1. Selected crystallographic data and structure refinement parameters of **36**

Compound reference	wk120 RM135
Chemical formula	$C_{23}H_{21}F_4N_3O_3$
Formula Mass	463.43
Crystal system	Monoclinic
a/Å	15.2900(12)
b/Å	17.4129(14)
c/Å	17.5994(14)
α/°	90.00
β/°	101.163(4)
γ/°	90.00
Unit cell volume/Å^3	4597.1(6)
Temperature/K	296(2)
Space group	$P2_1/n$
No. of formula units per unit cell, *Z*	8
Radiation type	Mo-K_α

Absorption coefficient, μ/mm^{-1}	0.111
No. of reflections measured	74587
No. of independent reflections	11301
R_{int}	0.0904
Final R_1 values ($I > 2\sigma(I)$)	0.0655
Final $wR(F^2)$ values ($I > 2\sigma(I)$)	0.1889
Final R_1 values (all data)	0.1755
Final $wR(F^2)$ values (all data)	0.2342
Goodness of fit on F^2	0.895
CCDC number	1849365

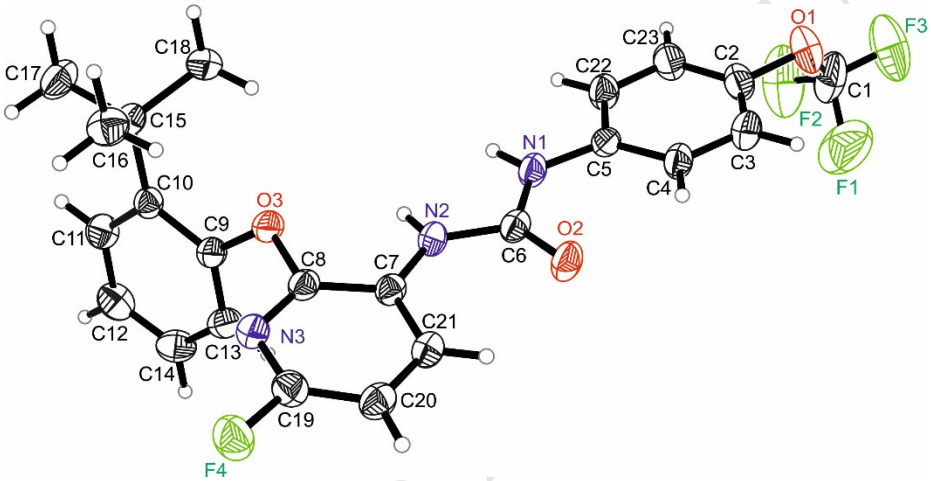

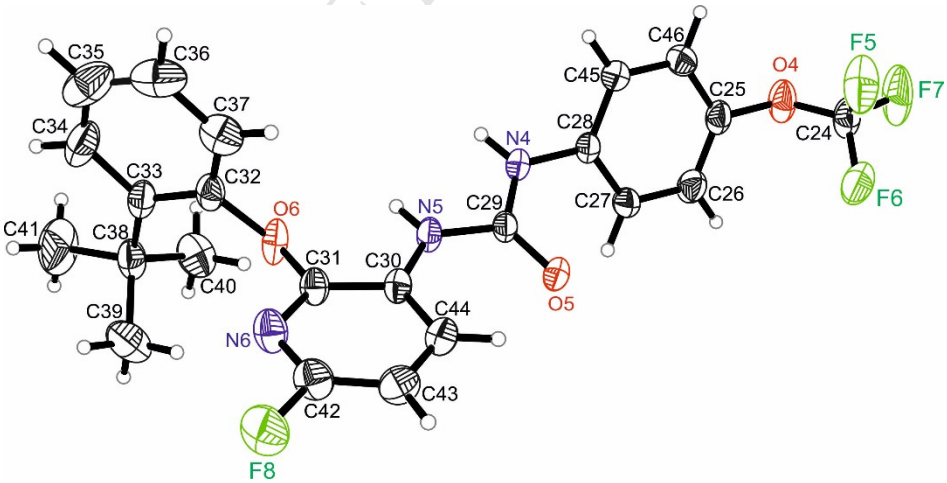

Figure 1. Ortep representation of the two different conformations of the molecules in the asymmetric unit of **36**. Atomic labelling shown with 30% probability displacement ellipsoids.

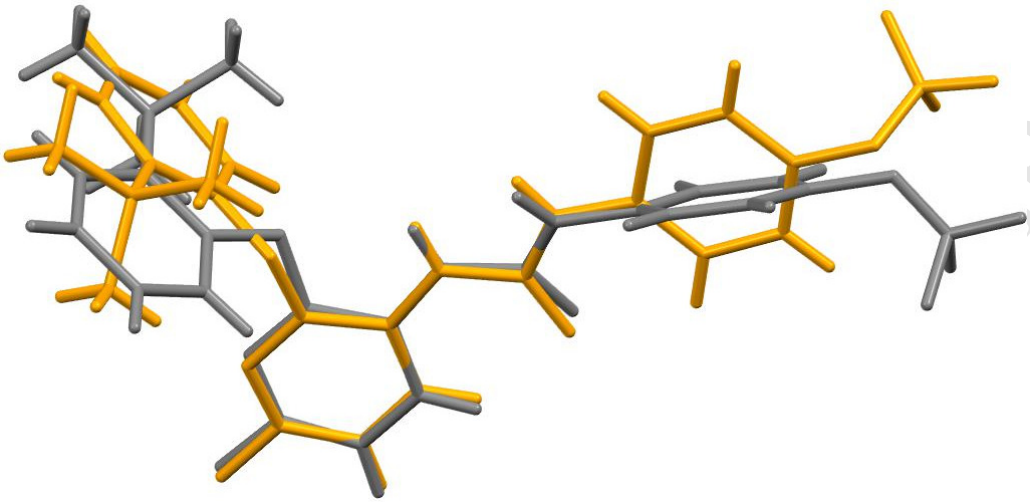

Figure 2. Overlay of the two different conformations.

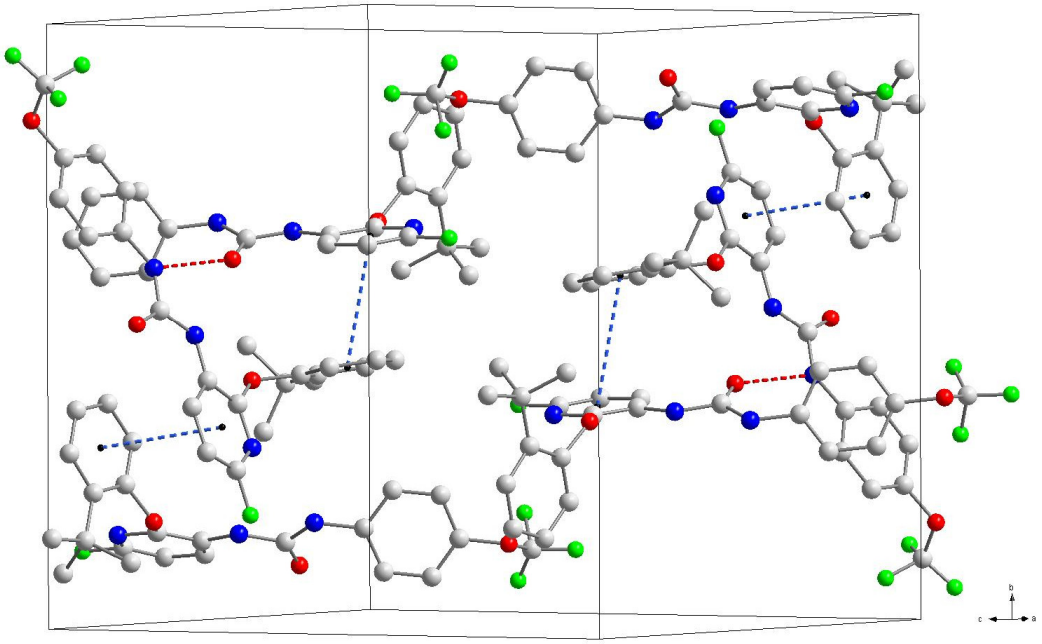

Figure 3. View of the unit cell of compound **36**. Hydrogen bonds are drawn as dashed red lines and π-π interactions as blue dashed lines. Hydrogen atoms omitted for clarity.

HPLC Chromatogram cpd. **7**

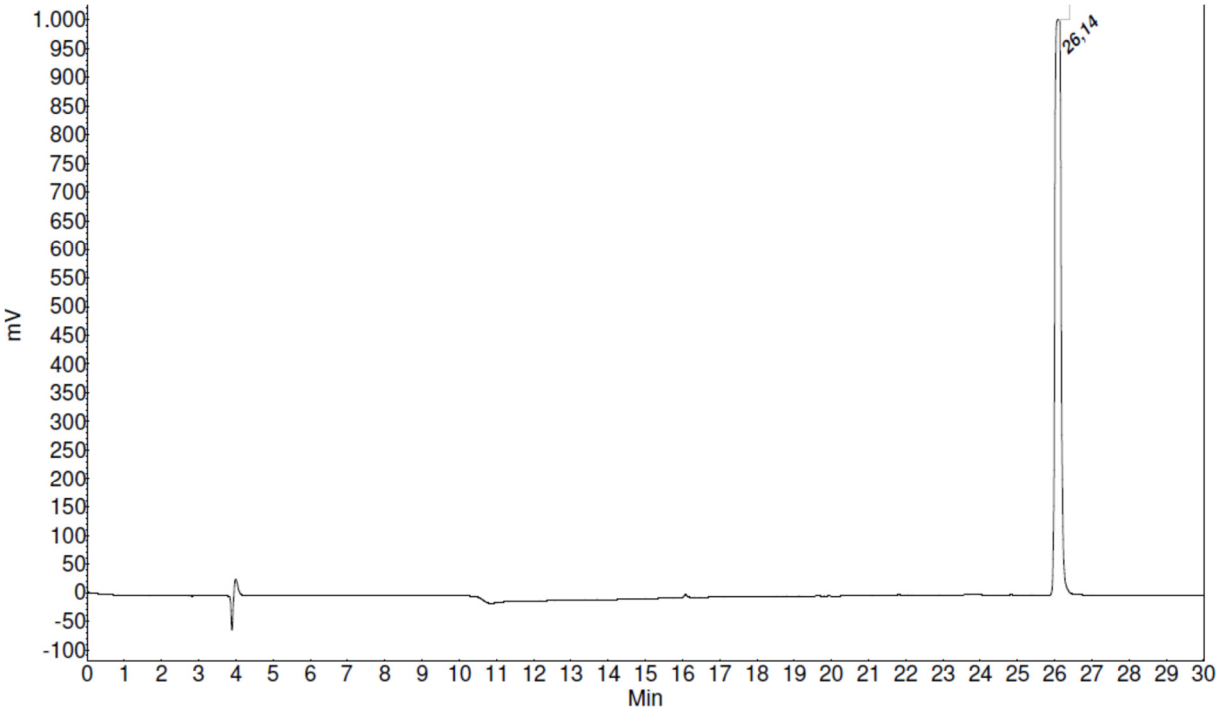

HPLC Chromatogram cpd. **18**

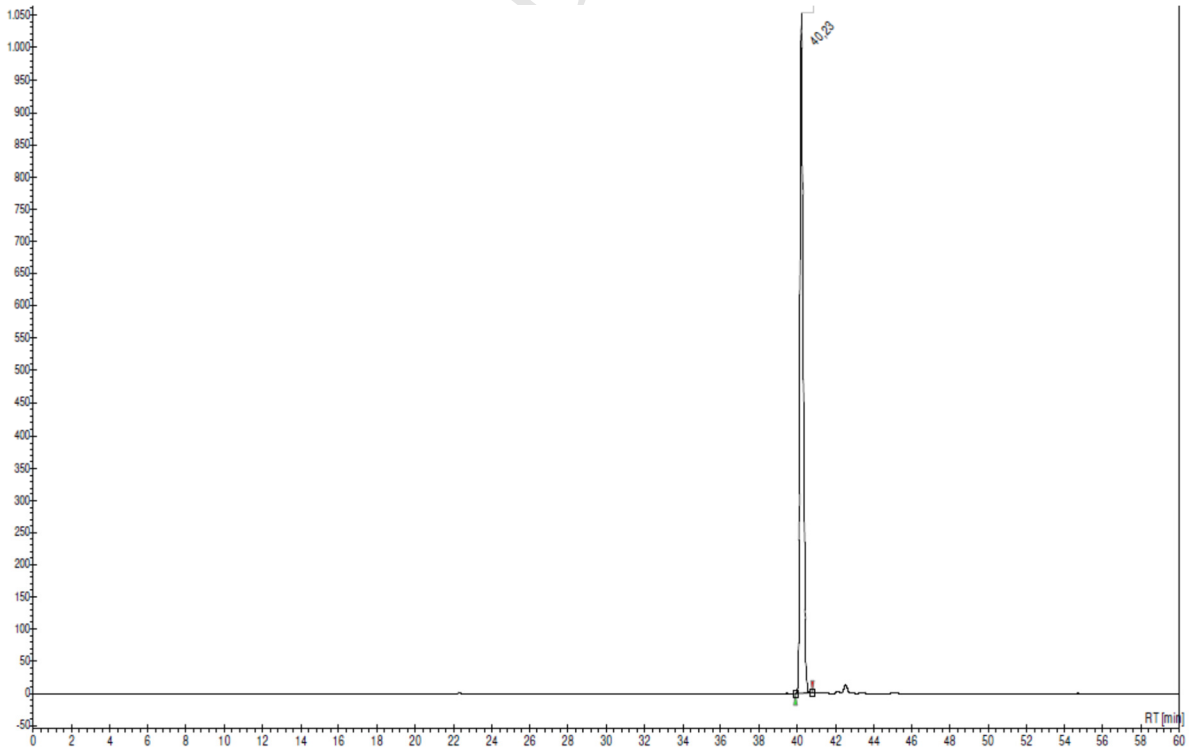

HPLC Chromatogram cpd. **19**

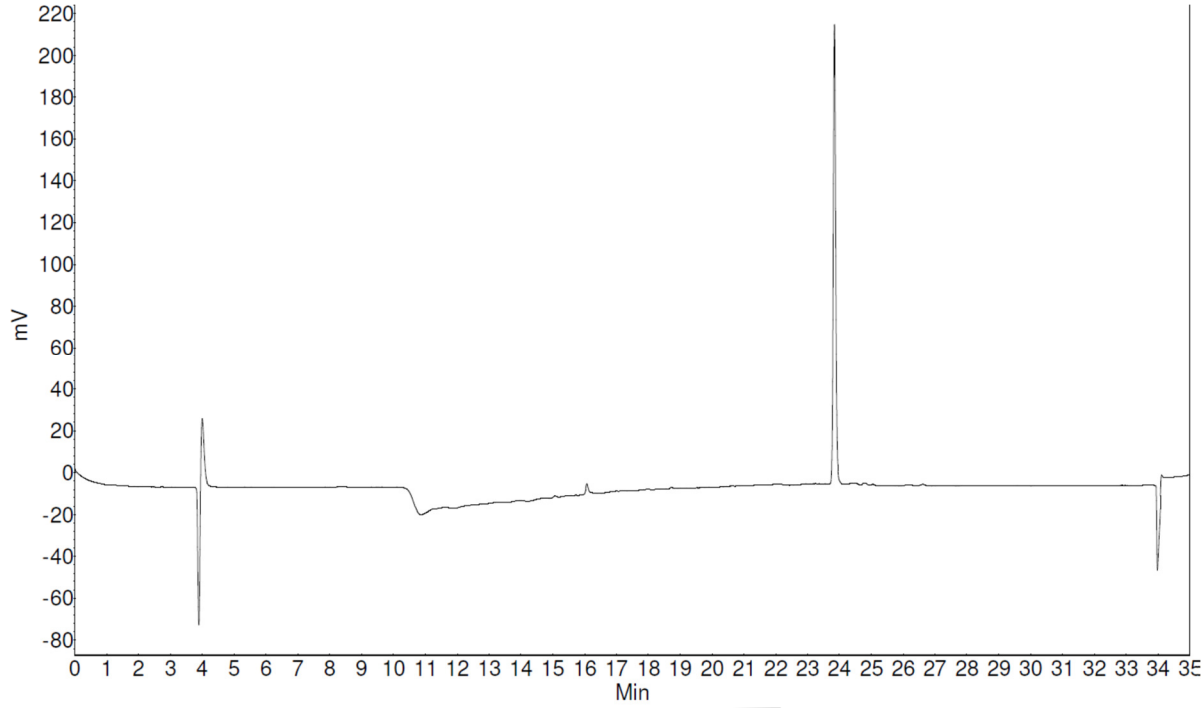

HPLC Chromatogram cpd. **22**

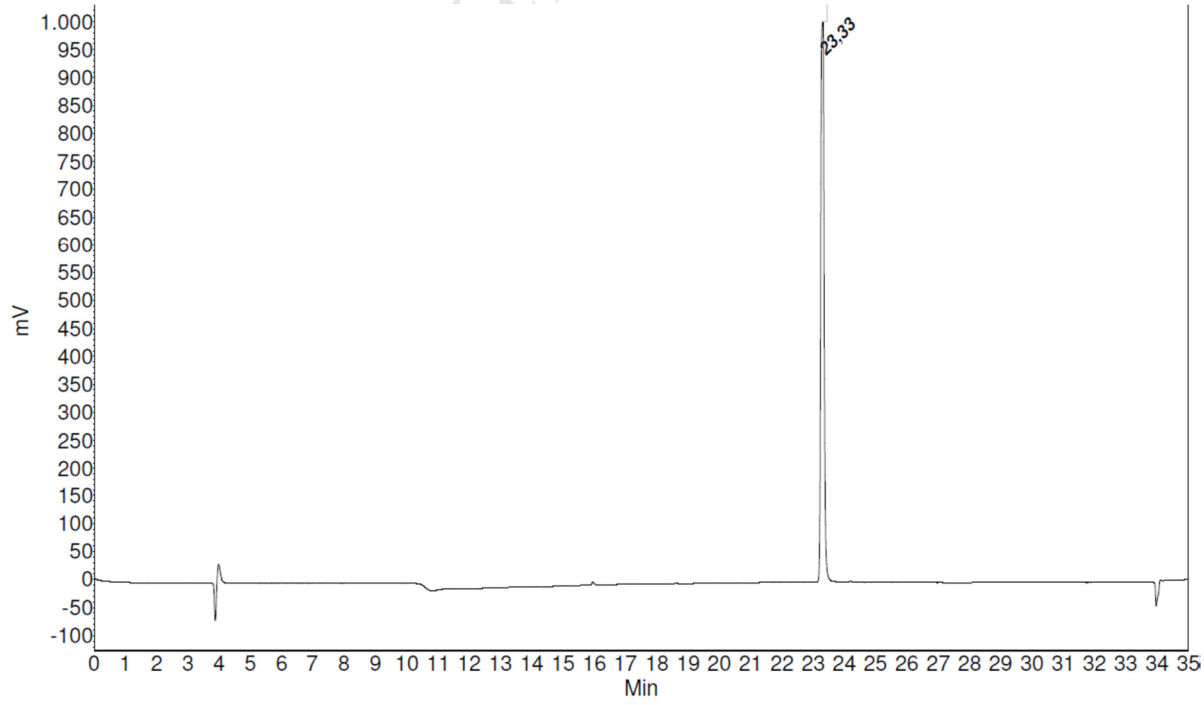

HPLC Chromatogram cpd. **23**

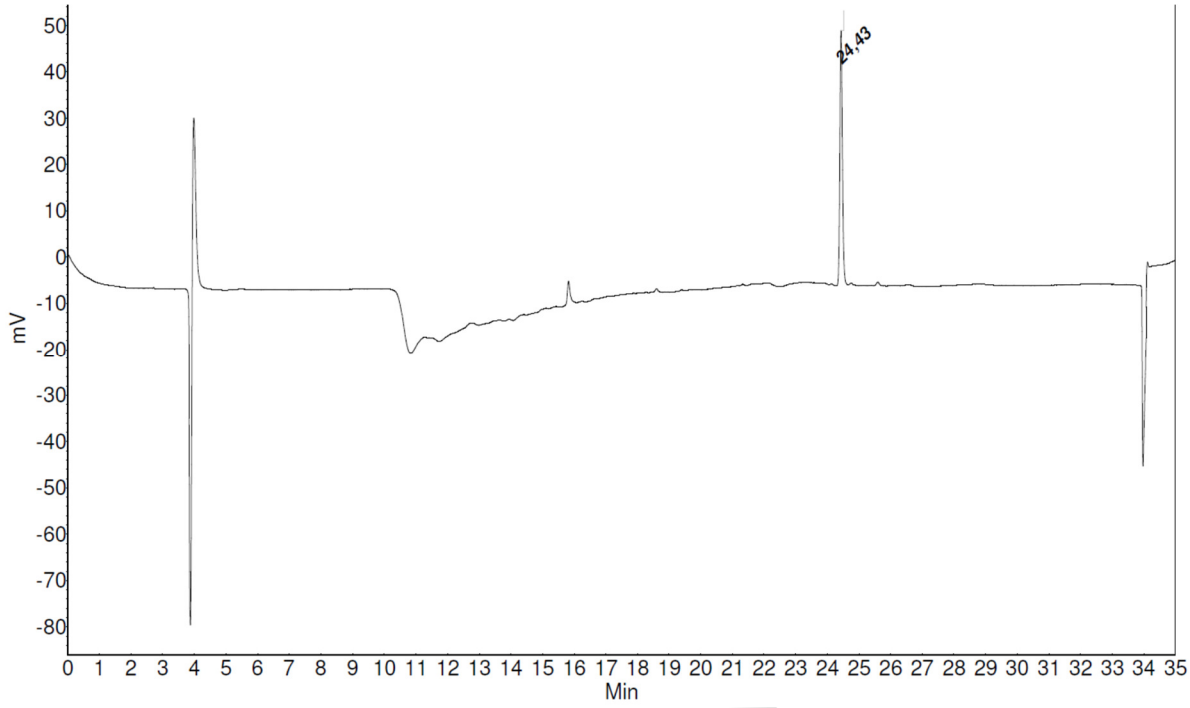

HPLC Chromatogram cpd. **24**

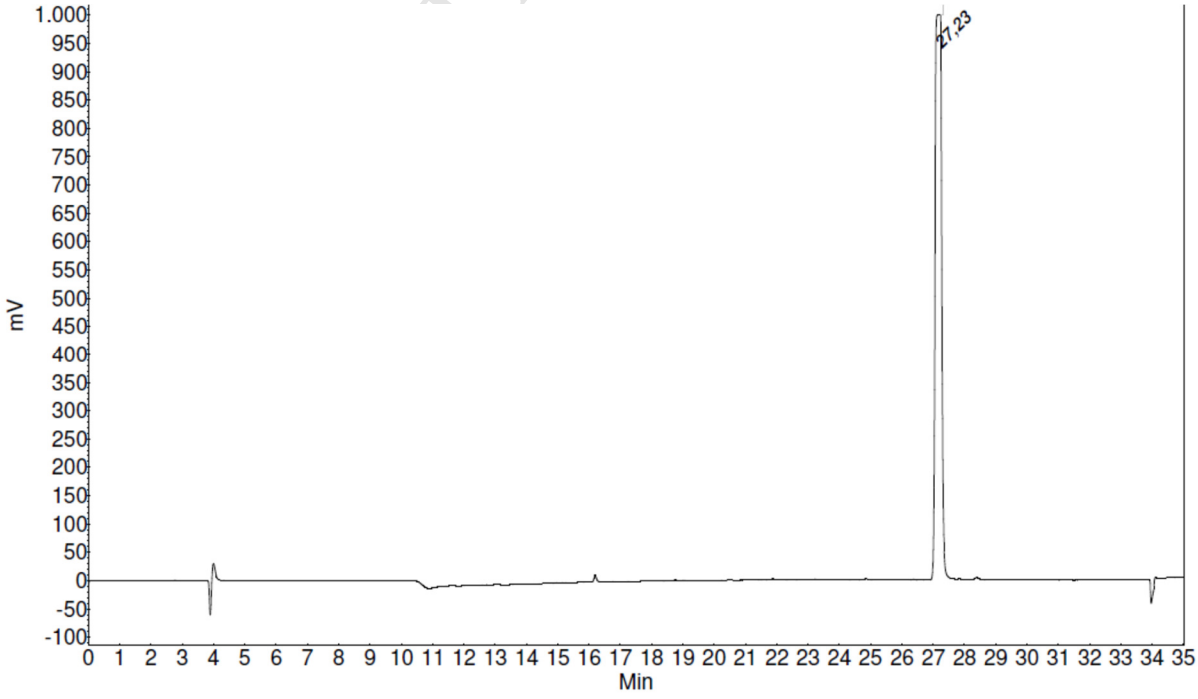

HPLC Chromatogram cpd. **25**

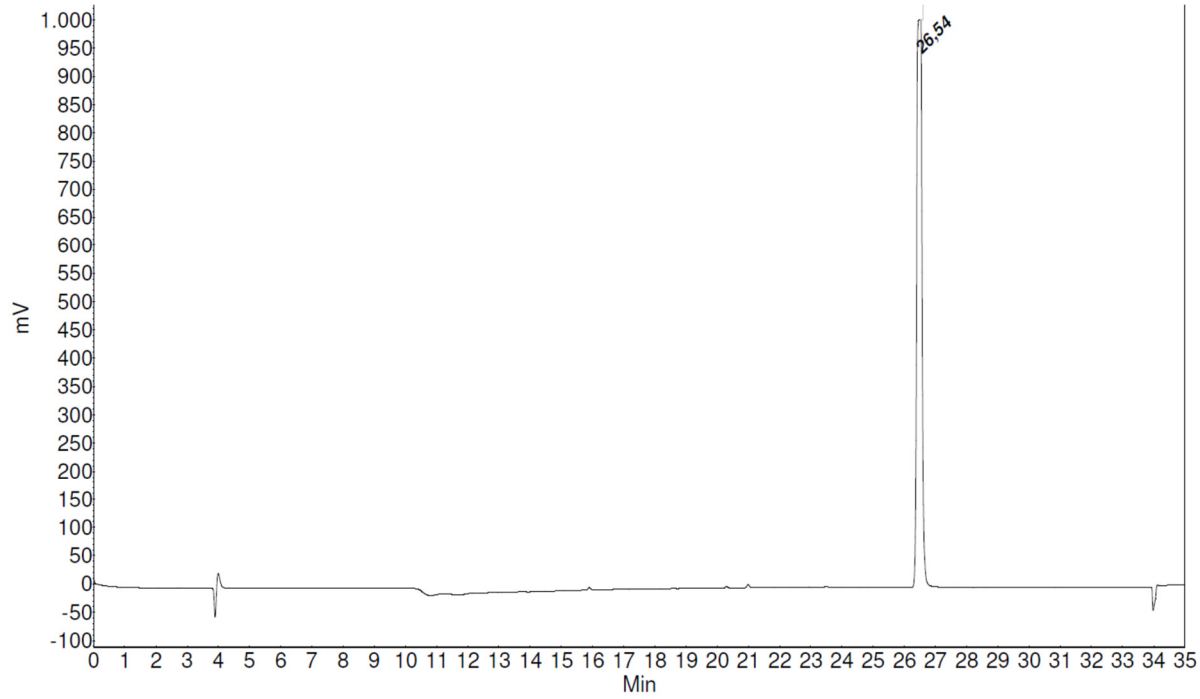

HPLC Chromatogram cpd. **28**

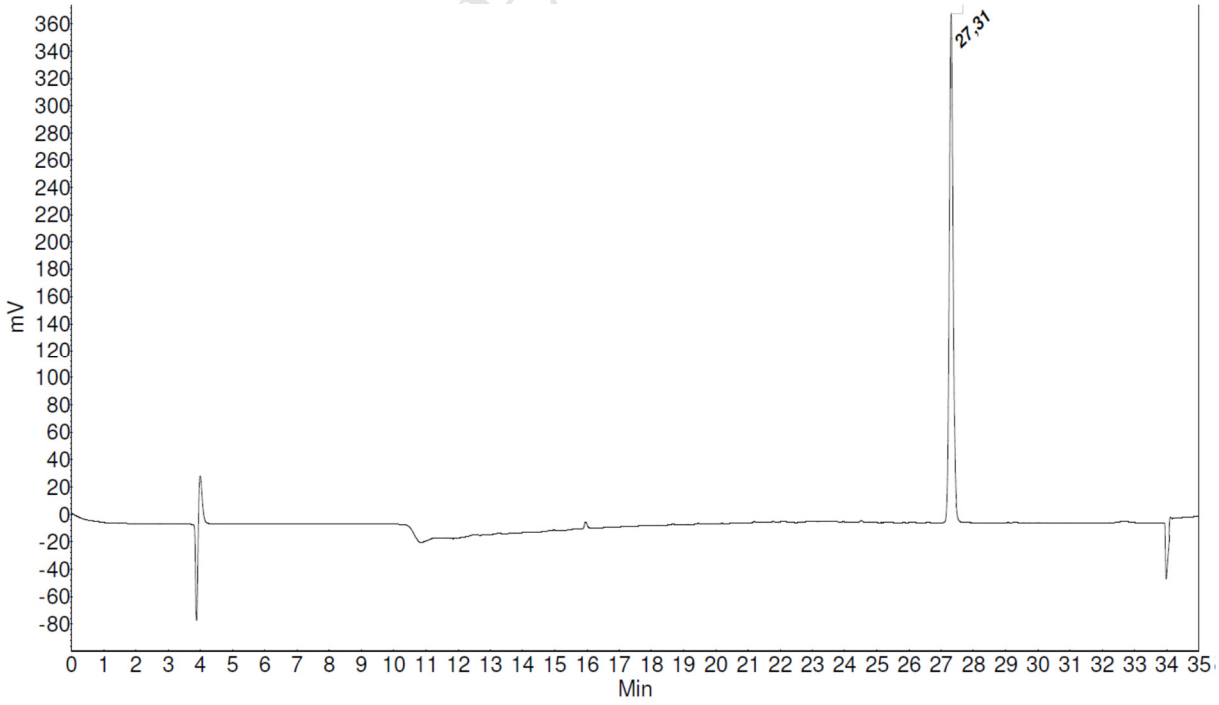

HPLC Chromatogram cpd. **29**

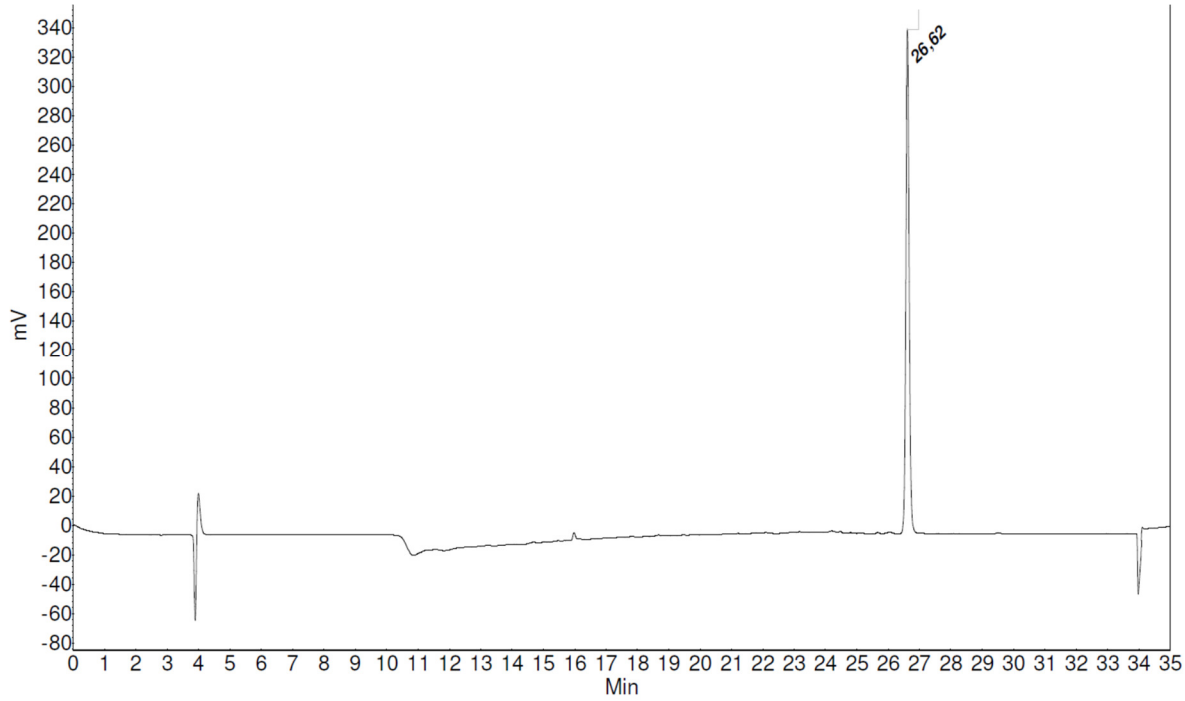

HPLC Chromatogram cpd. **30**

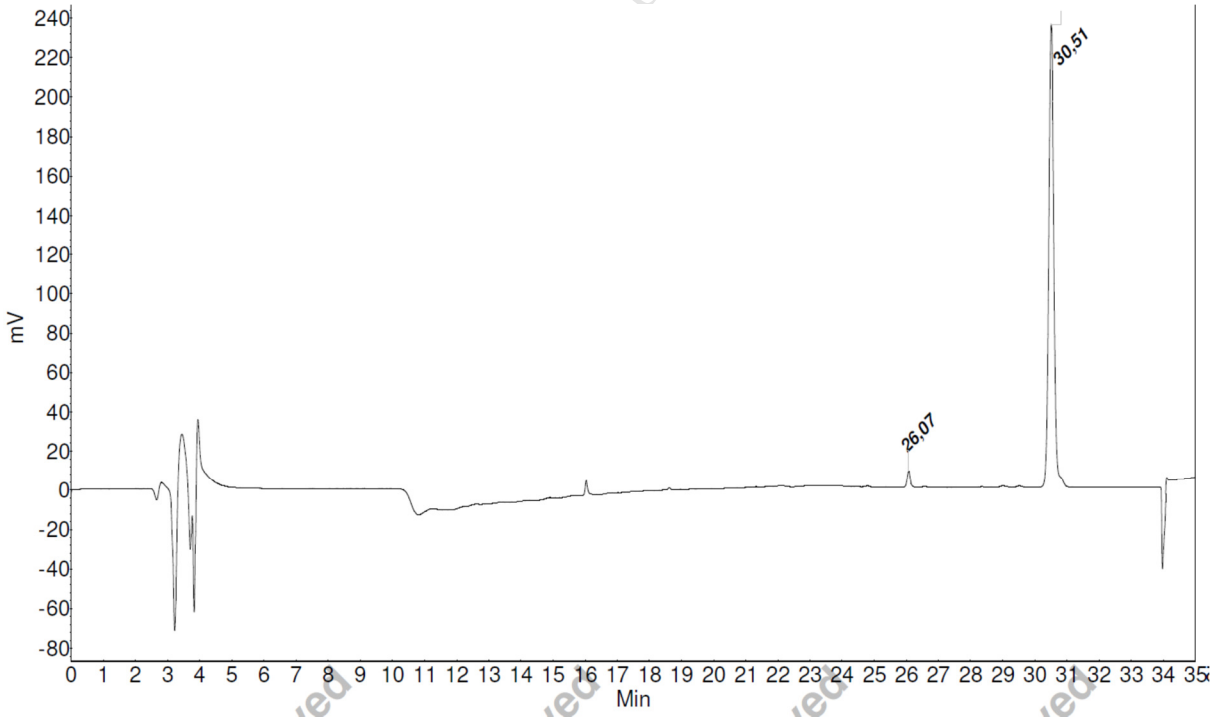

HPLC Chromatogram cpd. **32**

Index	Time [Min]	Quantity [% Area]	Height [mV]	Area [mV.Min]	Area % [%]	K'	Res. USP	Res. HW	Selectivity	As. 10%
2	19.86	2.58	32.1	2.3	2.583	0.00	0.00	0.00	0.00	1.31
1	28.69	97.42	544.4	87.8	97.417	0.00	47.75	48.78	1.44	1.13
Total		100.00	576.5	90.1	100.000					

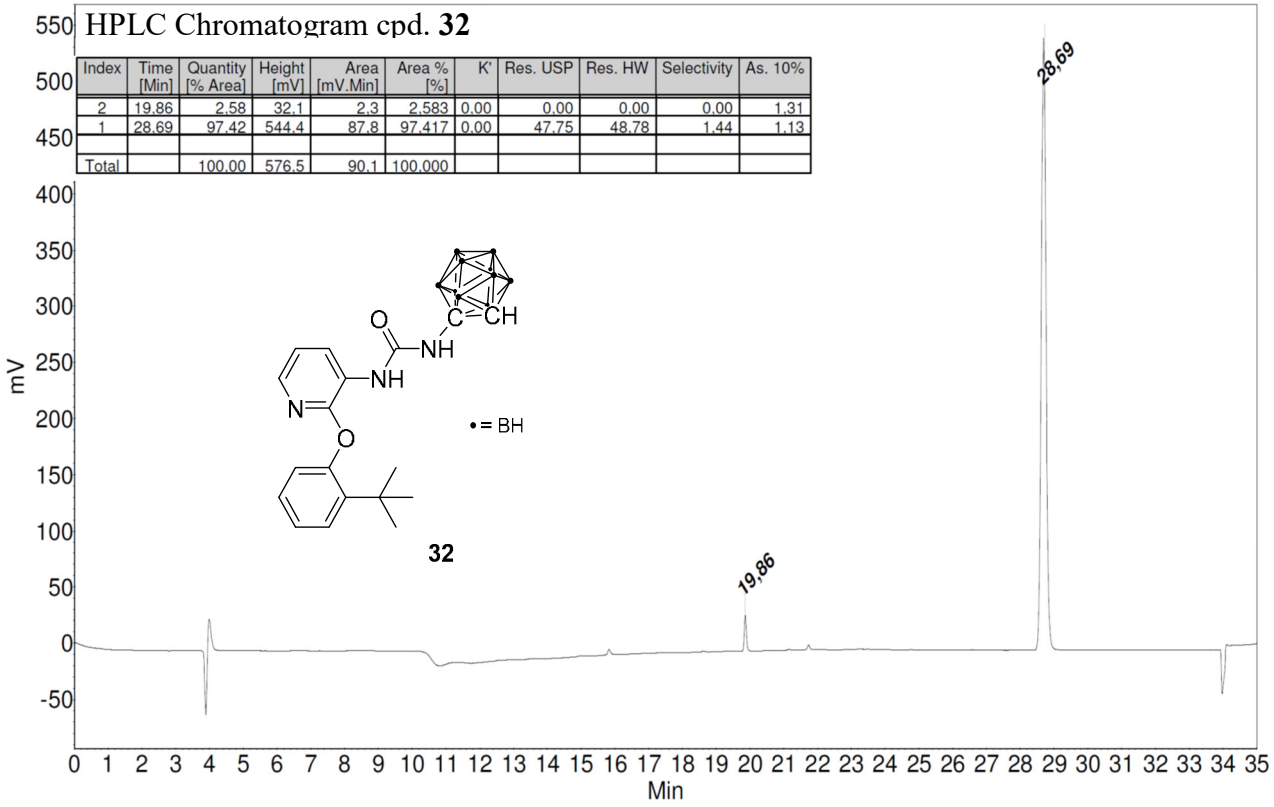

32

HPLC Chromatogram cpd. **36**

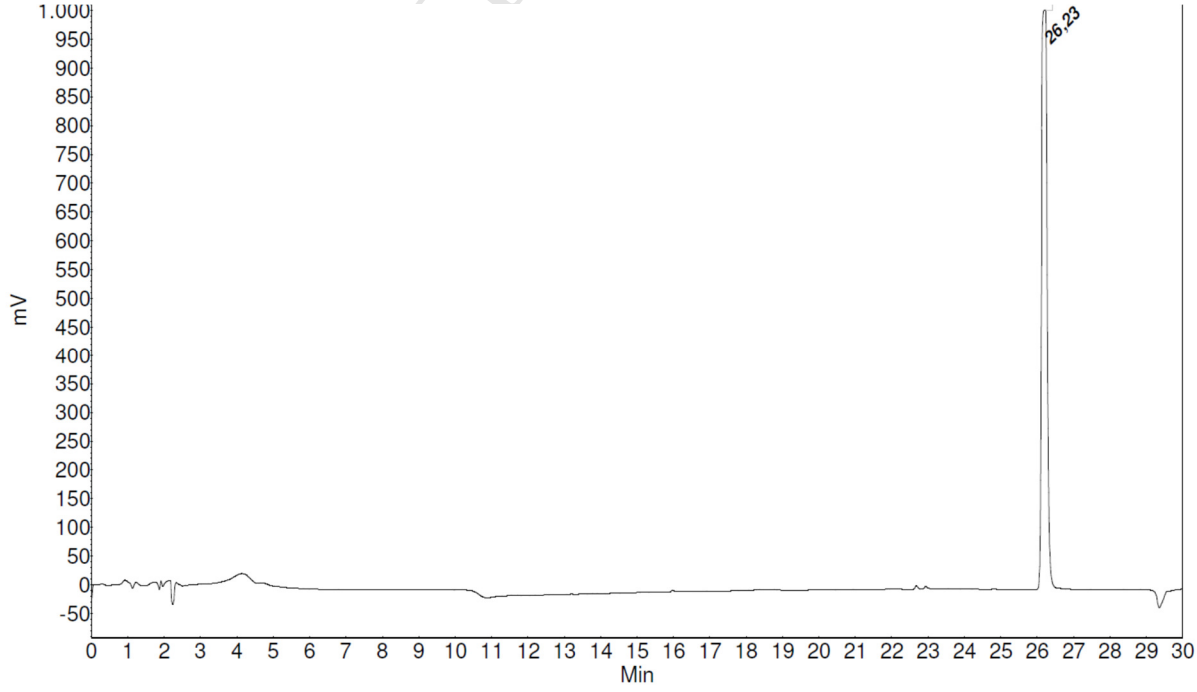

HPLC Chromatogram cpd. **37**

Index	Time [Min]	Quantity [% Area]	Height [mV]	Area [mV.Min]	Area % [%]	K'	Res. USP	Res. HW	Selectivity	As. 10%
1	28,15	97,91	999,4	217,6	97,910	0,00	0,00	0,00	0,00	0,54
2	30,72	2,09	24,8	4,6	2,090	0,00	8,96	8,07	1,09	1,14
Total		100,00	1024,2	222,3	100,000					

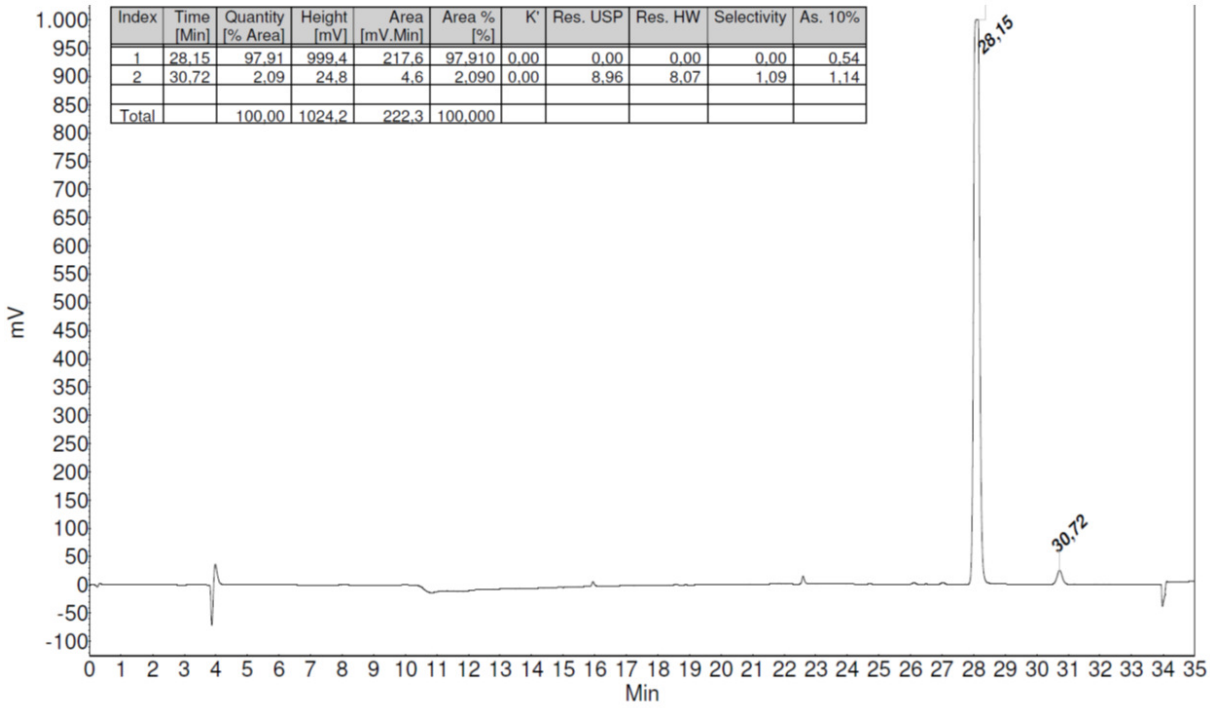

HPLC Chromatogram cpd. **38**

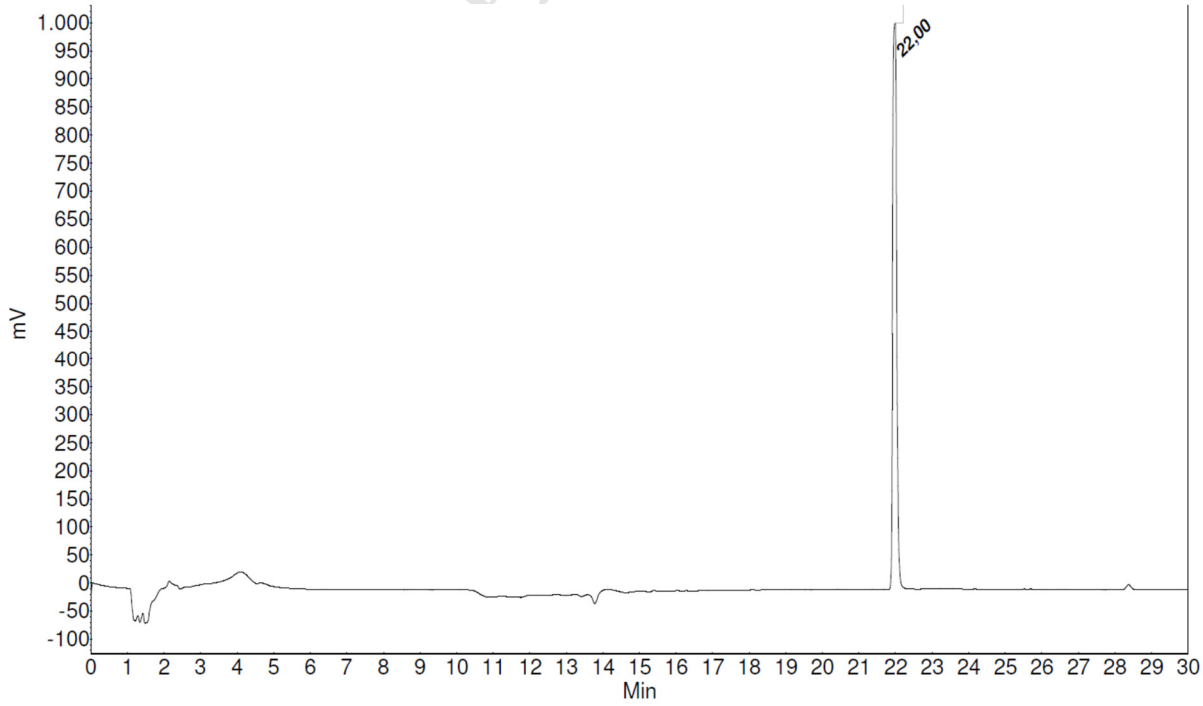

HPLC Chromatogram cpd. **39**

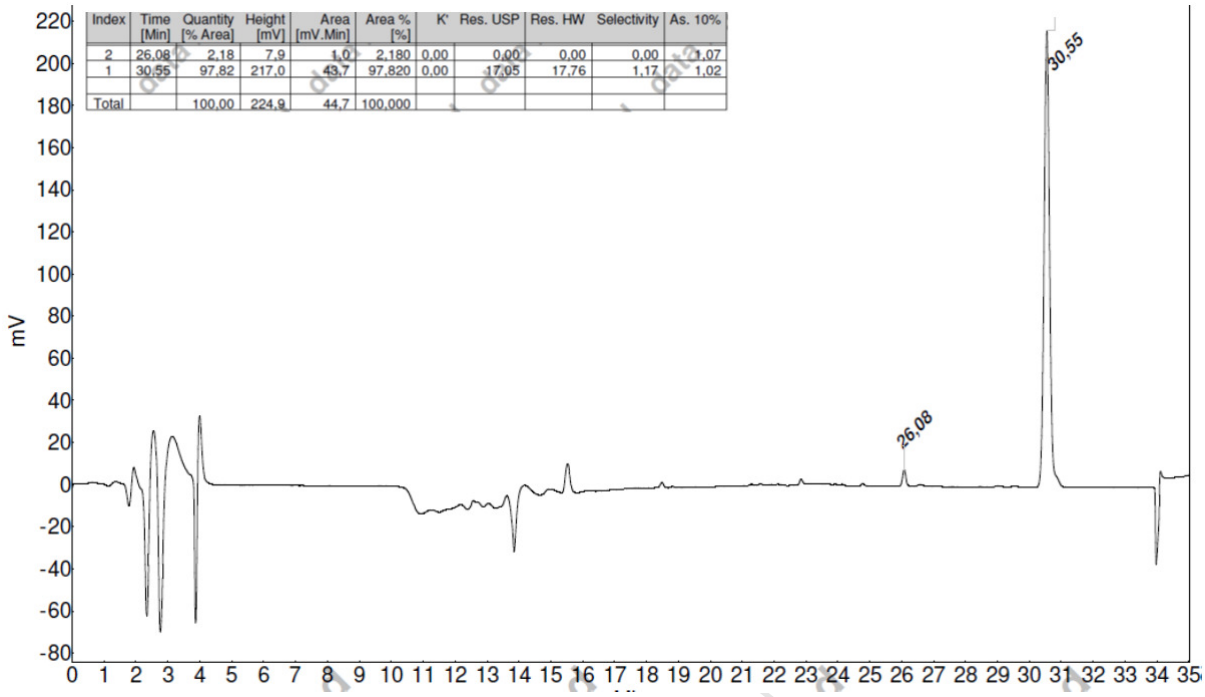

HPLC Chromatogram cpd. **40**

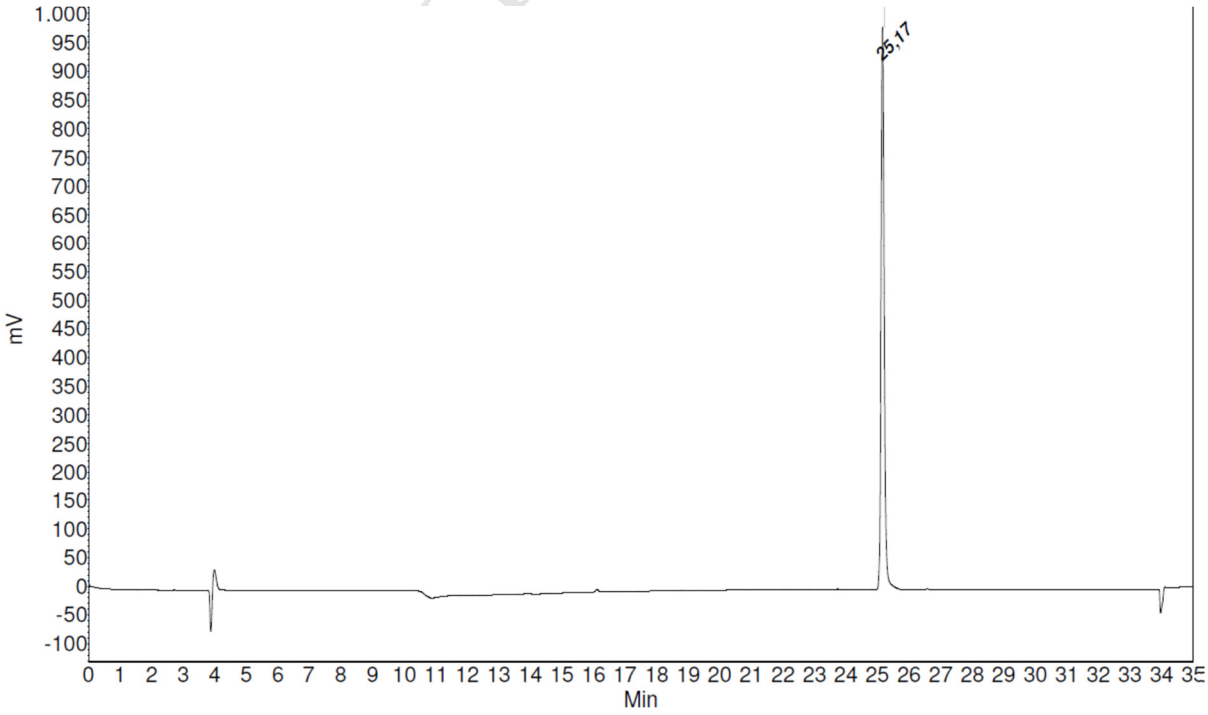

HPLC Chromatogram cpd. **41**

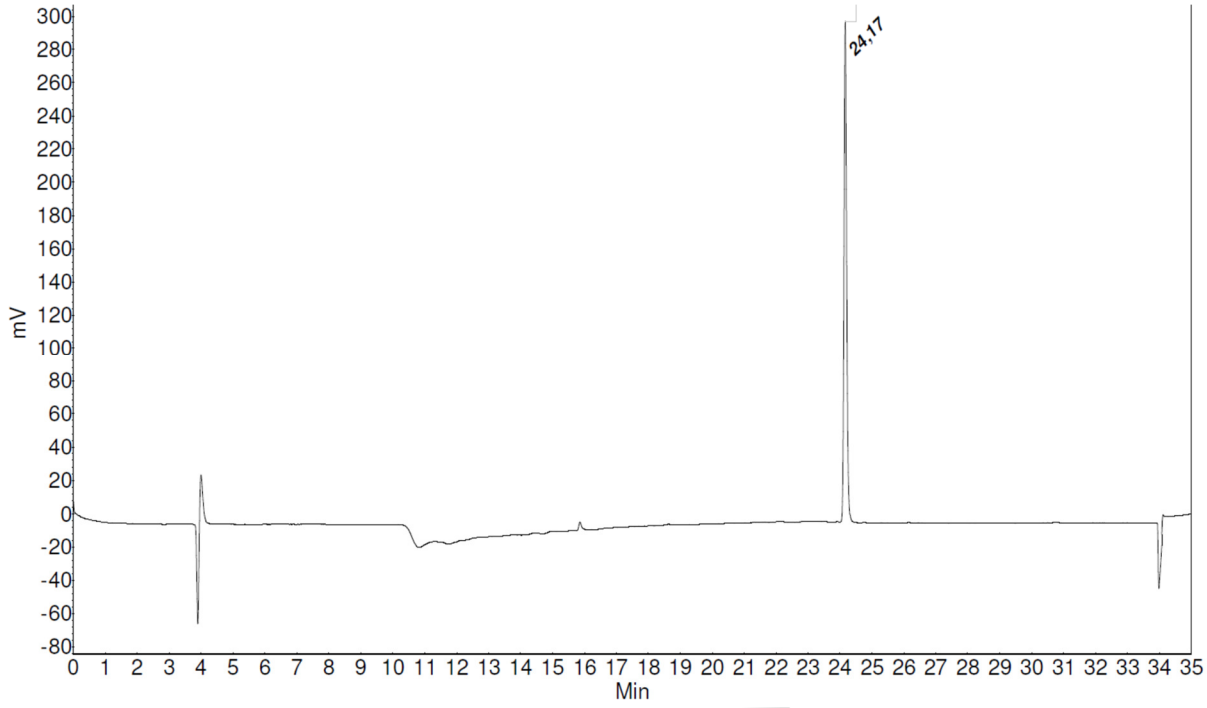

HPLC Chromatogram cpd. **42**

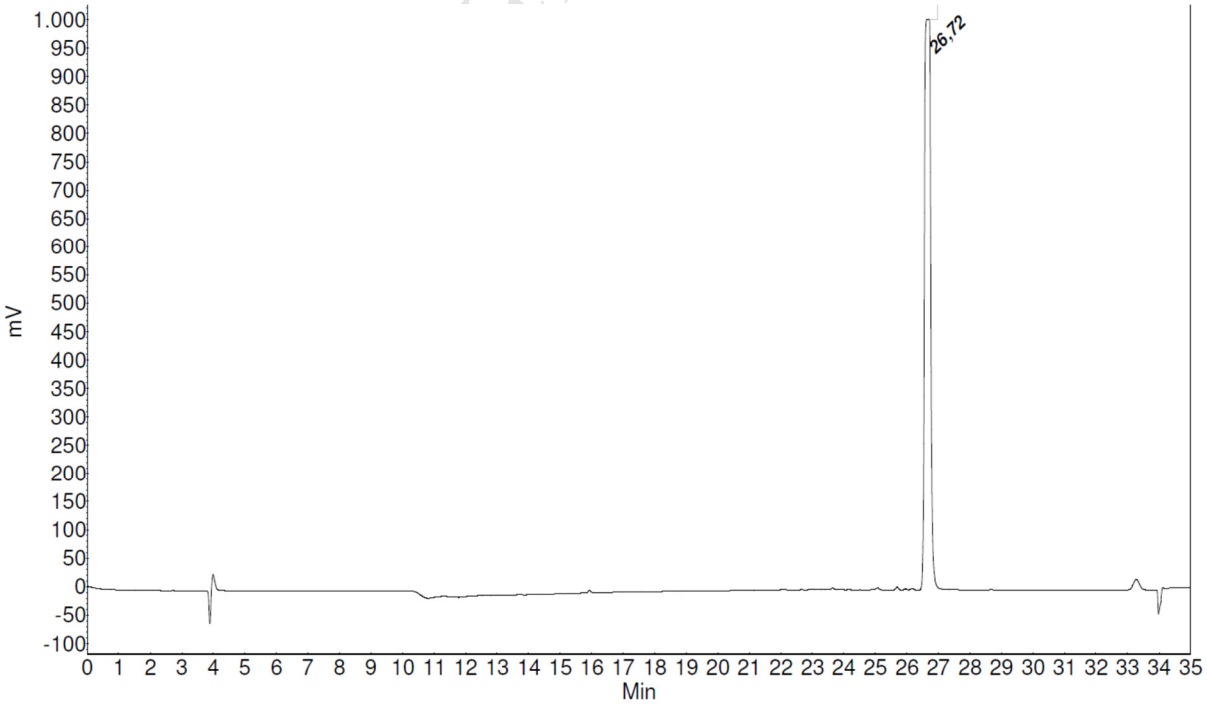

HPLC Chromatogram cpd. **43**

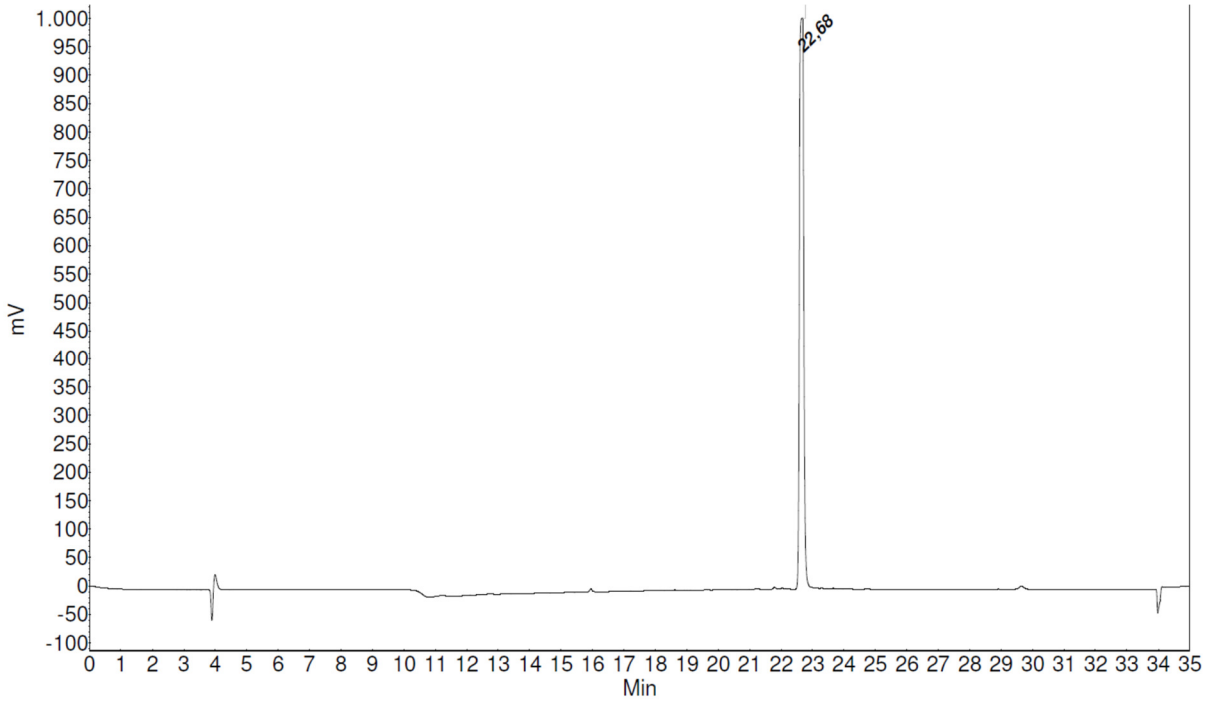

HPLC Chromatogram cpd. **47**

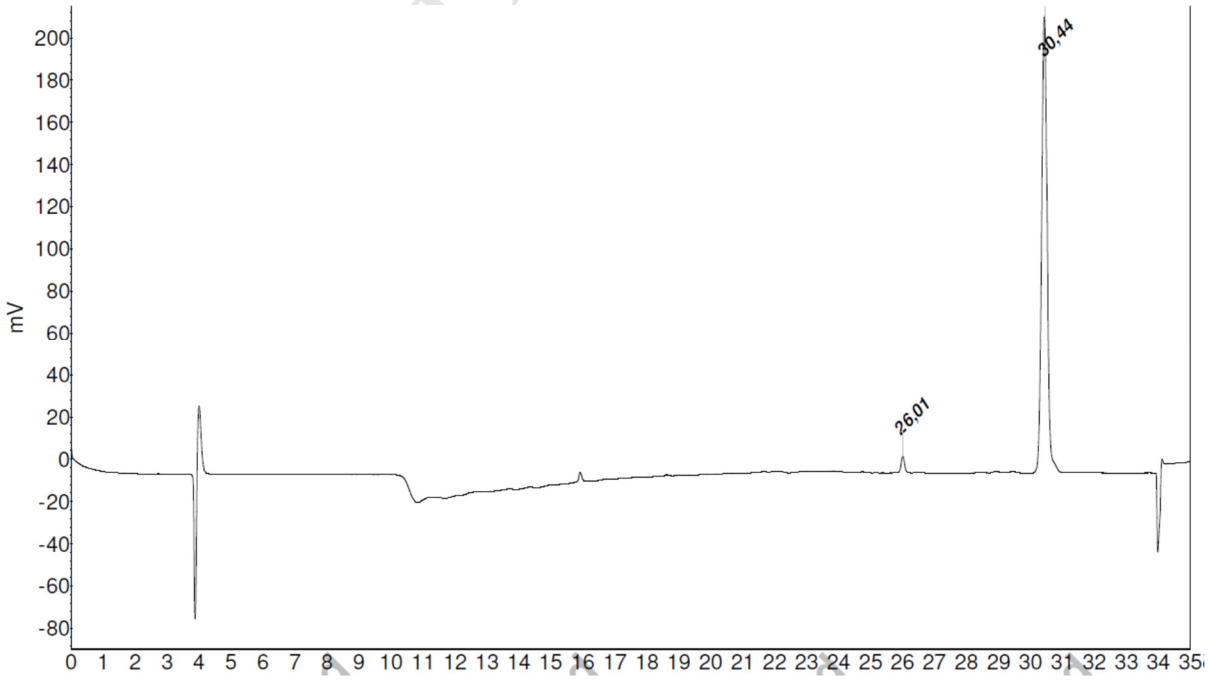

HPLC Chromatogram cpd. **48**

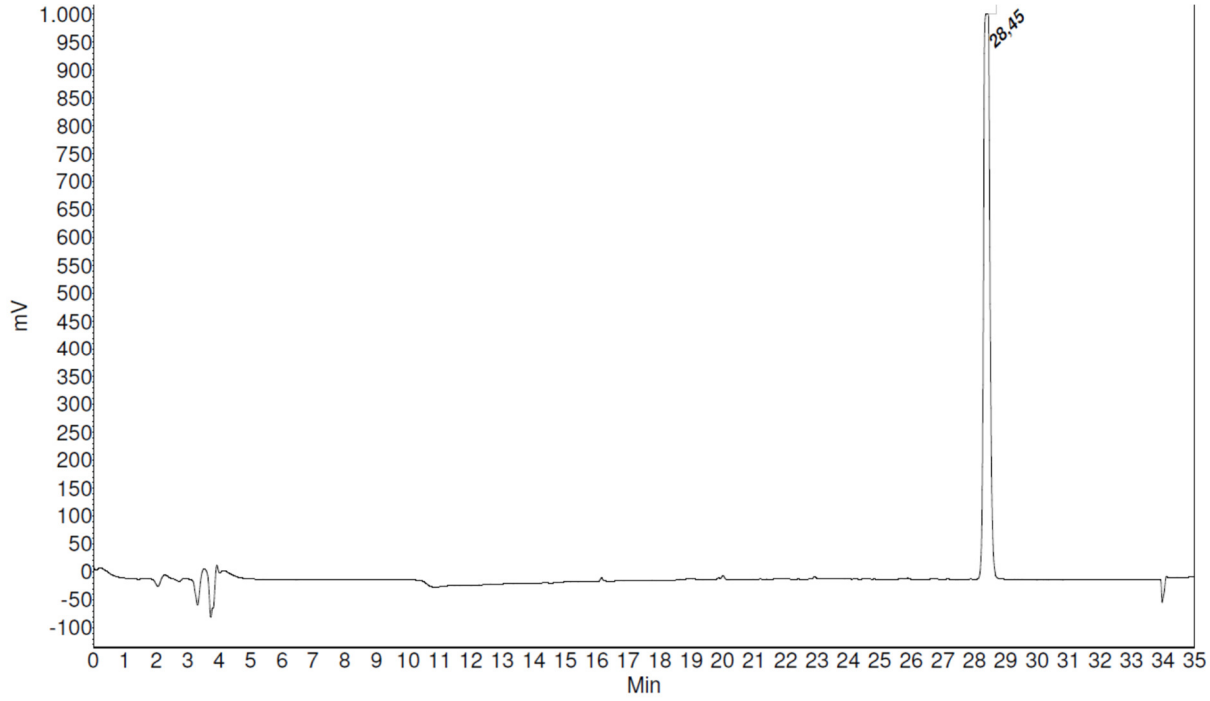

HPLC Chromatogram cpd. **49**

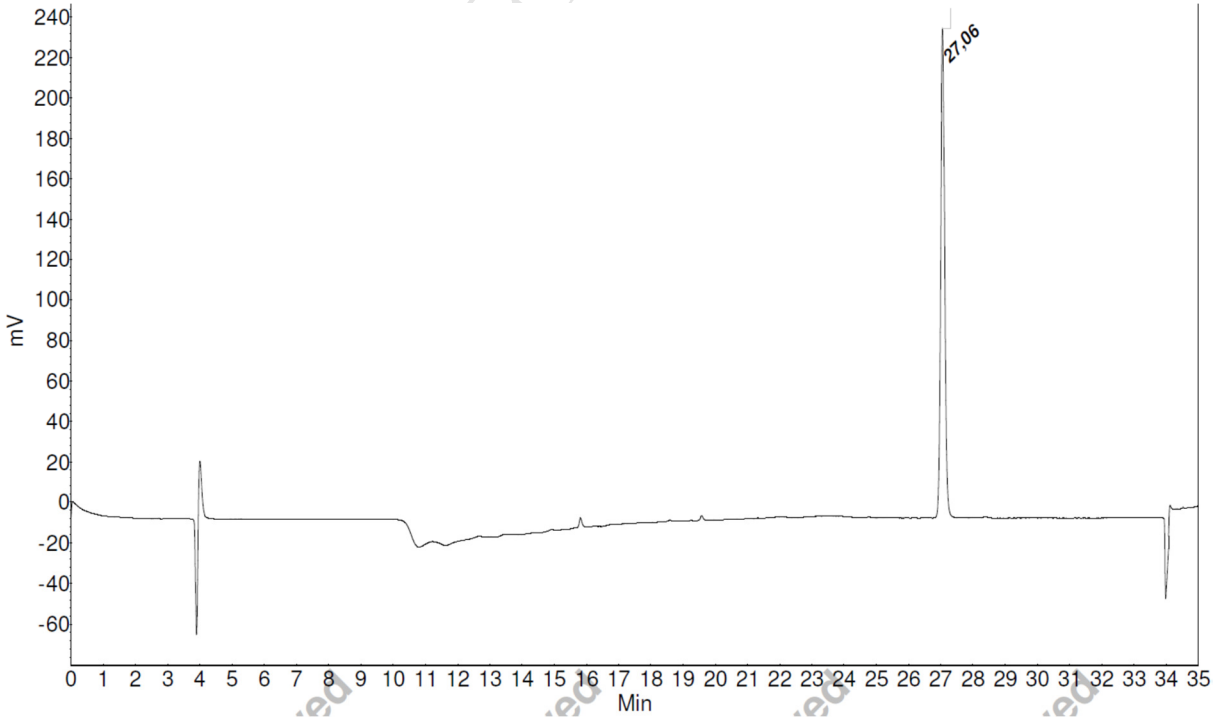

HPLC Chromatogram cpd. **53**

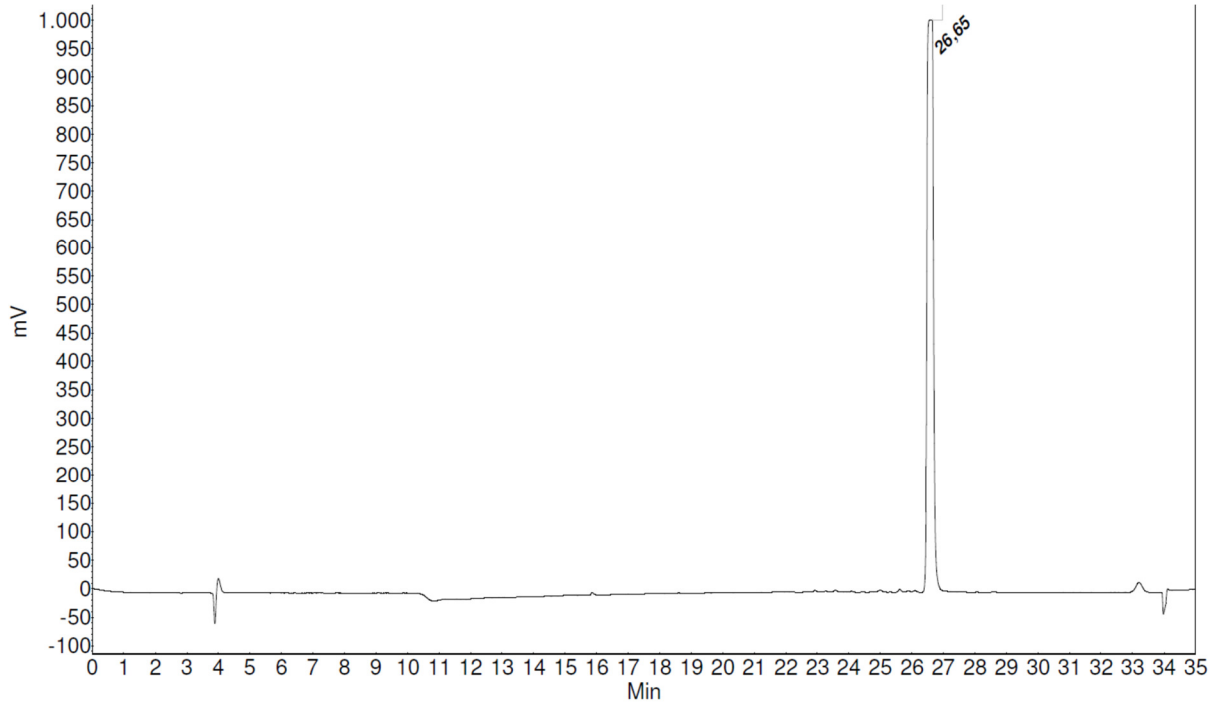

HPLC Chromatogram cpd. **54**

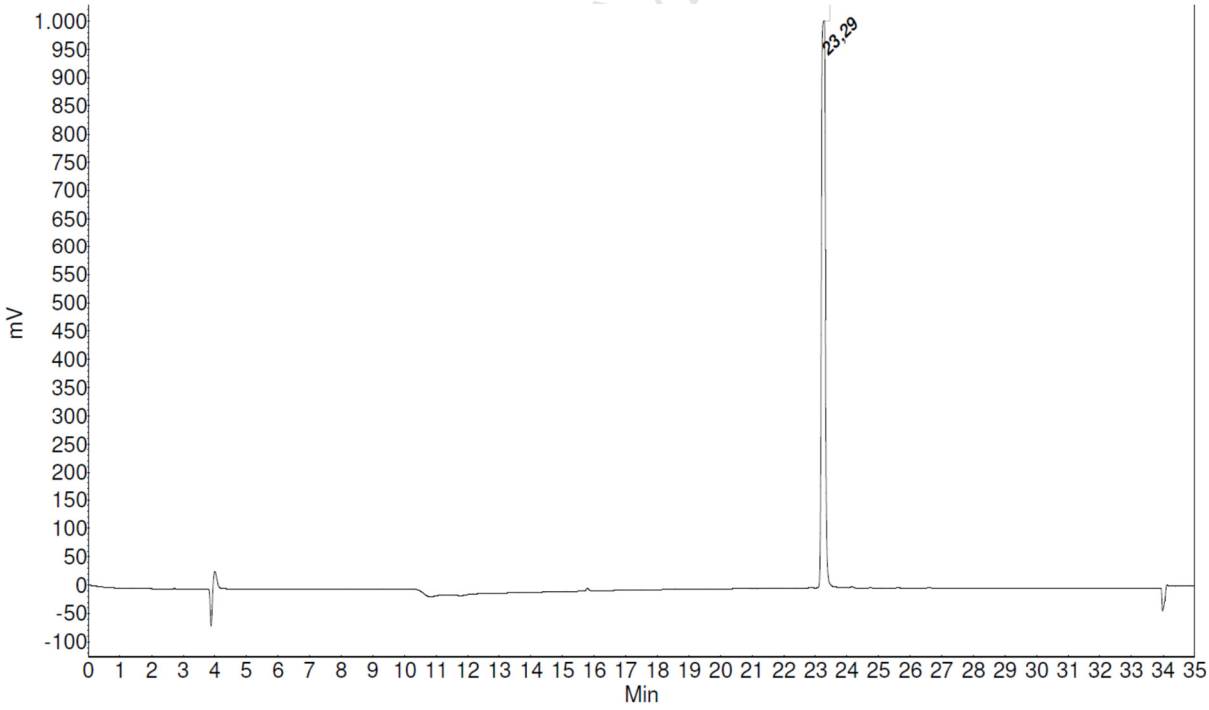

References

[1]G.M. Sheldrick, *Acta Crystallogr. Sect. A* 64 (**2008**) 112-122.